

H24/3649

MONASH UNIVERSITY
THESIS ACCEPTED IN SATISFACTION OF THE
REQUIREMENTS FOR THE DEGREE OF
DOCTOR OF PHILOSOPHY
ON..... 12 October 2004.....

.....
Sec. Research Graduate School Committee

Under the Copyright Act 1968, this thesis must be used only under the normal conditions of scholarly fair dealing for the purposes of research, criticism or review. In particular no results or conclusions should be extracted from it, nor should it be copied or closely paraphrased in whole or in part without the written consent of the author. Proper written acknowledgement should be made for any assistance obtained from this thesis.

**The Specificity of
Proteinase-Adhesins from
*Porphyromonas gingivalis***

Nafisa Ally

Department of Biochemistry and Molecular Biology
Monash University
Clayton, Victoria, Australia, 3800

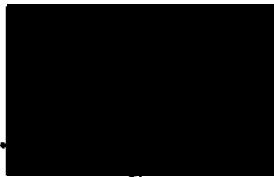
PhD Thesis

August 2003

For Dad and Mum

DECLARATION

I hereby declare that this thesis contains no material which has been accepted for the award of any other degree or diploma at any University or equivalent institution and that, to the best of my knowledge and belief, this thesis contains no material previously published or written by another person, except where due reference is made in the text of the thesis.



.....

Nafisa Ally

August 2003

PUBLICATIONS ARISING FROM THIS WORK

Abraham, L.A., Chinni, C., Jenkins, A.L., Loubakos, A., Ally, N., Pike, R.N., and Mackie, E.J. (2000), Expression of Protease-activated Receptor-2 by Osteoblasts, *Bone* **26**: 7-14.

Nuttall, S.D., Krishnan, U.V., Doughty, L., Nathanielsz, A., Ally, N., Pike, R.N., Hudson, P.J., Kortt, A.A., and Irving R. (2002), A naturally occurring NAR variable domain binds the Kgp protease from *Porphyromonas gingivalis*, *FEBS Letters* **516**: 80-6.

Ally, N., Whisstock, J.C., Sieprawska-Lupa, M., Potempa, J., Le Bonniec, B.F., Travis, J. and Pike, R.N. (2003), Characterisation of the specificity of Arginine-Specific gingipains from *Porphyromonas gingivalis* reveals active site differences between different forms of the enzymes. *Biochemistry* **42**: 11693-700.

ACKNOWLEDGEMENTS

I would like to acknowledge the assistance of the following people for their contribution to this thesis:

Dr. Rob Pike, my supervisor for giving me the opportunity to do a PhD in his laboratory, and for his invaluable advice, guidance, assistance and support throughout my PhD.

Dr. James Whisstock for modelling the catalytic domain of HRgpA and his discussions on the structure and specificity of gingipains.

Prof. James Travis for giving me the opportunity to work in his laboratory at the Department of Biochemistry and Molecular Biology, University of Georgia, Atlanta.

Dr. Jan Potempa for all his assistance and expert advice throughout my PhD.

Magdalena Sieprawska-Lupa for her contribution to the study on the adhesin domains.

Dr. Agnieszka Banbula for her scientific advice and assistance in the purification of RgpA_{cat} and Kgp_{cat}, and support and friendship during my stay in Georgia.

Dr. Neil O'Brien-Simpson for the synthesis of the peptide inhibitor substrates.

James Balmer for his utmost understanding, support and encouragement in the writing up of my thesis.

All my family and friends for their continual support and understanding throughout my studies.

TABLE OF CONTENTS

DECLARATION.....	i
PUBLICATIONS ARISING FROM THIS WORK.....	ii
ACKNOWLEDGEMENTS.....	iii
LIST OF FIGURES.....	viii
LIST OF TABLES.....	x
ABBREVIATIONS.....	xi
SUMMARY.....	xiii
CHAPTER 1 Introduction.....	1
1.0 General.....	2
1.1 Periodontal Disease.....	3
1.2 <i>Porphyromonas gingivalis</i>	6
1.2.1 Virulence Factors of <i>P. gingivalis</i>	6
1.2.2 Fimbriae.....	8
1.2.3 Lipopolysaccharide.....	10
1.3 Proteases of <i>P. gingivalis</i>	11
1.3.1 Importance of gingipains to pathogenesis.....	14
1.3.2 Gingipains.....	16
1.3.2.1 Arginine-Specific gingipains.....	20
1.3.1.2 Lysine-Specific Gingipain.....	21
1.4 Pathological Potential of Proteinases.....	22
1.4.1 Degradation of Connective Tissue Components.....	24

1.4.2 Deregulation of Complement Pathway.....	25
1.4.3 Deregulation of Kallikrein/Kinin System.....	25
1.4.4 Deregulation of the Coagulation pathway.....	28
1.4.5 Cytokines.....	28
1.5 Protease Activated Receptors.....	29
1.6 Bacterial Invasion of Cells.....	30
1.7 Aims of Study.....	31
CHAPTER 2 Purification of gingipains-R and gingipain-K and their catalytic domains RgpA_{cat} and Kgp_{cat} from <i>Porphyromonas gingivalis</i>.....	34
2.1 Introduction.....	35
2.2 Materials and Methods.....	37
2.2.1 Materials.....	37
2.2.2 Cultivation of Bacteria.....	37
2.2.3 Purification of Enzymes.....	37
2.2.3.1 HRgpA, Kgp and RgpB.....	38
2.2.3.2 Purification of KgpA _{cat} and Kgp _{cat}	40
2.2.4 Bradford Protein Assay.....	41
2.2.4.1 Macro-assay.....	41
2.2.4.2 Micro-assay.....	42
2.2.5 Activation of Gingipains.....	42
2.2.6 Active Site Titration of Gingipains-R and Gingipains-K.....	42
2.2.7 Tris-Tricine SDS Polyacrylamide Gel Electrophoresis (SDS-PAGE)..	43
2.2.8 Enzyme Assays.....	44
2.3 Results.....	46
2.3.1 Purification of HRgpA, Kgp and RgpB.....	46
2.3.2 Purification of RgpA _{cat} and Kgp _{cat}	55
2.3.3 Characterisation of Purified Enzymes.....	60
2.3.4 Kinetic Characterisation of Proteases.....	60
2.4 Discussion.....	62

CHAPTER 3 Characterisation of the specificity of Arginine-Specific gingipains from <i>Porphyromonas gingivalis</i> reveals active site differences between different forms of the enzymes.....	65
3.1 Introduction.....	66
3.2 Materials and Methods.....	69
3.2.1 Materials.....	69
3.2.2 Fluorescence-Quenched Substrates.....	69
3.2.3 Cultivation of the bacteria and purification of enzymes.....	70
3.2.4 Kinetic Studies.....	71
3.2.5 Modelling.....	72
3.2.6 ELISA of gingipain binding to extracellular matrix proteins.....	72
3.2.7 Analysis of degradation of proteins by SDS-PAGE.....	73
3.2.8 Western Blot analysis of the degradation of human plasma fibrinogen by Arg-gingipains.....	73
3.3 Results.....	75
3.3.1 HRgpA Specificity at P ₂ ' and P ₃ '.....	76
3.3.2 RgpB Specificity at P ₂ ' and P ₃ '.....	76
3.3.3 Modelling of RgpA.....	80
3.3.4 Comparison of the specificity of HRgpA, RgpB, and RgpA _{cat} at P ₂ ' and P ₃ '.....	82
3.3.5 Binding of gingipains to fibrinogen, fibronectin and laminin.....	84
3.3.6 Degradation of fibrinogen by the gingipains.....	86
3.4 Discussion.....	90
CHAPTER 4 Specificity studies of gingipains reveal co-operativity in binding of residues to the active sites of the enzymes.....	96
4.1 Introduction.....	97
4.2 Materials and Methods.....	99
4.2.1 Peptide Inhibitors for Primary screening.....	99
4.2.2 Kinetic Studies.....	99
4.2.3 Peptide Inhibitors for Secondary screening.....	101

4.3 Results.....	102
4.3.1 Primary Screening of gingipain specificity.....	104
4.3.1.1 Specificity of HRgpA	104
4.3.1.2 Specificity of RgpB.....	107
4.3.1.3 Specificity of Kgp.....	110
4.3.1.4 Comparison of HRgpA, RgpB and Kgp.....	113
4.3.2 Secondary screening of gingipain specificity.....	119
4.3.2.1 HRgpA Selectivity.....	120
4.3.2.2 RgpB Selectivity.....	124
4.3.2.3 Kgp Selectivity.....	128
4.4 Discussion.....	132
CHAPTER 5 Final Discussion.....	138
APPENDIX I.....	146
APPENDIX II.....	147
APPENDIX III.....	148
REFERENCES.....	149

LIST OF FIGURES

Figure 1.1. Progression of Periodontal disease.....	5
Figure 1.2. Electron Micrograph of <i>Porphyromonas gingivalis</i> cells.....	8
Figure 1.3. Schematic representations of isoforms of RgpA and RgpB proteases from <i>p. gingivalis</i>	19
Figure 1.4. The various externally and internally directed effects of the gingipains produced by <i>P. gingivalis</i>	23
Figure 1.5. Activation of the Kallikrein/kinin pathway by bacterial proteases to generate bradykinin.....	27
Figure 2.1. Gel filtration chromatography of the acetone precipitate from the culture fluid of <i>P. gingivalis</i> on Sephadex G-150.....	48
Figure 2.2. Affinity chromatography of the high molecular mass fraction from the Sephadex G-150 column on an arginine-Sepharose column.....	50
Figure 2.3. Anion exchange of the low molecular weight fraction from the Sephadex G-150 column on a Mono Q column.....	52
Figure 2.4. Gel filtration chromatography on Superdex-75 of fractions pooled from the first peak eluted from the Mono Q column.....	53
Figure 2.5. Tris-Tricine SDS-PAGE analysis of gingipains HRgpA, Kgp and RgpB.....	54
Figure 2.6. Chromatography of gingipains on Mono Q.....	56
Figure 2.7. Tris-Tricine SDS-PAGE to monitor Purification of RgpA _{cat} and Kgp _{cat}	57
Figure 2.8. Anion exchange chromatography of Kgp _{cat} on Mono Q.....	58
Figure 2.9. Tris-Tricine SDS-PAGE of RgpA _{cat} and Kgp _{cat}	59
Figure 2.10. Kinetic analysis of HRgpA, RgpB, and RgpA _{cat} against Z-Phe-Arg-AMC [Phe-Arg] and for Kgp against Z-Ala-Phe-Lys-AMC [AFK].....	61
Figure 3.1. The crystal structure of RgpB.....	81
Figure 3.2. Comparison of the K_m values of HRgpA, RgpA _{cat} and RgpB towards fluorescent quenched substrates with a glycine or an alanine at P ₃ ' and a histidine and a serine at the P ₂ ' position.....	83

Figure 3.3. Binding of gingipains to (A) Fibrinogen, (B) Fibronectin and (C) Laminin.....	85
Figure 3.4. Degradation of fibrinogen by HRgpA, RgpA _{cat} , and RgpB at 0, 2, 5, 10, 15, 30, 60 and 120 min.....	88
Figure 3.5. Cleavage of fibrinogen in plasma by gingipains.....	89
Figure 4.1. A comparison of inhibition constants of HRgpA, RgpB and Kgp towards peptides with varying amino acids at P1'.....	114
Figure 4.2. A comparison of inhibition constants of HRgpA, RgpB and Kgp towards peptides with varying amino acids at P2'.....	115
Figure 4.3. A comparison of inhibition constants of HRgpA, RgpB and Kgp towards peptides with varying amino acids at P3'.....	116
Figure 4.4. A comparison of inhibition constants of HRgpA, RgpB and Kgp towards peptides with varying amino acids at P2.....	117
Figure 4.5. A comparison of inhibition constants of HRgpA, RgpB and Kgp towards peptides with varying amino acids at P3.....	118
Figure 4.6. Inhibition constants (K_i) for HRgpA with the (A) P2DP3 and (B) P2NP3 series.....	122
Figure 4.7. Inhibition constants (K_i) for HRgpA with the (A) P2DP1' and (B) P2NP1' series.....	123
Figure 4.8. Inhibition constants (K_i) for RgpB with the (A) P2SP3 and (B) P2IP3 series.....	126
Figure 4.9. Inhibition constants (K_i) for RgpB with the (A) P2SP1' and (B) P2IP1' series.....	127
Figure 4.10. Inhibition constants (K_i) for Kgp with the (A) P2AP3 and (B) P2HP3 series.....	130
Figure 4.11. Inhibition constants (K_i) for Kgp with the (A) P2AP1' and (B) P2HP1' series.....	131

LIST OF TABLES

Table 2.1. Purification tables of (A) HRgpA and (B) Kgp.....	47
Table 3.1. Substrate Specificity of HRgpA and RgpB at P ₂ '.....	78
Table 3.2. Substrate Specificity of HRgpA and RgpB at P ₃ '.....	79
Table 4.1. Structure of peptide inhibitors used to investigate the specificity of HRgpA, RgpB and Kgp in the first round of screening.....	99
Table 4.2. The general sequence of the second round of inhibitors used to screen the specificity of the gingipain enzymes.....	101
Table 4.3. Inhibition constants (K_i) for HRgpA against peptide inhibitors with substitutions at P1', P2', P3', P2 and P3.....	106
Table 4.4. Inhibition constants (K_i) for RgpB against peptide inhibitors with substitutions at P1', P2', P3', P2 and P3.....	109
Table 4.5. Inhibition constants (K_i) for Kgp against peptide inhibitors with substitutions at P1', P2', P3', P2 and P3.....	112

ABBREVIATIONS

Abz	2-aminobenzoyl
AFK	Z-Ala-Phe-Lys-7-amino-4-methylcoumarin
AMC	7-amino-4-methylcoumarin
BAPNA	Bz-L-Arg-pNA
BCIP	5-Bromo-4-chloro-3-indolyl phosphate
BSA	bovine serum albumin
DMF	N, N- Dimethylformamide
Dnp	2,4-dinitrophenyl
ELISA	enzyme linked immunosorbent assay
FPRck	Phe-Pro-Arg-chloromethylketone
GCF	gingival crevicular fluid
GEC	gingival epithelial cells
HRgpA	high molecular weight arg-gingipain
IL-8	interleukin-8
KB cells	oral epithelial cells
Kgp	lysine-specific gingipain
Kgp _{cat}	catalytic domain of Kgp
K _i	inhibition constant
LPS	lipopolysaccharide
MMP	matrix metalloprotease
NBT	nitroblue tetrazolium
PAR	protease activated receptor
PBS	phosphate buffered saline

Phe-Arg	Z-Phe-Arg-7-amino-4-methylcoumarin
RgpA	arginine-specific gingipain
RgpA _{cat}	catalytic domain of RgpA
RgpB	low molecular weight arg-gingipain
SDS-PAGE	sodium dodecylsulfate polyacrylamide gel electrophoresis
TBS	tris-buffered saline
TEMED	N, N, N', N', tetramethyl ethylene diamine
TLCK	N α -p-Tosyl-L-lysine-chloromethyl ketone
TNF- α	tumour necrosis factor- α
Z-FKck	benzyloxycarbonyl-Phe-Lys-chloromethylketone

SUMMARY

Periodontal disease is one of the major causes of tooth loss today. It is an inflammatory disease of the gingival and supporting structure of the periodontium. Although there are several bacteria that are associated with the disease, one of the main bacteria associated with the onset of the disease is *Porphyromonas gingivalis*, a Gram-negative bacterium. The bacterium has been shown produce a variety of different virulence factors, including lipopolysaccharides, fimbriae, proteinases and haemagglutinins/adhesins. The proteinases produced by the bacterium are termed "gingipains", and are thought to be very important virulence factors. The bacteria produce arginine- and lysine-specific gingipains, with the two major forms of the gingipains-R being HRgpA, a 95 kDa catalytic domain covalently linked to additional adhesin/haemagglutinin domains and RgpB, a 50 kDa catalytic domain with an Ig-like domain. Kgp, the lysine-specific gingipain is a 105 kDa proteinase composed of a catalytic domain and additional adhesin/haemagglutinin domains like HRgpA. Functions of the gingipains and their role in helping the bacteria grow and colonise within the host environment, makes them important targets in combating the progression of periodontal disease.

The main focus of this study was to determine the specificity of the gingipains, to gain maximum knowledge to aid in the design and development of a specific inhibitor. Initially, work was carried out to purify the individual gingipains, HRgpA, RgpB and Kgp, in their active forms. During the purification of the gingipains, RgpA_{cat}, the catalytic domain of HRgpA, and Kgp_{cat}, the catalytic domain of Kgp, were also purified. The purification of Kgp_{cat} was an important achievement, as this

study was the first to describe its purification from the culture supernatant of *P. gingivalis*. Purified RgpA_{cat} was used in a study to help establish the differences in specificity between HRgpA and RgpB at P₂' and P₃'. The study on the P₂' and P₃' specificity of the gingipains showed that there was a difference in specificity between the two gingipains. Comparison of the catalytic domain of HRgpA and RgpB found the catalytic domains of the two gingipains to be identical except for a four amino acid substitution in the active site of HRgpA compared to RgpB. RgpA_{cat} was used to determine that the difference in specificity was due to the amino acid substitutions in the active site and not the additional adhesin domains. Further experiments to establish the function of the adhesin domains indicated that they helped the gingipains attach to a protein or peptide substrate, but played no role in determining the specificity of the gingipains.

An extensive study to determine the specificity of gingipains-R and gingipain-K was carried out to gain an insight into the effect of residues at each site from P₃- P₃' in a substrate, in order to design and develop specific inhibitors to target the respective gingipains. Primary sets of peptides were screened for specificity of each gingipain at positions P₃- P₃', following which a second series of peptide inhibitors were designed using the results from the first round of screening. The second set of peptides was designed with substitutions of amino acids that were found to be the "best" peptide inhibitors in the first round of screening. The method of design used in the second set of peptides was based on the principle of additivity in the binding of substrate residues to the enzymes, which assumes that each individual enzyme subsite interaction with the substrate would add to the overall interaction in an independent

manner, such that the overall interaction was a simple sum of the interaction at each subsite.

The study reported in this thesis determined not only a difference in specificity of the three gingipains, but also established that mechanism of specificity for gingipains towards substrates is not additive but cooperative. The mechanism of cooperativity is based on the principle that binding of each amino acid in the substrate at each subsite would affect binding of amino acids at other subsites. The finding that the binding mechanism for gingipains towards substrates is cooperative, makes this mechanism difficult to predict for a P_3 - P_3' substrate, as the number of interactive and cooperative effects which might be occurring would be enormous. Thus, the principle of rational inhibitor design is most likely not an appropriate approach for the design of inhibitors for gingipains. Instead, random inhibitor screening appears to be a more suitable approach for the design of peptide inhibitors for the gingipains.

The study in this thesis not only determined the specificity of gingipains and established the underlying principle for the binding of gingipains to substrates, but also determined that rational inhibitor design is most likely not suitable for the gingipains.

CHAPTER ONE

INTRODUCTION

1.0 General

Periodontal infections are recognised as one of the most common diseases affecting humans. Not only does the disease cause great discomfort and economic loss, recent epidemiological evidence suggests that the infection may have systemic consequences, such as cardiovascular diseases and the delivery of pre-term infants and low birth rate babies (Beck *et al.*, 1996; Page, 1998). The oral cavity is home to a menagerie of bacterial species. This makes the etiology of periodontal disease a major focus of oral research. Although over 300 different bacterial species reside in the subgingival niche, only a few of the species are responsible for the initiation and progression of the disease, namely *Actinobacillus actinomycetemcomitans*, *Fusobacterium nucleatum*, *Bacteroides forsythus*, *Campylobacter rectus*, *Prevotella intermedia*, *Treponema vincentii*, *T. denticola*, *T. pectinovorum*, *Selenomonas sputigena* and *Porphyromonas gingivalis* (Holt *et al.*, 1999). Nevertheless, a consistent association has emerged between *Porphyromonas gingivalis* and severe manifestations of periodontal disease (Schenkein, 1998). There are several distinct clinical stages of periodontitis, with the most common form being chronic periodontitis (adult periodontitis), in which *P. gingivalis* has been implicated as the major causative agent (Haffajee and Socransky, 1994).

1.1 Periodontal Disease

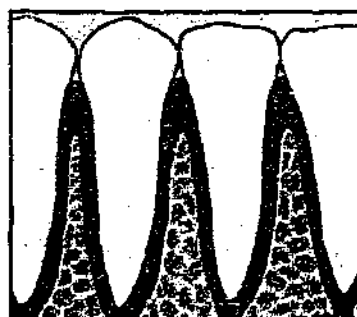
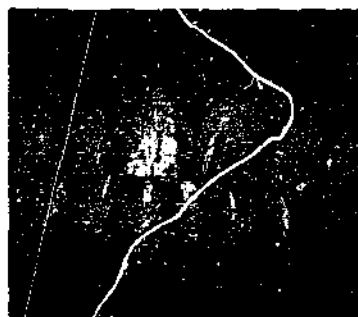
Periodontal disease is a group of inflammatory diseases of the gingiva and the supporting structures of the periodontium. The disease is characterised by a group of infections leading to chronic inflammation of the gingivae termed gingivitis, which results in bleeding of the gums, gingival redness, oedema, increased flow of gingival crevicular fluid (GCF) and changes in the structure of the gingiva (Cimasoni, 1983; Greenstein, 1984), eventually leading to periodontitis. Periodontitis is the destruction of the periodontal tissue, which results in loss of periodontal ligament and connective tissue attachment to the teeth, swollen, red and bleeding gums, and loss of alveolar bone, which leads to the undesired event of tooth loss (Lamont and Jenkinson, 1998) (Fig. 1.1).

Periodontal disease is classified into several distinct clinical stages; chronic periodontitis, aggressive periodontitis, periodontitis as a manifestation of systemic diseases, necrotizing periodontal disease and many other forms (Armitage, 1999; Wiebe and Putnins, 2000). The two main types of periodontal disease are chronic periodontitis and aggressive periodontitis. Both types of the disease are sub-classified into two different stages, localised and generalised, dependent on the severity of the disease. Chronic periodontitis (adult periodontitis) is characterised as occurring mostly in adults 35 years or older, but at times can also be seen in younger people. Chronic periodontitis progresses slowly with occasional bursts of destruction. Aggressive (early-onset) periodontitis is associated with individuals 35 years or younger (Loesche and Grossman, 2001). This form of periodontitis is characterised by rapid loss of attachment and bone destruction (Armitage, 1999).

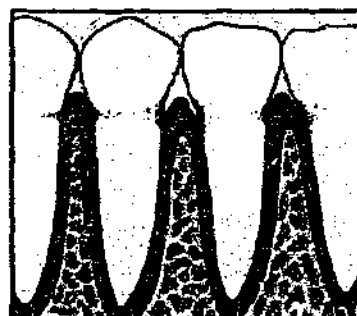
The plaque biofilm that forms on the soft and hard tissue of the oral cavity is a dynamic system that is composed of diverse microbial species. Each periodontopathic bacterial species possesses or secretes a large number of biologically active molecules that act on the host tissue and cause its destruction. In fact, many of the virulence factors have been shown to have a direct pathogenic effect on the host by triggering the host inflammatory system. Many of the host-derived hydrolytic enzymes and destructive cytokines produced in response to the bacterial virulence factors cause destruction of the host tissue and alveolar bone surrounding the tooth root.

P. gingivalis has been shown to be highly prevalent in plaque samples from patients with chronic periodontitis (Loesche and Grossman, 2001). Since the clinical symptoms of periodontal disease are almost always significantly associated with the overgrowth of *P. gingivalis*, along with *B. forsythus* and *T. denticola* in the subgingival plaque, treatments or methods to suppress the growth of the bacteria and eliminate them from the sites of infection have been the focus of many studies (Moore *et al.*, 1982; Socransky and Haffajee, 1992; Socransky *et al.*, 1998; Loesche and Grossman, 2001). Studies carried out have detected an increased prevalence of *P. gingivalis* at diseased periodontal sites (Socransky *et al.*, 1991). The strong association of the bacterium with the progression of the disease makes it an ideal candidate for further investigation.

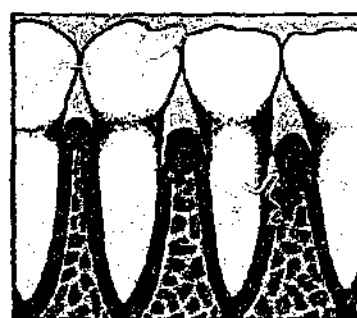
1. Healthy gums
Healthy pink gums



2. Gingivitis
Tender, inflamed and bleeding gums



3. Periodontitis
Receding gums and formation of pockets between the teeth and gums



4. Advanced Periodontitis
Destruction of bone and periodontal ligament resulting in loose teeth.

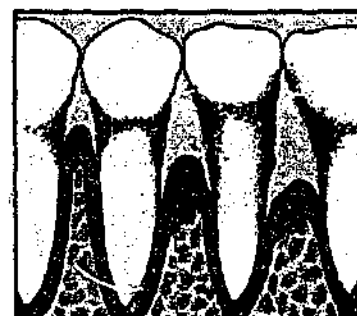


Figure 1.1. Progression of Periodontal disease

Photographs and schematic representation of individuals with 1) Healthy gingiva; 2) Gingivitis; 3) Periodontitis and 4) Advanced Periodontitis (Taken from the website with address http://www.dentalgentlecare.com/picture_gum_disease.htm)

1.2. *Porphyromonas gingivalis*

Porphyromonas gingivalis, a Gram-negative, black-pigmented anaerobe is a non-sporing, non-motile and fimbriated, short rod, which has been implicated as the major etiological agent of periodontal disease (Fig. 1.2). The organism is asaccharolytic, and is dependent on nitrogenous substrates such as amino acids and peptides for nutrition (Shah and Gharbia, 1989). Iron is an essential requirement for the growth of the bacteria, and is acquired mainly from hemin (Bramanti and Holt, 1991). The proteolytic processing of a number of hemin containing compounds such as haemoglobin, myoglobin, haemopexin, haptoglobin and methaemoglobin can also be a source of hemin (Barua *et al.*, 1990; Fujimura *et al.*, 1995). *P. gingivalis* stores hemin on its cell surface, giving rise to the characteristic black-pigmented appearance of its colonies (Genco, 1995).

1.2.1 Virulence factors of *P. gingivalis*

The first step in colonisation and pathogenicity is the adherence of a bacterium to its host. *P. gingivalis* survives and accomplishes colonisation in a hostile environment by producing a variety of virulence factors including lipopolysaccharides, a polysaccharide capsule, haemagglutinins, outer membrane vesicles, fimbriae, hemolysins and proteases (Lamont and Jenkinson, 1998). Virulence factors produced by the bacteria are active against a variety of host proteins and provide mechanisms for successful evasion of the host antimicrobial defenses (Holt *et al.*, 1999). One protective mechanism of the bacterium is the production of a polysaccharide capsule, which functions as an antiphagocytic virulence factor. The thick capsule of various *P. gingivalis* strains is mainly composed of sugars, and functions by increasing

resistance of the bacterium to opsonisation and phagocytosis (Chen *et al.*, 1987; Haapsalo *et al.*, 1989). Although, *P. gingivalis* produces several virulence factors, the main focus of this thesis is the cysteine proteases, which have been shown to be important in the pathogenesis of the bacteria. The fimbriae of this organism, along with the lipopolysaccharides it produces, have been investigated thoroughly, and have also been found to play an important role in the pathogenesis by the bacteria, and thus will be discussed in detail in the following sections.



Figure 1.2. Electron Micrograph of *Porphyromonas gingivalis* cells

Electron micrograph of the bacteria, which are 0.5-0.8 by 1.0-3.5 μm in diameter.

(Taken from <http://www.pgingivalis.org>)

1.2.2 Fimbriae

The primary phase in most bacterial infections is adherence to host tissue (Ofek and Doyle, 1994). *P. gingivalis* possesses fimbriae, which are fine fibrillar appendages arranged in a peritrichous manner on its cell surface. The major fimbriae found on the surface of the bacteria are composed of fimbrillin (FimA), a monomer of 43 kDa (Lantz *et al.*, 1991). Adherence of the bacterium has been shown to be at least partly mediated by the fimbriae, which have affinity for binding to fibroblasts, epithelial cells, and components of the extracellular matrix such as collagen, fibrinogen, fibronectin and laminin (Holt *et al.*, 1999; Lamont and Jenkinson, 1998; Hamada *et al.*, 1994; Naito *et al.*, 1993; Kontani *et al.*, 1996). The binding of the fimbriae is

enhanced by proteases that the bacterium produces, suggesting an important role of the proteases in the initial attachment of the bacteria (Kontani *et al.*, 1996). The fimbriae are capable of eliciting several important host-mediated responses that could cause destruction *in vivo*. Some of the responses include stimulating IL-1, IL-6, IL-8 and tumour necrosis factor- α (Ogawa, 1994).

fimA is directly responsible for many of the adhesive properties of *P. gingivalis*. Binding has been shown to be mediated via a number of domains located throughout the molecule, but clustered predominantly at the C-terminus (Lamont and Jenkinson, 2000). The *fimA* gene occurs as a single copy, with four genes downstream of *fimA* whose products might be associated with the fimbriae (Dickinson *et al.*, 1988; Watanabe *et al.*, 1996). Hemin concentration, temperature and salivary molecules are all factors that affect the expression of *fimA* (Xie *et al.*, 1997). Since the expression of *fimA* can be controlled by various environmental factors, the *fimA* gene could thus assist in the survival of the organism in the oral cavity.

1.2.3 Lipopolysaccharide

Lipopolysaccharide (LPS), a major component of the gram-negative bacterial cell membrane, is a key inflammatory mediator and is recognised by various host defence proteins. LPS produced by *P. gingivalis* evokes highly unusual host cell responses, activating human monocytes by a CD14-dependent mechanism, but inhibiting endothelial cell expression of E-selectin and interleukin 8 (IL-8), which are normally induced by other bacteria (Shapira *et al.*, 1994; Darveau *et al.*, 1995). Although the endotoxic activity of *P. gingivalis* LPS is very low compared to that of LPS isolated from enterobacteria, it is a potent inducer of bone resorption, TNF- α secretion, inhibition of bone formation, polyclonal B-cell activation and fibroblast proliferation (Darveau *et al.*, 1995; Ogawa, 1994; Reife *et al.*, 1995; Mayrand and Holt, 1988; Millar *et al.*, 1986; Mundy, 1991; Aleo, 1980; Shapira *et al.*, 1994).

LPS is estimated to be in the range of 10kDa and larger. The hydrophilic end of the molecule consists of the polysaccharide or O-antigen, which is on the outer surface of the membrane and is exposed to the environment. The hydrophobic end of the molecule is the core region, buried within the outer leaflet, which connects the O-antigen to the hydrophobic end of the molecule or lipid A (Holt *et al.*, 1999).

Although LPS is generally considered a bacterial component that alerts the host to infection, *P. gingivalis* LPS may selectively modify the host response as a means of facilitating colonization.

1.3 Proteases of *P. gingivalis*

Although the primary function of proteases produced by asaccharolytic bacteria such as *P. gingivalis* is to provide peptides for growth, proteases are also directly involved in tissue invasion and destruction by bacteria and in evasion and modulation of host immune defences. The potentially most significant virulence characteristic of *P. gingivalis* is the large number of hydrolytic enzymes that are produced by essentially all of the known strains (Kuramitsu, 1998; Curtis *et al.*, 1999). The majority of these enzymes are exposed at the surface (on the outer membrane) of the bacterium where they can come in contact with host cells and tissues, within the periplasmic space from where they are capable of being transported to the cell surface, and in outer membrane vesicles, which are sloughed from the outer membrane during growth. The bacterial proteases have been shown to degrade the major serum immunoglobulins, which leak into the gingival crevice during the course of inflammation (Kilian, 1981). The proteases also degrade complement C3, which reduces the opsonisation of the bacteria and component C5, which releases the neutrophil attractant C5a, thus causing both retarding and stimulatory effects on inflammation components (Jagels *et al.*, 1996; Schenkein *et al.*, 1995). In addition to degrading immunoglobulins and complement components, the proteases have been shown to degrade various cytokines, including tumour necrosis factor- α , IL-1, IL-6 and IL-8 (Calkins *et al.*, 1998; Darveau *et al.*, 1998; Fletcher *et al.*, 1997; Huang *et al.*, 1998). The proteinases include trypsin-like, cysteine- and caseinolytic proteinases, and two peptidases, glycylopropylpeptidase and glycylopropyldipeptidylaminopeptidase, all of which contribute to the progression of periodontal disease by causing tissue invasion by the bacteria and the destruction of

host cells and tissue (Holt and Bramanti, 1991; Kuramitsu *et al.*, 1995; Travis *et al.*, 1997).

Proteinases constitute one of the largest functional groups of proteins, with more than 560 members actually described (Barrett and Rawlings, 2001). These enzymes play a crucial role in organisms spanning the whole phylogenetic tree, by hydrolysing one of the most important bonds present in biomolecules, the peptide bond (Supuran *et al.*, 2002). The understanding that proteinases are important targets for drug design has led to greater research in the field. Proteinases have been classified according to their catalytic functions or specificity, with four major classes of proteases identified: aspartate, metallo-, serine and cysteine proteases. The terminology used in describing the specificity of a proteinase is based on a model proposed by Schechter and Berger (1970), in which the catalytic site is considered to be flanked on one or both sides by specificity subsites, each being able to accommodate the side chain of a single substrate amino acid residue. The sites are numbered from the catalytic site, S1, S2, ...Sn towards the amino terminus of the substrate, and S1', S2',...Sn' towards the carboxyl terminus. The residues of the substrate they accommodate are numbered P1, P2,...Pn, and P1', P2',...Pn', respectively. The same nomenclature is used for enzyme inhibitors that bind to the catalytic site of an enzyme:

SUBSTRATE/INHIBITOR: -P3-P2-P1*P1'-P2'-P3'-

ENZYME: -S3-S2-S1↑S1'-S2'-S3'-

where the asterisk indicates the scissile peptide bond and the arrow denotes the catalytic site of the enzyme.

The proteases shown to be critical for pathogenesis by *P. gingivalis* are collagenases, aminopeptidases and trypsin-like proteinases (Curtis *et al.*, 1999). Proteases which cleave C-terminal to arginine (Arg-Xaa) or lysine (Lys-Xaa) residues are referred to as "trypsin-like" proteases. They may also be further classified as Arg- or Lys-specific proteases should they in fact be specific for cleavage after only those amino acids. The major trypsin-like enzymes of *P. gingivalis* are members of the cysteine protease family, which includes enzymes of the papain superfamily, clostripain (*Clostridium spp.*), calpains and streptopains (*Streptococcus spp.*). The enzymes from *P. gingivalis* are thus given the name, gingipains. The activity of proteinases belonging to the family of cysteine proteinases depends on a catalytic dyad of cysteine and histidine residues (Barrett and Rawlings, 2001). Cysteine proteinases are divided into 21 different families according to the similarity in their primary structure, especially around the active site (Barrett and Rawlings, 2001). The papain family of cysteine proteinases is the best known with more than 140 members. Although *P. gingivalis* has been shown to produce a variety of different enzymes, the gingipains have received the most interest and have been shown to play a critical role in the progression of periodontal disease.

1.3.1 Importance of gingipains to pathogenesis

The importance of gingipains produced by *P. gingivalis* in the pathogenesis of infection by the bacteria has been shown in several studies. Null mutants of the gingipains, along with studies using gingipains as immunogens, have all demonstrated the importance of the enzymes in the pathogenesis of periodontitis. *P. gingivalis* mutants lacking Arg-gingipain or Lys-gingipain activity were shown to be susceptible to the bactericidal activity of human serum (Grenier *et al.*, 2003). Rajapakse *et al.* (2002) showed that immunization with RgpA-Kgp complexes from *P. gingivalis* W50 strain (Bhogal *et al.*, 1997) restricted periodontal bone loss and colonization by the bacteria in rats.

Curtis *et al.* (2002) found Kgp to be an important factor for both nutrition and virulence of *P. gingivalis*. Isogenic mutants with mutations in *kgp* using the *P. gingivalis* W50 strain were found to have a significant reduction in virulence in murine models. The bacterium containing the Kgp mutant had an inability to lyse erythrocytes, degrade hemin and hence release hemin for accumulation at the cell surface (Curtis *et al.*, 2002). Furthermore, pre-treatment of wild-type cells with a slow reversible Kgp inhibitor 1-(3-phenylpropionyl)piperidine-3(*R,S*)-carboxylic acid-[4-amino-1(*S*)-benzothiazole-2-carbonyl]butyl] amide (A71561) prior to inoculation into mice led to a significant reduction in virulence, emphasising the importance of Kgp inhibitors as a potential therapeutic agent. Similarly, a study carried out to determine the virulence of isogenic mutants of the invasive W50 strain lacking the RgpA, RgpB and Kgp proteinases in a murine lesion model found the Kgp mutant to be least virulent (O'Brien-Simpson *et al.*, 2001). The mutant

displayed a non-pigmented phenotype due to the lack of accumulation of heme, one of the main functions of Kgp in the bacteria. The mutant's reduced ability to accumulate heme, which is essential for the growth and virulence of *P. gingivalis*, was thought to be a major factor in the reduced virulence in the murine lesion model (O'Brien-Simpson *et al.*, 2001).

Several immunization studies have also revealed the importance of the gingipains as potential vaccine candidates. A mouse model immunized with the amino-terminal region of the catalytic domain of gingipain-R was shown to induce a protective response against *P. gingivalis* (Genco *et al.*, 1998). Immunisation with the RgpA-Kgp complex was shown to protect against challenge with invasive and non-invasive strains of *P. gingivalis* in murine models (O'Brien-Simpson *et al.*, 2000). Mice immunized with plasmid DNA carrying *rgpA* were found to be resistant to an invasive *P. gingivalis* W50 challenge and sera from these mice inhibited the binding of the bacteria to a type I collagen sponge (Yonezawa *et al.*, 2001). Immunization of mice with RgpA has been shown to protect against oral bone loss elicited by *P. gingivalis* (Gibson and Genco, 2001).

Thus results from all the above-mentioned studies, along with several others carried out to date, emphasise the important role played by *P. gingivalis* proteases in the progression of the disease caused by the bacteria.

1.3.2 Gingipains

Although research using molecular biological approaches has indicated there might be several cysteine protease activities, there are at least three different genes that code for the main proteolytic activity seen in *P. gingivalis* (Curtis *et al.*, 1999). The genes encode a lysine-gingipain (Lys-gingipain, Kgp) and two arginine-specific gingipains (Rgp's). The first gene to be successfully cloned and fully sequenced was denoted *rgp-1* (arg-gingipain1) from strain HG66 by Pavloff *et al.* (1995), followed by *prpR1* (protease polyprotein Arg1) from strain W50, *rgpA* (arg-gingipain A) from strain 381, *prtR* (protease R) from strain W50 and the recently cloned *hagE* from strain 381 (Aduse-Opoku *et al.*, 1995; Okamoto *et al.*, 1995; Kirsbaum *et al.*, 1995). The only significant variation between these genes is in the coding sequence of *rgpA* in strain 381, due to a large deletion, thus overall there is a high degree of similarity between the translations of the genes (Curtis *et al.*, 1999). The *prtH* gene from strain W83, which was cloned and sequenced in 1994 is now recognised as an *rgp-1* like gene with an alternative start site. All of the above genes represent homologous loci in different strains (Curtis *et al.*, 1999). The deduced translations of the *rgp-1* like genes revealed an N-terminal pro-peptide domain adjacent to a 50 kDa catalytic domain, followed by a long C-terminal extension. Polypeptides with the possible function of hemagglutination were found within the C-terminal extension and were co-purified with the 50 kDa arginine-specific protease from the culture supernatant of *P. gingivalis* (Pike *et al.*, 1994; Aduse-Opoku *et al.*, 1995). Proteolytic processing of the large initial translation product of the gene results in the formation of multifunctional arginine-specific protease/heamagglutinin molecules (Curtis *et al.*, 1999).

The *rgpB* gene from strain 33277 was the first complete sequence to appear in the database, followed by the *rgp-2* gene from strain HG66, *prtR11* (W50) and the incomplete sequence of *prtK2* (W50) (Nakayama *et al.*, 1997; Mikolajczyk-Pawlinska *et al.*, 1998; Slakeski *et al.*, 1998; Rangarajan *et al.*, 1997). Thus the main arginine-specific proteases of *P. gingivalis* are derived from the products of two highly related genes, one of which has the potential to code for a polypeptide(s) with an additional role in hemagglutination/adherence (Curtis *et al.*, 1999).

The *prtP* from strain W12 was the first gene from the lysine-specific protease family to be cloned (Barkocy-Gallagher *et al.*, 1996), followed by *kgp* from strains HG66 and 381, *kgp* (*381*)-*hagD* from strain 381, *prtP* from strain W83 and *prtK* from W50 (Lewis *et al.*, 1998; Pavloff *et al.*, 1997; Okamoto *et al.*, 1996; Slakeski *et al.*, 1999). The genomic organization of these loci is similar to that of the arginine-specific protease/haemagglutinin gene, with the translation product consisting of a propeptide and catalytic domain followed by a long C-terminal extension (Curtis *et al.*, 1999). Translations of the deduced lysine protease genes indicated they are highly homologous, particularly in the propeptide and catalytic domains, with significant differences in the C-terminal region. The lysine-specific protease activity of *P. gingivalis* is derived from a single gene product and *kgp*, *prtK* and *prtP* represent homologous loci in different strains (Curtis *et al.*, 1999). A single gene encodes the *P. gingivalis* lysine-specific protease, the product of which is specific only for lysyl peptide bonds.

A comparison of the translation of the *rgp-1* gene with the lysine-specific protease sequence shows considerable conservation within the adhesin/haemagglutinin domain and also the pro-peptide and catalytic domain, indicating a common ancestral gene for the two loci (Curtis *et al.*, 1999).

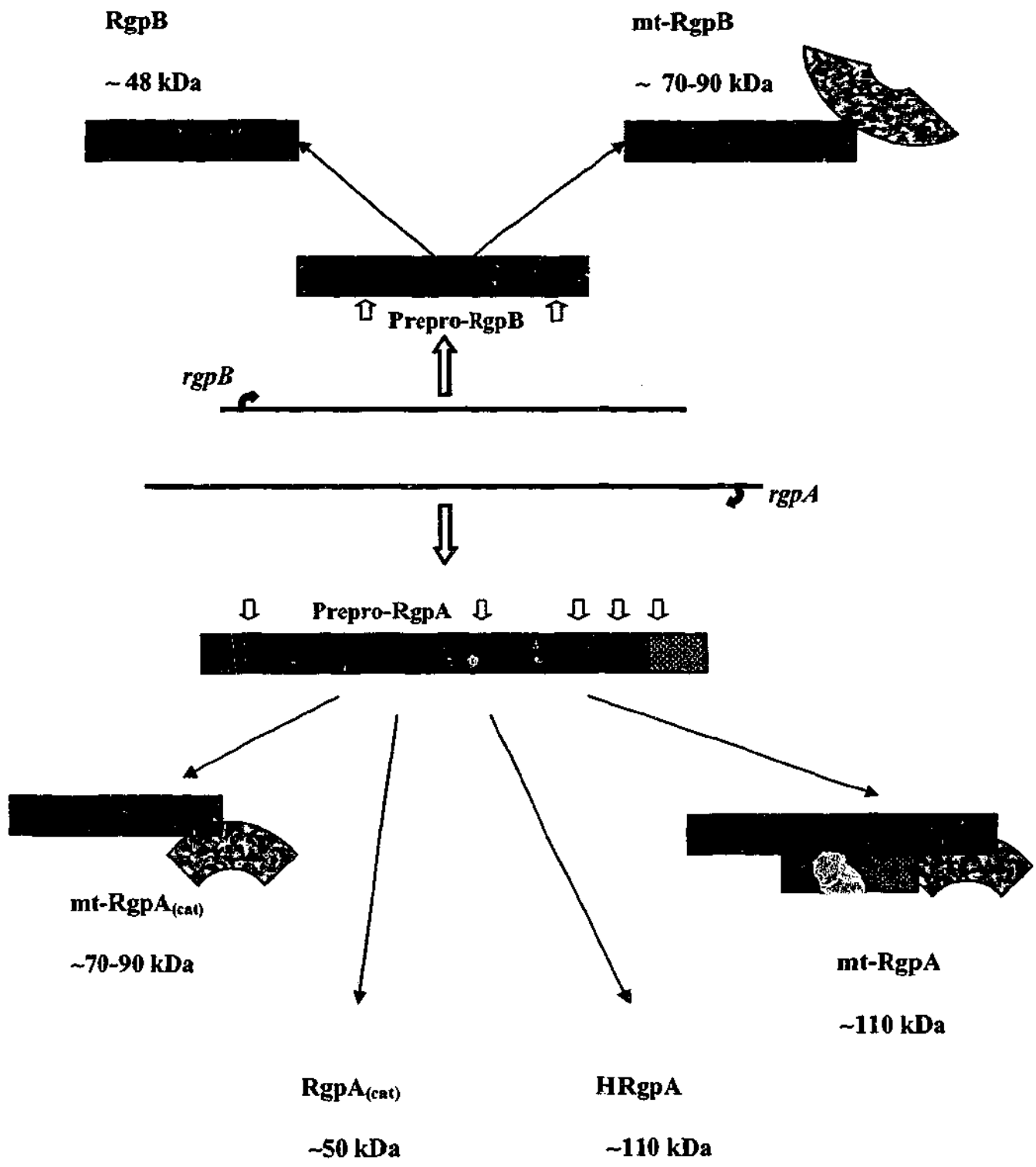


Figure 1.3. Schematic representations of isoforms of RgpA and RgpB proteases from *P. gingivalis*. (Adapted from Travis and Potempa, 2000)

1.3.2.1 Arginine-Specific Gingipains

As elucidated above, the major arginine-specific protease activity of *P. gingivalis* is derived from two separate genes. The arginine-specific protease (denoted RgpA) with the associated haemagglutinin/adhesin subunits is encoded by the *rgp-1* gene, while the *rgp-2* gene encodes the arginine-specific protease without the additional adhesin subunits (denoted RgpB). A complex processing pathway of the two genes produces many isoforms of the arg-specific proteases as seen in Figure 1.3. The proteases exist as (a) heterodimers or multimers of RgpA comprising the catalytic domain non-covalently bonded with the adhesin(s), (b) monomeric, soluble forms of the catalytic domains of RgpA and RgpB and (c) membrane-bound monomers containing large post-translational modifications (Chen *et al.*, 1992; Pike *et al.*, 1994; Slakeski *et al.*, 1998; Rangarajan *et al.*, 1997). The 110 kDa, high molecular weight complex consisting of the catalytic and additional adhesin/haemagglutinin domains is referred to as HRgpA. The catalytic domain of RgpA is referred to as RgpA_(cat) and the membrane associated modified form of this monomer is mt-RgpA_(cat) (mt refers to membrane type). RgpB and mt-RgpB are the terms used for the soluble and membrane bound forms of the *rgpB*-derived proteases.

The crystal structure of RgpB has given a better insight into the general structure of the gingipain's catalytic domain (Eichinger *et al.*, 1999). The shape of the RgpB molecule has been described as a crooked one root "tooth", made up of a 'crown' formed by the catalytic domain, while the 'root' is made by the last 84 residues resembling an immunoglobulin superfamily domain (Ig-like domain) (Eichinger *et al.*, 1999). The catalytic domain of RgpB is subdivided into A- and B- sub-domains,

with each subdomain consisting of a central β -sheet and additional hairpins flanked by helices on either side. The surface of the active-site of RgpB is relatively flat, except for the entrance 'hole' to the S1 pocket and is characterised by a negative electrostatic potential (Eichinger *et al.*, 1999). The active-site of RgpB was found to be similar to that of caspases, with an identical arrangement of the secondary structure elements along with an almost identical active-site, indicative of a close evolutionary relationship. Although the function of the Ig-like domain in RgpB is not obvious, it could represent the attachment site for anchoring the haemagglutinin domains in the high molecular weight Rgps. The determination of the three dimensional structure of RgpB, is a unique tool, offering the possibility of design and development of a selective, potent inhibitor against the gingipain, using the principle of rational inhibitor design.

1.3.2.2 Lysine-Specific Gingipain

The proteases specific for lys-X peptide bonds are products of a single gene, referred to as *kgp* (Lys-gingipain). The high molecular weight form of the *kgp*-derived enzymes, comprising catalytic and adhesin subunits is referred to as Kgp. For the monomeric and membrane type isoforms, a similar system to that used for *rgpA*-derived proteases is used (Figure 1.3).

1.4 Pathological potential of the gingipains

There is building evidence that suggests that *P. gingivalis* depends on the gingipains for growth and proliferation. Gingipains account for at least 85% of the total proteolytic activity produced by the bacterium (Potempa *et al.*, 1997). These trypsin-like enzymes that were originally isolated and partially characterized by Sawyer *et al.* (1962), have been found to have a variety of functions as seen in Figure 1.4, which not only help the bacteria to avoid host defences, but also to obtain sufficient nutrients for its growth and proliferation. The proteases also have the ability to activate the host immune responses, which aids the bacteria not only by causing destruction of the host tissue and assisting in host evasion, but in the process also indirectly aids in nutrient accumulation.

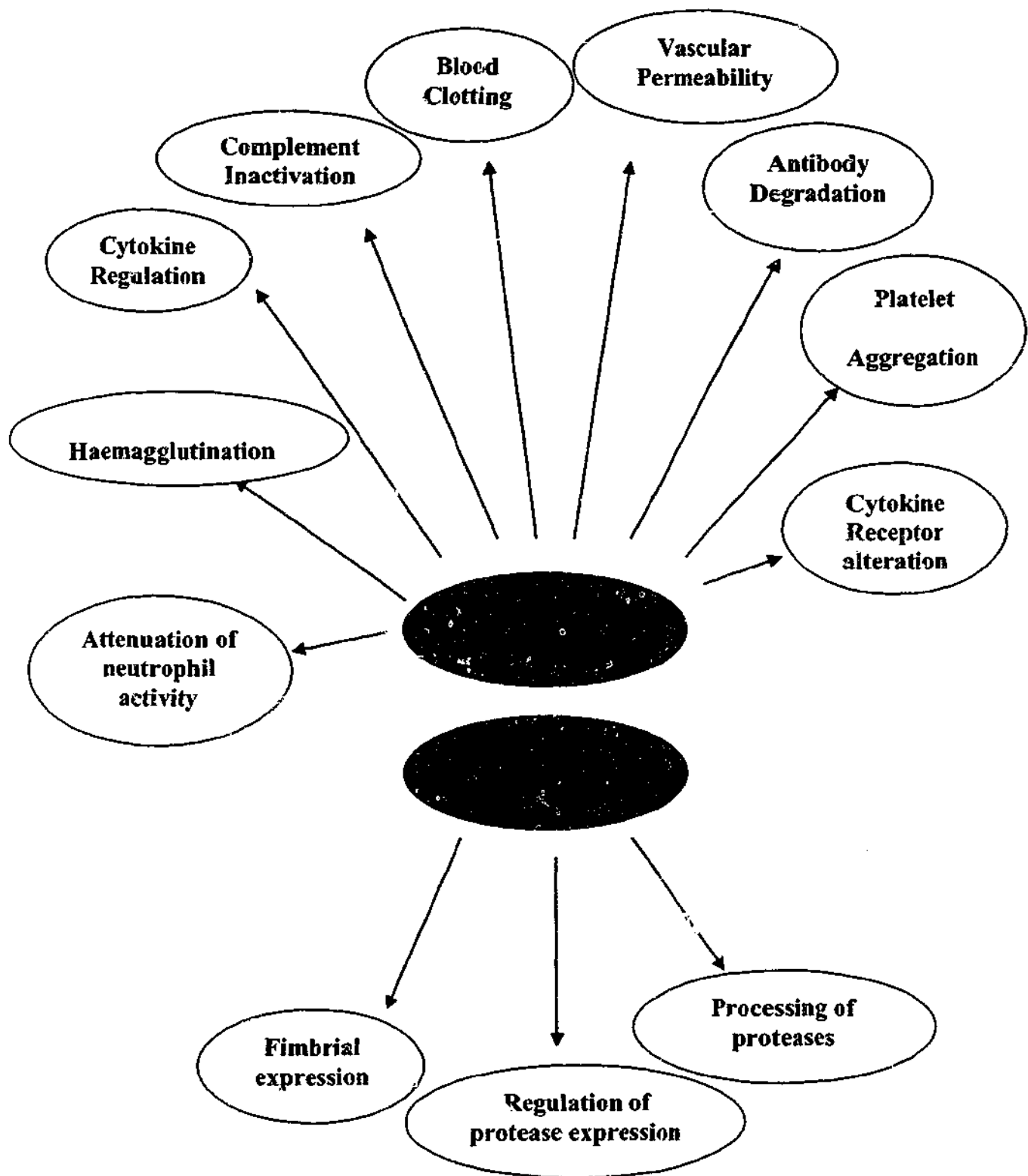


Figure 1.4. The various externally and internally directed effects of the gingipains produced by *P. gingivalis*.

1.4.1 Degradation of Connective Tissue components

The major components of connective tissue are collagen, elastin and proteoglycans, and the abnormal turnover of these components is the hallmark of disease development in the progression of both pulmonary emphysema and periodontitis, where in both cases there is significant tissue destruction (Travis *et al.*, 1994). The formation of periodontal pockets is caused by the degradation of collagen containing tissue at the dento-epithelial junction, where the redox levels are considerably low, favouring the growth of anaerobic species (Harrington, 1996). In general, the breakdown of collagen and elastin during tissue destruction is mainly due to host proteases released by phagocytic cells such as neutrophils and macrophages that are recruited to the site of infection (Sorsa *et al.*, 1992; Potempa and Travis, 1996; Travis and Potempa, 2000). *Porphyromonas gingivalis* proteases thus act not only via direct, but also indirect mechanisms to cause the damage to connective tissue. The bacterial proteases induce the expression of matrix metalloprotease (MMP) enzymes from host cells, which have the capacity to degrade most of the extracellular matrix proteins, including collagen, laminin and fibronectin (Birkedal-Hansen, 1993). The gingipains-R in particular can activate human fibroblasts to express MMP-1 and human neutrophils to express MMP-8 (Sorsa *et al.*, 1992). The proteases also induce plasminogen activator to be secreted from fibroblasts, which leads to plasmin activation of pro-collagenases (Birkedal-Hansen, 1993).

1.4.2 Deregulation of Complement Pathway

A primary innate host response for defence against pathogen invasion is the activation of the complement pathway. Proteases produced by *P. gingivalis* are capable of activating or deregulating the complement pathway, thereby assisting in the evasion of the host defences. The gingipain-R enzymes cleave the complement factor C5 very efficiently at two specific sites, to yield the potent chemotactic factor C5a, causing an infiltration of phagocytic cells into the site (Wingrove *et al.*, 1992).

1.4.3 Deregulation of the Kallikrein/Kinin System

Bacterial pathogens require a continuous source of nutrients for their growth and proliferation. Most bacterial species acquire their nutrients through the degradation of connective tissue or plasma exudate. An alternative method used by *P. gingivalis* involves the acquisition of plasma proteins via the deregulation of the kallikrein/kinin system, which results in the over production of bradykinin, a peptide hormone that increases capillary permeability (Maeda and Yamamoto, 1996; Travis *et al.*, 1995). Bradykinin is released from high molecular weight kininogen due to proteolytic cleavage by plasma kallikrein (Maeda and Yamamoto, 1996). Kallikrein is a serine protease produced by the action of a number of host proteases (plasmin, Hageman factor, etc.) on its zymogen precursor prekallikrein (Kaplan *et al.*, 1997). The kinin generating pathway can be activated at many steps, as can be seen in figure 1.5 and many bacterial pathogens can activate the kallikrein/kinin cascade to release bradykinin from kininogens. This usually leads to the development of oedema, which is the main source of plasma exudate, caused by the binding of bradykinin to receptors on vascular endothelial cells, contraction of the cells and leaky capillaries

(Imamura *et al.*, 1994; Travis and Potempa, 2000). Gingipain-R is capable of releasing bradykinin and inducing vascular permeability by directly activating plasma prekallikrein (Imamura *et al.*, 1994).

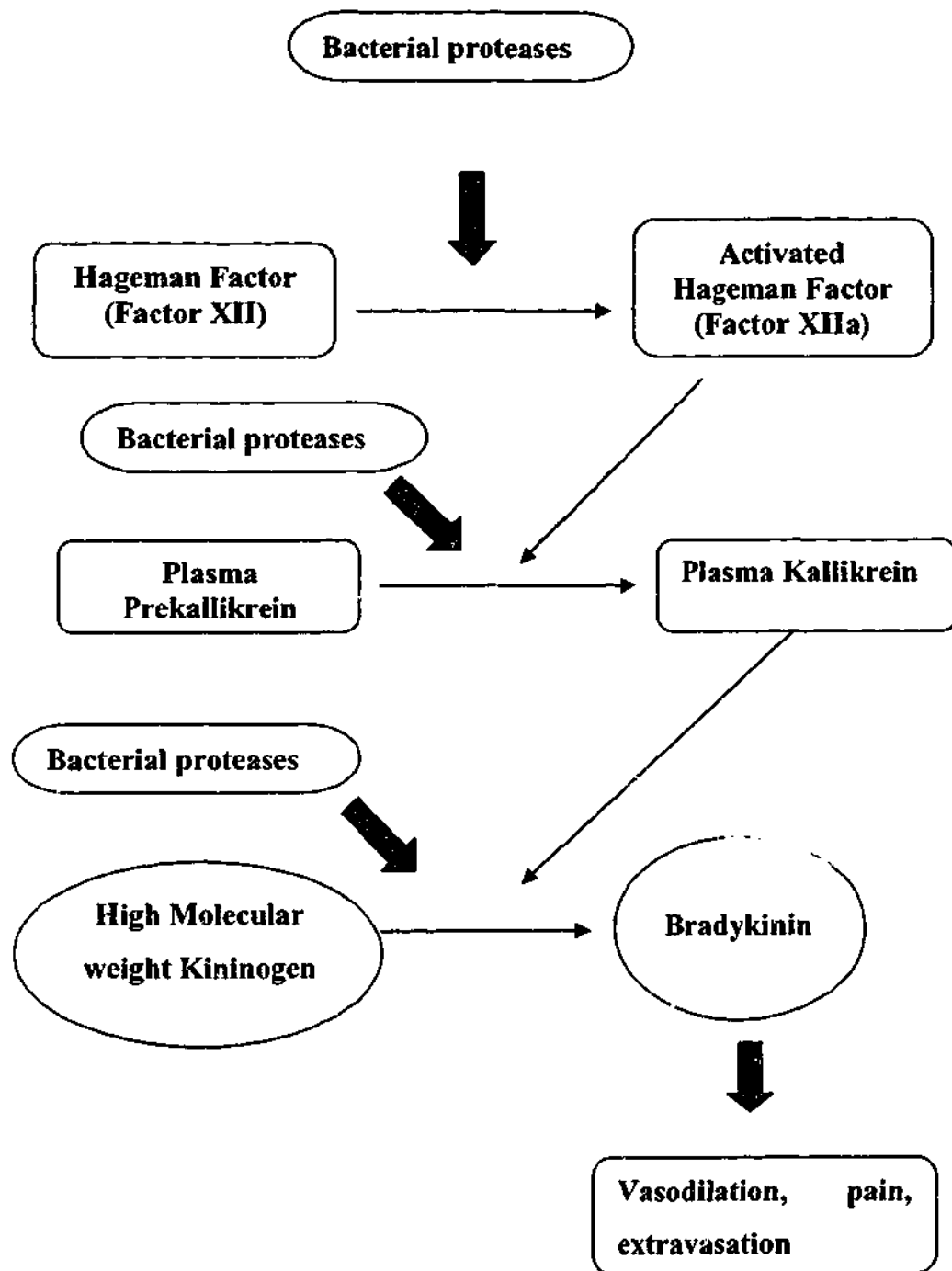


Figure 1.5. Activation of the Kallikrein/kinin pathway by bacterial proteases to generate bradykinin (adapted from Maeda and Yamamoto, 1996).

1.4.4 Deregulation of the coagulation pathway

Gingipains are capable of disrupting the coagulation pathway by activating various coagulation factors. Gingipains-R can activate factor X, prothrombin and protein C, and cause deregulation of the coagulation pathway (Imamura *et al.*, 1997; Hosotaki *et al.*, 1999). The arg-specific gingipains cleave the zymogen forms of these three coagulation factors at the same sites that are recognised during normal coagulation events to produce active forms of the proteases. Essentially, it seems that any bacterial protease with the cleavage specificity at Arg-X residue may have the potential to activate the coagulation pathway. Clostripain, a cysteine protease produced by *Clostridium histolyticum*, with specificity for cleaving after arginine residues, is also an activator of the coagulation cascade (Bordusa *et al.*, 1997).

1.4.5 Cytokines

Porphyromonas gingivalis and its virulence factors induce the expression of a variety of cytokines and chemokines. The bacterial proteases have been shown to not only stimulate an increase in the production, but also degrade proinflammatory cytokines such as IL-1 β , TNF- α , IL-1, IL-6 and IL-8, which not only promote inflammation, but also stimulate tissue destruction and bone resorption (Calkins *et al.*, 1998; Darveau *et al.*, 1995; Fletcher *et al.*, 1997; Huang *et al.*, 1998). Cytokines promote the release of tissue-derived enzymes, such as the MMPs, which are destructive to the extracellular matrix and alveolar bone (Offenbacher, 1996; Birkedal-Hansen, 1993).

1.5 Protease Activated Receptors

Proteases produced by *P. gingivalis* have been shown to cleave and activate protease-activated receptors. Protease-activated receptors (PARs), are a family of seven transmembrane G-protein-coupled receptors, activation of which is initiated by the cleavage of the N-terminus by a serine protease, resulting in the generation of a tethered ligand that interacts with loop-2 of the receptor. Binding of the tethered ligand to the body of the receptor leads to its activation. To date four PARs have been identified, PAR-1, PAR-2, PAR-3 and PAR-4 (Coughlin, 2000). PAR-1, -3 and -4 are cleaved by thrombin (Ishihara *et al.*, 1997; Kahn *et al.*, 1998; Xu *et al.*, 1998). PAR-2 is activated by trypsin and mast cell tryptase (Dery *et al.*, 1998). RgpB cleaves and activates protease-activated receptor 2 (PAR-2) on human neutrophils (Lourbakos *et al.*, 1998) and PAR-1 and PAR-2 on oral epithelial cells (KB cells) (Lourbakos *et al.*, 2001a). Protease activation of the PARs in oral epithelial cells has also been shown to stimulate production of IL-6, a powerful proinflammatory cytokine (Lourbakos *et al.*, 2001a). These studies indicate another mechanism via which proteases produced by *P. gingivalis* mediate inflammatory responses in the host system. Arg-gingipains, HRgpA and RgpB have also been shown to activate PAR-1 and -4 expressed on the surface of human platelets and cause platelet aggregation (Lourbakos *et al.*, 2001b). Since gingipains are known to activate the coagulation cascade, activation of PARs on platelets has been suggested as the underlying mechanism stimulating cellular processes linking periodontitis and cardiovascular disease (Lourbakos *et al.*, 2001b).

1.6 Bacterial Invasion of cells

Invasion of cells by *P. gingivalis* has been proposed as a possible mechanism of pathogenesis in periodontal disease and more recently cardiovascular disease (Loesche, 1993; Dorn *et al.*, 1999; Deshpande *et al.*, 1999). The initial event in many infectious diseases involves adhesion of pathogens to host tissue, followed by subsequent invasion. Upon invasion of cells, bacterial pathogens establish an intracellular niche for survival and replication, which provides an increased concentration of protein substrates for their metabolic pathways and also protects them from the host's defence mechanisms (Dorn *et al.*, 2001). Primary gingival epithelial cells (GEC) and the oral epithelial KB cells have been used to research the invasive nature of the periodontopathogen (Lamont and Yilmaz, 2002). The invasion of GEC cultured from basal epithelium extracted from gingival explants by *P. gingivalis in vitro* was first reported in 1992 by Lamont *et al.* *Porphyromonas gingivalis* is capable of invading endothelial cells, and the intracellular bacteria are contained in vacuoles that resemble autophagosomes, a mechanism which allows the bacteria to evade host defenses and provide nutrients for its growth and survival (Dorn *et al.*, 2001).

1.7 Aims of Study

Gingipains produced by *P. gingivalis* have been shown to be involved in tissue invasion and destruction, evasion of host defenses and modulation of the host immune system during infection and inflammation (Travis *et al.*, 1995). Involvement of gingipains in critical processes such as colonization and evasion of host immune defenses, all of which lead to the pathogenesis by *P. gingivalis*, makes the proteases important and attractive targets for the development of novel types of antibiotics, since inhibition of such critical enzymes would presumably lead to the death of the invading pathogen (Supuran *et al.*, 2002). In order to develop a selective and potent inhibitor that will target only the respective gingipains, the substrate/inhibitor specificity of the gingipains needs to be determined. Amongst the active site residues of most proteolytic enzymes, positions S3-S3' are important in determining the specificity of the enzyme. The design of a selective target inhibitor requires an extensive knowledge of the specificity of an enzyme towards its peptide substrate/inhibitor. Determining the substrate specificity of an enzyme, and narrowing down the selectivity of amino acids at particular subsites in the substrate/inhibitor, would lead to acquisition of information that would aid in the design and development of a specific inhibitor.

The main aim and underlying theme of this study was to determine the specificity of gingipains-R and gingipain-K, to gain maximal knowledge of their active site in order to design and develop selective inhibitors to target the enzymes. In order to carry out the specificity studies, pure and active forms of the gingipains were an essential requirement, and thus one of the first aims of this study was to purify the

gingipains HRgpA, RgpB and Kgp, and the catalytic domains RgpA_{cat} and Kgp_{cat}. Initially, the specificity of HRgpA and RgpB at P2' and P3' was investigated in this study. Results from this study also led to an investigation into the role of adhesin domains in the specificity of gingipains. Following the first specificity study, more extensive study was carried out to determine the specificity of HRgpA, RgpB and Kgp. The principle of rational inhibitor design was used, where a primary set of peptide inhibitors were designed, developed and screened against the gingipains. Following the first round of screening, the underlying principle of additivity, which is used in rational drug design, was used to design a second series of inhibitor peptides were designed and screened. The second series of peptide inhibitors were designed using the results from the first round of screening, where the 'best' amino acid residue was substituted for the 'best' subsite in the substrates for each respective gingipain.

The initial specificity study in Chapter 3, on HRgpA and RgpB at P2' and P3' indicated a difference in the specificity of the two gingipains. Modelling of the catalytic domain of HRgpA on the catalytic domain of RgpB, showed the catalytic domains of the two gingipains to be identical, except for a four amino acid substitution in the active site of HRgpA compared to RgpB. The difference in specificity observed was thus thought to be due to the additional adhesin domains in HRgpA, leading to the use of RgpA_{cat}, the catalytic domain of HRgpA, lacking the additional adhesin domains to further investigate this finding. Specificity of HRgpA and RgpA_{cat} was found to be similar, indicating that it is most likely the four amino acid substitution in the active site of gingipains-R, which is responsible for the

difference in specificity. Investigation into the role of adhesin domains on the influence of specificity indicated that the adhesins do not influence the substrate specificity of the gingipains, but most likely aid the gingipains in binding to the substrate.

The specificity study of the gingipains, spanning the P3-P3' positions on a substrate, which utilised the principle of rational design of inhibitors, found that the specificity of the gingipains towards residues in a substrate is cooperative, rather than additive. This finding was contrary to the assumption which is generally made for the specificity of most proteolytic enzymes, where the specificity towards a substrate is thought to be additive. The finding has broadened our understanding of the specificity and mechanism underlying the binding affinity of gingipains to substrates/inhibitors and will help in the selection of a more appropriate method of peptide inhibitor design for the enzymes in the future. The method of random screening of peptide inhibitors used by Curtis *et al.* (2002), appears to be a more suitable method of designing and developing inhibitors for gingipains.

Development of a specific inhibitor that binds irreversibly to the gingipains and blocks their enzymic activity, without having any effects on the human cells, would provide an exquisite means of blocking the activities of the enzymes that are crucial to the pathogenesis of *P. gingivalis*-associated periodontal disease. Development of such inhibitors will lead to the emergence of novel treatment therapies for periodontal disease in the early twenty-first century.

CHAPTER TWO

PURIFICATION OF GINGIPAINS-R AND GINGIPAIN-K AND THEIR CATALYTIC DOMAINS $RgpA_{cat}$ AND Kgp_{cat} FROM *PORPHYROMONAS* *GINGIVALIS*

2.1 Introduction

The gram-negative anaerobic bacterium *Porphyromonas gingivalis* produces potent cysteine proteinases that have been shown to be important virulence factors. The organism produces two main types of proteinases, an arginine-specific proteinase, gingipain-R and a lysine-specific proteinase, gingipain-K (Kuramitsu, 1998). There are two main forms of gingipain-R, HRgpA, a 95kDa high molecular weight form and RgpB, a 50kDa low molecular weight gingipain (Curtis *et al.*, 1999). HRgpA is composed of a catalytic subunit non-covalently bound to additional adhesin subunits, whereas RgpB is composed of the catalytic domain and an associated Ig-like domain. The lysine-specific gingipain, Kgp, has a molecular weight of 105kDa and, like HRgpA, is composed of a catalytic subunit covalently linked to additional adhesin subunits.

Methods for the purification of the gingipains from the culture fluid of strain HG66 of *P. gingivalis* have been established previously by Pike *et al.* (1994) and have been used with great success. In this chapter, the previously used method of purification was used to purify HRgpA, RgpB and Kgp (Pike *et al.*, 1994) and the catalytic domains of HRgpA and Kgp were also purified. The main theme of this thesis is the determination of the substrate specificity of the gingipains, which requires highly pure forms of each of the enzymes. The importance of RgpA_{cat}, the catalytic domain of HRgpA is evident in Chapter 3, where it was used to determine the difference in the specificity between HRgpA and RgpB. This study also succeeded in producing a purified form of Kgp_{cat}, the catalytic domain of the lysine-specific gingipain, Kgp, from the culture supernatant of *P. gingivalis*. Fujimura *et al.* (1998) previously

purified a 48 kDa form of Kgp from membrane extracts of *P. gingivalis* strain ATCC 33277, but the molecular weight of the enzyme was not confirmed by gel filtration. Although Kgp_{cat} was not directly used in the studies carried out as part of this thesis, the purification of the catalytic domain in its active form may help further studies to elucidate the roles of the adhesin and catalytic subunits of Kgp.

2.2 Materials and Methods

2.2.1 Materials

Bz-L-Arg-pNA (BAPNA) was purchased from Sigma (Sydney, Australia). Z-L-Lys-pNA was from Novabiochem (Darmstadt, Germany). Protein molecular weight markers for SDS-PAGE (Wide Range Molecular Weight Standards) were purchased from Novex (Australia).

2.2.2 Cultivation of Bacteria

The HG66 strain of *P. gingivalis* was used in this study and was a gift of Dr. Jan Potempa (Department of Biochemistry and Molecular Biology, University of Georgia, Athens, USA) and was grown as described previously (Chen *et al.*, 1992). The bacteria was cultivated in broth containing 3% (w/v) trypticase soy broth, 0.5% (w/v) yeast extract and 0.5 mg/ml (w/v) cysteine-HCL in distilled water, with the pH adjusted to 7.4. The broth was boiled and then cooled on ice and gassed with 85% N₂, 10% H₂ and 5% CO₂. The flask was sealed with a rubber bung and wire and autoclaved. The broth was stored at room temperature until use, 1 µg/ml hemin and 1 µg/ml menadione were added to it, along with a 1% inoculation of culture stock using a syringe and the culture was grown for 2 days at 37°C.

2.2.3 Purification of Enzymes

The gingipains-R, HRgpA and RgpB and the gingipain-K, Kgp, were purified from the HG66 strain culture fluid as described previously (Pike *et al.*, 1994; Potempa *et al.*, 1998).

2.2.3.1 HRgpA, Kgp and RgpB

The whole culture (2000 ml) was centrifuged (6000 x g, 30 min, 4°C) to obtain the culture supernatant (1930 ml). Chilled acetone (one and a half times the volume of the culture fluid) was added to the supernatant over a 15 min period of time, with the temperature of the supernatant being maintained below 0°C at all times using an ice/salt bath. The mixture was centrifuged (6000 x g, 30 min, -15°C) and a precipitate was obtained, which was redissolved in 190 ml of 20 mM Bis-Tris-HCl, 150 mM NaCl, 5 mM CaCl₂, 0.02% (w/v) NaN₃, pH 6.8 (Buffer A). The precipitate was dialysed against Buffer A containing 1.5 mM 4,4'-dithiopyridine disulfide for 4 hrs, followed by two changes of buffer A overnight at 4°C. The dialysed fraction was centrifuged (27,000 x g, 30 min, 4°C), and concentrated to 100 ml by ultrafiltration using an Amicon PM-10 membrane. The concentrated fraction was applied to a Sephadex G-150 column (90 x 5 cm, 1800 ml), which had been equilibrated with buffer A, and the column was run at 30 ml/h (1.5 cm/h). Fractions (10 ml) were collected and assayed for Arg- and Lys-specific activity using BAPNA and Z-L-Lys-pNA (Fig. 2.1). Two peaks of activity were obtained with the two substrates, with the high molecular mass peak containing activity against both BAPNA and Z-L-Lys-pNA. The fractions from the first peak were pooled and dialysed against two changes of 50 mM Tris-HCl, 1 mM CaCl₂, 0.02% (w/v) NaN₃, pH 6.5 (Buffer B) overnight at 4°C.

An arginine-Sepharose column (1.5 x 30 cm, 15 ml) was equilibrated with buffer B and the dialysed high molecular weight fraction was applied to the column at a flow rate of 30 ml/h. The column was washed with two column volumes of buffer B,

following which a 500 mM NaCl step gradient was applied in buffer B. The column was washed with 500 mM NaCl until the baseline for activity against both substrates was zero, following which it was equilibrated with buffer B. A gradient of 0-750 mM L-lysine was applied to the column (over a total volume of 80 ml), followed by re-equilibration of the column with buffer B and a second gradient of 100 mM L-arginine over a total volume of 80 ml. Fractions of 5 ml were collected and assayed for activity. A major peak of activity against Z-L-Lys-pNA was eluted with the lysine gradient and activity against BAPNA was eluted with the arginine gradient. Fractions from the peak were pooled and dialysed against two changes of 20 mM Bis-Tris-HCl, 1 mM CaCl₂, 0.02% (w/v) NaN₃, pH 6.4 (buffer C) and concentrated to 10 ml using an Amicon PM-10 membrane. The pH of buffer C used initially was 7.3, but this was found to reduce the activity of the enzymes, rendering them almost inactive. The pH of the buffer was decreased to 6.4 to help retain the activity of the enzymes. The purified enzyme samples were used for specificity studies.

The second peak of activity against BAPNA from the Sephadex-G150 column was concentrated to 1 ml and dialysed against two changes of buffer C. The dialysed fraction was applied to a Mono Q column equilibrated with buffer C at a flow rate of 30 ml/h, using a Bio Rad HR chromatography system. The column was washed with two column volumes of buffer C, following which a 200 mM NaCl gradient was applied to the column. A single peak with activity against BAPNA was collected. Fractions with activity were pooled, dialysed against two changes of 25 mM Bis-Tris, 1 mM CaCl₂, 0.02% (w/v) NaN₃, pH 6.5, overnight, and applied to a Superdex 75 gel filtration column (10 x 300 mm, 24 ml). A monomeric form of

RgpB with activity against BAPNA was eluted with 200 mM NaCl, 25 mM Bis-Tris, 1 mM CaCl₂, 0.02 % (w/v) NaN₃, pH 6.5 buffer (flow rate 30 ml/h) and used for specificity studies.

2.2.3.2 Purification of RgpA_{cat} and Kgp_{cat}

Purification of the catalytic domain of HRgpA and Kgp was carried out in Professor James Travis' laboratory in the Department of Biochemistry and Molecular Biology at the University of Georgia. The low molecular weight peak with activity against BAPNA from the Sephadex G-150 column was pooled, concentrated and dialysed against two changes of 50 mM Bis-Tris, 1 mM CaCl₂, pH 6.5 (Buffer D) overnight and loaded onto a DE-52 cellulose column, equilibrated with buffer D at a flow rate of 20 ml/h. The column was washed with buffer D until the A₂₈₀ baseline fell to zero, following which a gradient of 0-200 mM NaCl was applied in a total volume of 200 ml. Fractions (5 ml) were collected and assayed for activity against BAPNA and Z-L-Lys-pNA for activity. Some activity was found in the void volume of the column against both of these substrates. The void volume was pooled and dialysed overnight against two changes of 25 mM Bis-Tris, pH 6.3 overnight. The fraction containing the void volume was applied to a Mono Q column and the column was eluted at 30 ml/h. A gradient of 0-1.5% (15 mM) 1 M NaCl was applied to the column for a 10 min period, following which a gradient of 1.5%-100% of 1 M NaCl was applied to the column. Fractions of 0.6 ml were collected and assayed against BAPNA and Z-L-Lys-pNA for activity. Three peaks were collected from the column, the first peak, which corresponded to the void volume of the column, contained activity against Z-L-Lys-pNA. Peak two, which was eluted with 15 mM

NaCl, contained activity against BAPNA, as did peak three, which was eluted in the second gradient step (Fig. 2.6). Fractions from the individual peaks were pooled, and samples from each peak were electrophoresed on SDS-PAGE (Fig. 2.7). The pooled fractions from each peak were loaded onto the Mono Q under the same conditions as mentioned above (Fig. 2.8). The void volume contained activity against Z-L-Lys-pNA and two separate peaks with activity against BAPNA were eluted by the salt gradient (Fig. 2.9).

2.2.4 Bradford Protein Assay

The Bradford dye-binding assay (Bradford, 1976) was used for protein determination. The dye reagent consisted of Serva blue G dye (50 mg) dissolved in 88% (v/v) phosphoric acid (50 ml) and 99.5% (v/v) ethanol (23.5 ml), made up to 500 ml with distilled water. The solution was stirred for 1 hr filtered through Whatman No.1 paper and stored in a brown bottle. A standard protein solution of bovine serum albumin (BSA) 1 mg/ml was made up in distilled water and used to construct a standard curve (0-25 μ g). The standard solution was diluted to 100 μ g/ml for the micro-assay.

2.2.4.1 Macro-assay

The standard BSA solution (0-25 μ l), or sample protein, was diluted to a final volume of 100 μ l with distilled water to give the desired protein concentration (0-25 μ g). Dye reagent (5 ml) was added and the mixture was vortexed. The colour was allowed to develop for 2 min and the A_{595} of the solution was read in 3 ml plastic cuvettes, against a blank of distilled water for the standard proteins, or buffer

for the samples. Assays for the standard curve were carried out in triplicate at five concentrations of BSA.

2.2.4.2 Micro-assay

Protein standard (0-50 μ l of the 100 μ g/ml solution or 1-5 μ g) or sample was diluted to 50 μ l with distilled water or buffer. Dye reagent (950 μ l) was added, and mixed well. The colour was allowed to develop for 2 min after mixing, and the A_{595} was read in 1 ml plastic cuvettes, as mentioned above. Assays for the standard curve were carried out in triplicate at five concentrations of BSA.

A linear standard curve was plotted and results for the protein samples were calculated from the equation generated by linear regression analysis of the standard curve.

2.2.5 Activation of Gingipains

Gingipains were activated by incubation in activation buffer containing 0.2 M Tris-HCl, 1 mM CaCl_2 , 10 mM cysteine, pH 7.6, at 37°C for 10 min.

2.2.6 Active Site Titration of Gingipains-R and Gingipains-K

The concentration of active gingipain-R (HRgpA, RgpB and RgpA_{cat}) was calculated by active site titration of the enzyme with the inhibitor FPRck, and for gingipain-K (Kgp and Kgp_{2cat}) the active concentration was calculated by active site titration of the enzyme with Z-FKck (Potempa *et al.*, 1997). The enzyme was diluted to 2 μ M (using

the Bradford protein estimation assay) in buffer containing 0.2 M Tris-HCl, 1 mM CaCl₂, 10 mM cysteine, pH 7.6 and incubated at 37°C for 5 min. Immediately, prior to use, the inhibitor FPRck or Z-FKck was diluted (0-1.25 μM) in 0.1 M HEPES, 2 mM CaCl₂, pH 7.6. Aliquots (95 μl) of the different inhibitor concentrations were added to 5 μl of activated enzyme and incubated at room temperature for 15 min. Aliquots (5 μl) of the enzyme-inhibitor mix were taken and assayed against 0.5 mM BAPNA in the case of gingipain-R and Z-L-Lys-pNA in the case of gingipain-K. Assays were carried out in 96 well plates and were read at 405 nm using a microplate reader (Thermomax, Molecular Probes).

2.2.7 Tris-Tricine SDS Polyacrylamide Gel Electrophoresis

(SDS-PAGE)

The purity of enzyme samples was monitored by Tris-Tricine SDS-PAGE using the Tris-HCl/Tricine buffer system (Shägger and von Jagow, 1987). The gels were poured and electrophoresed using the Mini-Protean II dual slab gel apparatus (Bio-Rad). The resolving gel was made with 1.1 M Tris-HCl, pH 8.45, 0.1% (w/v) SDS, 18% (w/v) acrylamide, 2.2% (w/v) bis-acrylamide, 0.2% (w/v) ammonium persulphate, 0.15% (v/v) TEMED and milli-Q water to a final volume of 6.76 ml. The stacking gel contained 0.6 M Tris-HCl, pH 8.45, 0.02% (w/v) SDS, 4% (w/v) acrylamide, 0.2% (w/v) bis-acrylamide, 0.1% (w/v) ammonium persulphate, 1.9% (v/v) TEMED and milli-Q water to a final volume of 6 ml. The gels were electrophoresed using anode buffer containing 0.2 M Tris-HCl, pH 8.9 and cathode buffer containing 0.1 M Tris-HCl, 0.1 M Tricine, 0.1% SDS, pH 8.25 in the tank. The gels were electrophoresed at a constant voltage of 250 V. Samples were

loaded in 10x sample buffer containing 0.1 M Tris-HCl, pH 6.8, 10% (w/v) SDS, 0.04% (w/v) bromophenol blue, 20% (v/v) glycerol, 5.5% (v/v) β -mercaptoethanol.

Gels were stained in a staining solution containing 40% (v/v) methanol, 10% (v/v) acetic acid and 0.25% (v/v) Coomassie brilliant blue dye. The gel was then destained in destaining solution containing 40% (v/v) methanol and 10% (v/v) acetic acid.

2.2.8 Enzyme Assays

The arginine- or lysine-specific activity of enzymes was measured using 0.5 mM of BAPNA and Z-L-Lys-pNA substrates, respectively. Samples were incubated in activation buffer for 10 min at 37°C in a 96-well plate, following which substrate was added to the samples and the amidolytic activity was measured at 405 nm using a microtitre plate reader (Thermomax, Molecular Probes). The K_m values for HRgpA, RgpB and RgpA_{cat} were determined using the fluorescent substrate Z-Phe-Arg-amino-4-methylcoumarin (Z-Phe-Arg-AMC) and for Kgp using the substrate Z-Ala-Phe-Lys-amino-4-methylcoumarin (Z-Ala-Phe-Lys-AMC). K_m values were measured at 37°C using substrates at concentrations ranging from 1-50 μ M, with a final concentration of active site titrated enzyme of 1.0 nM in 0.2 M Tris-HCl, 5 mM CaCl₂, 10 mM cysteine, 0.1 M NaCl, pH 7.6. The assay was performed in a total volume of 200 μ l in microplates and was carried out in triplicate. Enzyme solution (100 μ l) was added to 100 μ l of substrate solution and the initial velocity was recorded (usually over 10 min) at 7 different substrate concentrations at 370/460 nm on a fluorescent plate reader (FLUOstar Galaxy,

BMG Labtechnologies, Australia). The initial velocities were plotted against substrate concentrations and the lines were fitted to a single site binding equation using non-linear regression analysis in the program Graph Pad Prism®. The K_m values were derived from the fitted line.

2.3 Results

2.3.1 Purification of HRgpA, Kgp and RgpB

The gingipains, HRgpA, Kgp and RgpB were all purified from whole culture fluid of *P. gingivalis*. The enzymes were initially precipitated out of the culture supernatant using the method of acetone precipitation. The acetone precipitate of the culture fluid contained high arginine- and lysine-specific activity, with the total activity for gingipains-R being slightly higher than that for Kgp (Table 2.1). Following the acetone precipitation step, the precipitate was resuspended in buffer and the high molecular weight gingipains, HRgpA and Kgp, were separated from the low molecular weight RgpB by gel filtration chromatography on a Sephadex-G150 column. The gel filtration chromatography of the precipitate solution yielded only two active peaks as opposed to the three peaks obtained by Pike *et al.* (1994) (Fig. 2.1). The two active peaks obtained contained the same activity as seen by Pike *et al.* (1994), where the high molecular mass peak contained both lysine- and arginine-specific activity (Kgp and HRgpA) and the low molecular mass peak contained only measurable arginine-specific activity (RgpB) (Fig. 2.1).

(A) HRgpA

Fraction	Volume (ml)	Protein (mg)	Total Activity (units)	Specific Activity (units/mg)	Purification -fold	Yield %
Culture	1930	22,154	163,000	7.3	1	100
Supernatant						
Acetone	100	378	120,000	317	43	74
Precipitate						
Sephadex- G150	215	62	64,000	1032	141	39
Arginine- Sephadex	30	16	28,000	1750	239	17

(B) Kgp

Fraction	Volume (ml)	Protein (mg)	Total Activity (units)	Specific Activity (units/mg)	Purification -fold	Yield %
Culture	1930	22,154	144,000	6.5	1	100
Supernatant						
Acetone	100	378	98,000	259	43	68
Precipitate						
Sephadex- G150	215	62	54,000	870	133	37
Arginine- Sephadex	45	9.8	22,000	2244	345	15

Table. 2.1 Purification tables of (A) HRgpA and (B) Kgp. Units for total activity are in mmol/min.

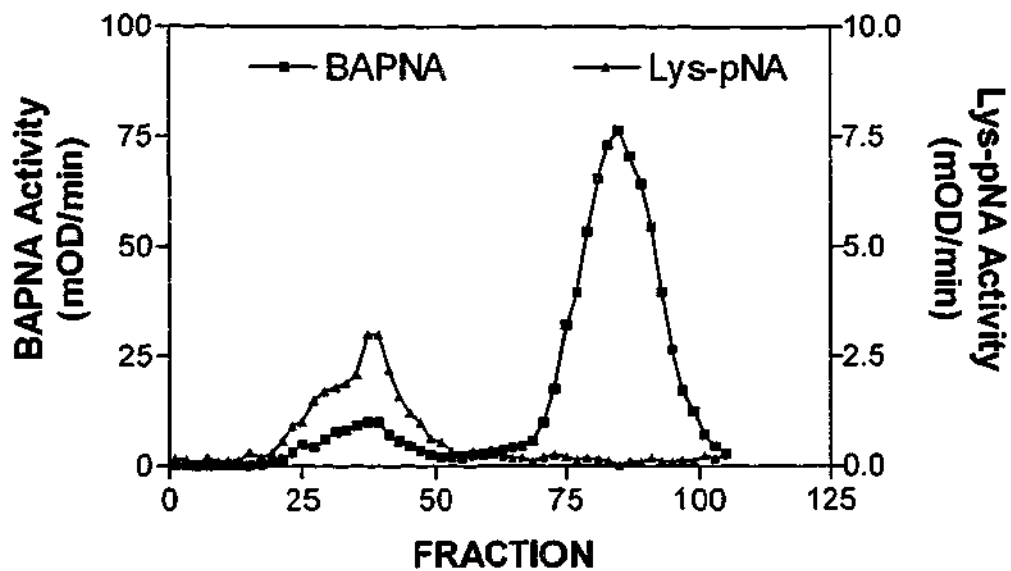


Figure 2.1 Gel filtration chromatography of the acetone precipitate from the culture fluid of *P. gingivalis* on Sephadex G-150. The acetone precipitate was applied to a Sephadex G-150 column (90 x 5 cm, 1800 ml) and fractions (10 ml) collected were assayed for activity against BAPNA and Z-L-Lys-pNA. Proteins were eluted with 20 mM Bis-Tris-HCl, 150 mM NaCl, 5 mM CaCl₂, 0.02% (w/v) NaN₃, pH 6.8, at a flow rate of 30 ml/h.

The high molecular weight peak, in which HRgpA and Kgp were eluted, was pooled and applied to an arginine-Sepharose column. The two high molecular weight gingipains, HRgpA and Kgp, were eluted in two separate peaks on this column (Fig. 2.2). A NaCl step gradient was initially used to remove relatively inactive material, following which a lysine gradient was used to elute Kgp and an arginine gradient was used to elute HRgpA. Kgp was eluted in a slightly larger volume (45 ml) compared to HRgpA (30 ml). The yield of the individual gingipains obtained from this step of purification was very similar, with a 17% yield for HRgpA and a 15% yield for Kgp.

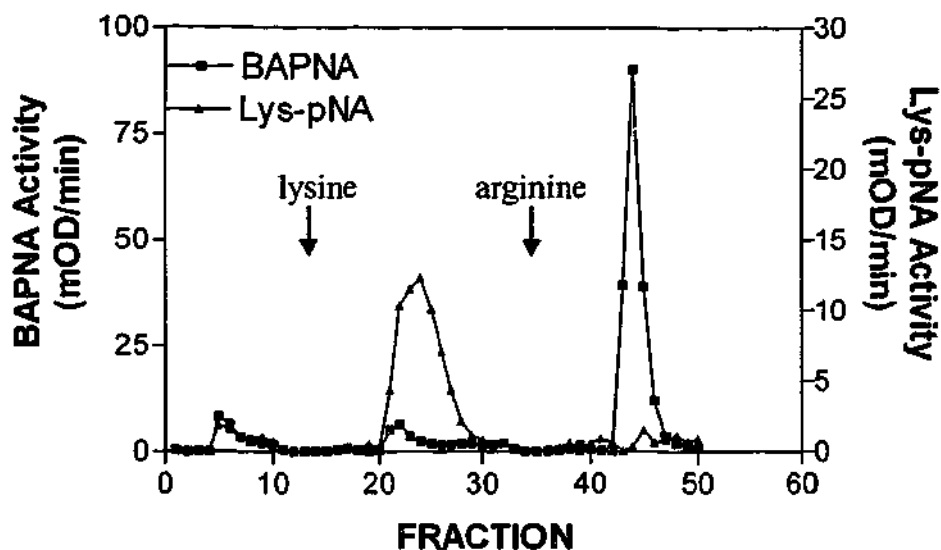


Figure 2.2. Affinity chromatography of the high molecular mass fraction from the Sephadex G-150 column on an arginine-Sepharose column. Fractions (5 ml) were collected and assayed against BAPNA and Z-L-Lys-pNA. Proteins were eluted with 50 mM Tris-HCl, 1 mM CaCl₂, 0.02% (w/v) NaN₃, pH 6.5, at a flow rate of 30 ml/h from the column (1.5 x 30 cm, 15 ml). Arrows indicate the application of gradient of lysine and arginine, as detailed in the text (section 2.2.3.1).

RgpB was purified from the low molecular mass peak obtained from the gel filtration chromatography as previously described (Potempa *et al.*, 1998). The low molecular mass peak eluted from the Sephadex G-150 column was subjected to anion exchange chromatography on a Mono Q column (Fig. 2.3), where a peak with activity against BAPNA was eluted (peak1, Fig 2.3). This peak was pooled and applied to a Superdex-75 gel filtration column for further purification to yield a pure form of RgpB (Fig. 2.4). Purity of RgpB, and HRgpA and Kgp was monitored on Tris-Tricine SDS-PAGE gels (Fig. 2.5). Electrophoresis of these proteins yielded bands at 50, 44, 27 and 14 kDa for HRgpA, 60, 44, 27 and 17 kDa for Kgp and a single 50 kDa band for RgpB.

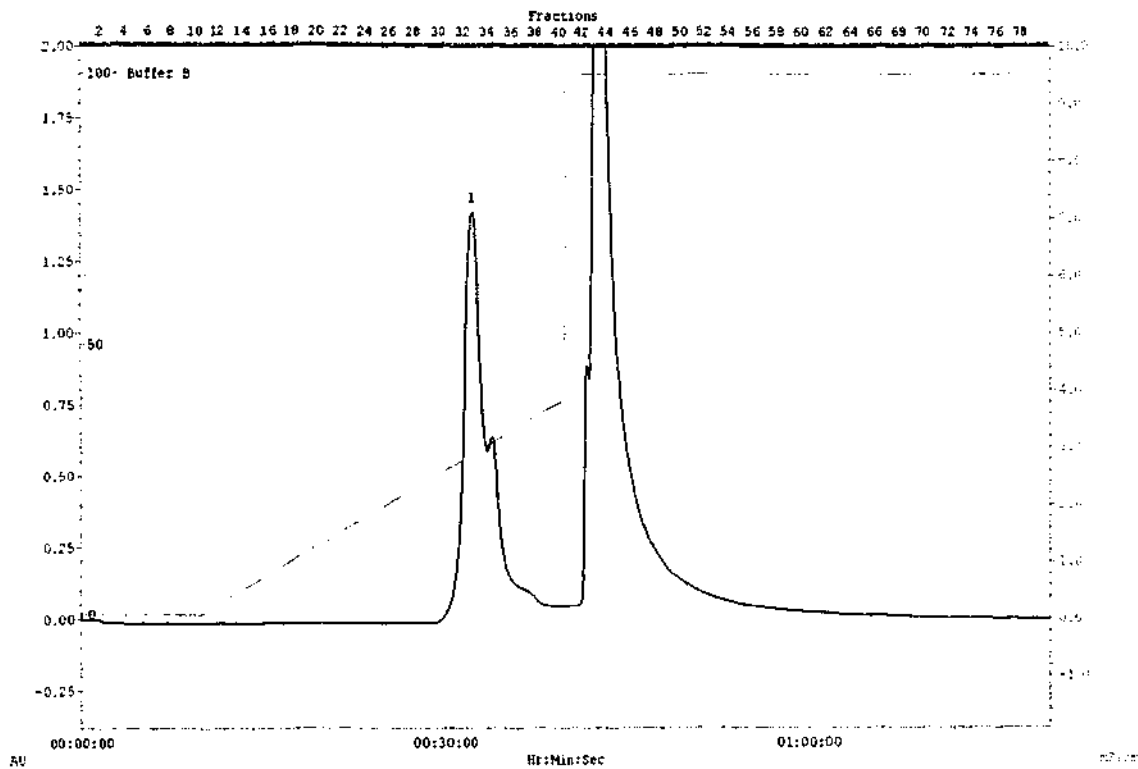


Figure 2.3. Anion exchange of the low molecular weight fraction from the Sephadex G-150 column on a Mono Q column. A gradient of 0-500 mM NaCl in 25 mM Bis-Tris, 1 mM CaCl₂, 0.02% (w/v) NaN₃, pH 6.5 buffer was applied to the column (7 x 52 mm, 2 ml) at a flow rate of 30 ml/h, to elute the proteins. Fractions collected (1 ml) were assayed against BAPNA for activity. (—) Absorbance at 280 nm. (---) NaCl gradient.

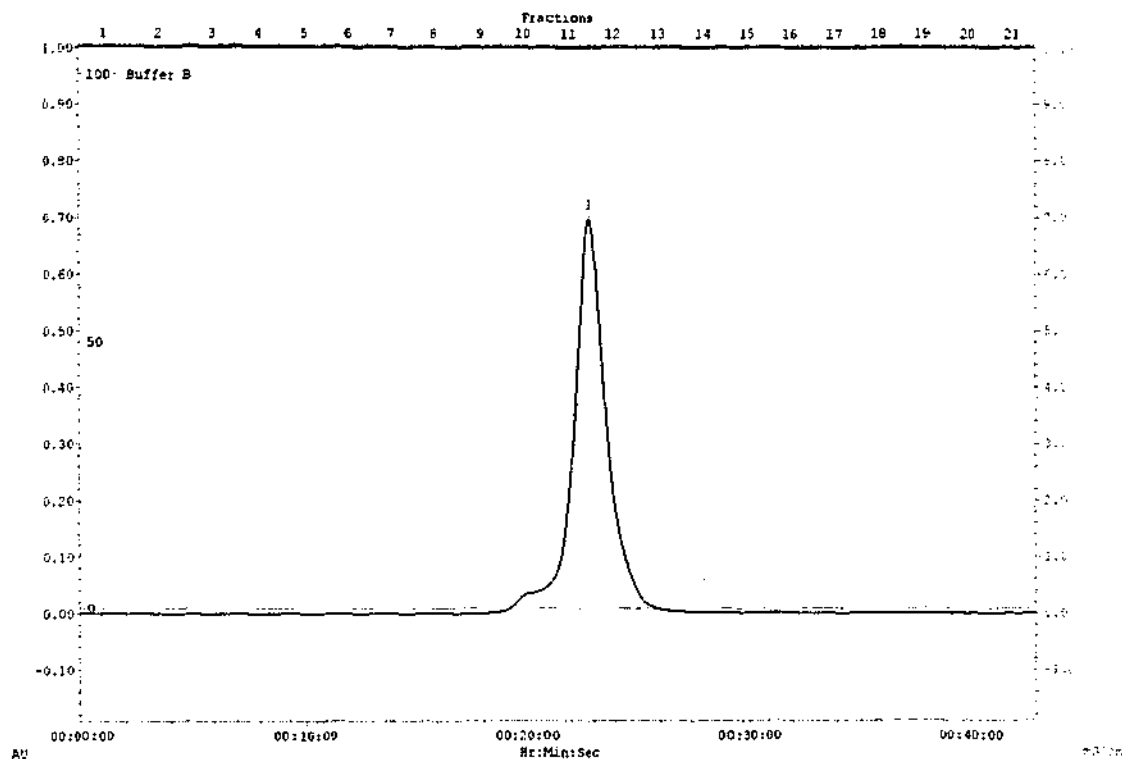


Figure 2.4. Gel filtration chromatography on Superdex-75 of fractions pooled from the first peak eluted from the Mono Q column. Fractions were eluted with 200 mM NaCl, 25 mM Bis-Tris, 1 mM CaCl₂, 0.02 % (w/v) NaN₃, pH 6.5 buffer at a flow rate of 30 ml/h, from the column (10 x 300 mm, 24 ml) and assayed for activity against the substrate BAPNA. (-) Absorbance at 280 nm.

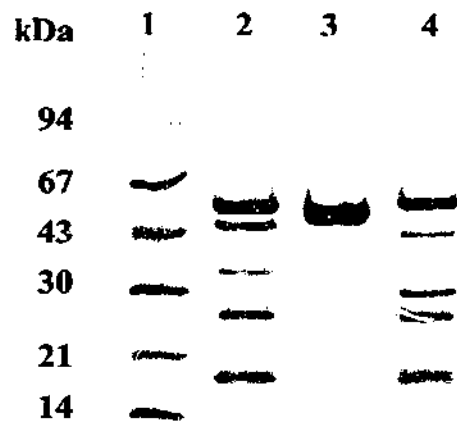


Figure 2.5. Tris-Tricine SDS-PAGE analysis of gingipains HRgpA, Kgp and RgpB. Samples of HRgpA, RgpB and Kgp were boiled in reducing loading buffer and electrophoresed on a Tris-Tricine gel. Lane, (1) Molecular weight markers (shown in kDa to the left of the gel picture), (2) HRgpA, (3) RgpB and (4) Kgp.

2.3.2 Purification of RgpA_{cat} and Kgp_{cat}

RgpA_{cat} and Kgp_{cat} were both purified from the culture supernatant of *P. gingivalis* as described for the whole gingipains. Fractions from the low molecular weight peak eluted on the Sephadex G-150 column with activity against BAPNA (containing RgpB) and very little activity against Z-L-Lys-pNA were pooled and applied onto a DE-52 cellulose column. Fractions from the collected void volume contained BAPNA and Z-L-Lys-pNA activity (results not shown). The fractions containing the void volume were pooled and applied to a Mono Q anion-exchange column. Three peaks with activity were eluted from this column (Fig. 2.6), the first peak contained activity against the Z-L-Lys-pNA substrate only and was eluted in the void volume. The remaining two peaks were eluted in the NaCl gradient and contained only BAPNA activity. Sample aliquots from pooled fractions of the peak were electrophoresed on Tris-Tricine-SDS-PAGE gels to monitor purity (Fig. 2.7). Fractions from the first peak containing only Z-L-Lys-pNA activity were pooled and applied to the Mono Q column once again. A single peak was eluted with a 1 M NaCl gradient, containing only Z-L-Lys-pNA activity (Fig. 2.8). Fractions from the peak containing highly purified Kgp_{cat} were pooled and stored at -80°C. Samples from the pooled fractions of the two peaks containing only BAPNA activity were electrophoresed on a Tris-Tricine-SDS-PAGE gel and were found to contain pure forms of RgpA_{cat} (Fig. 2.9).

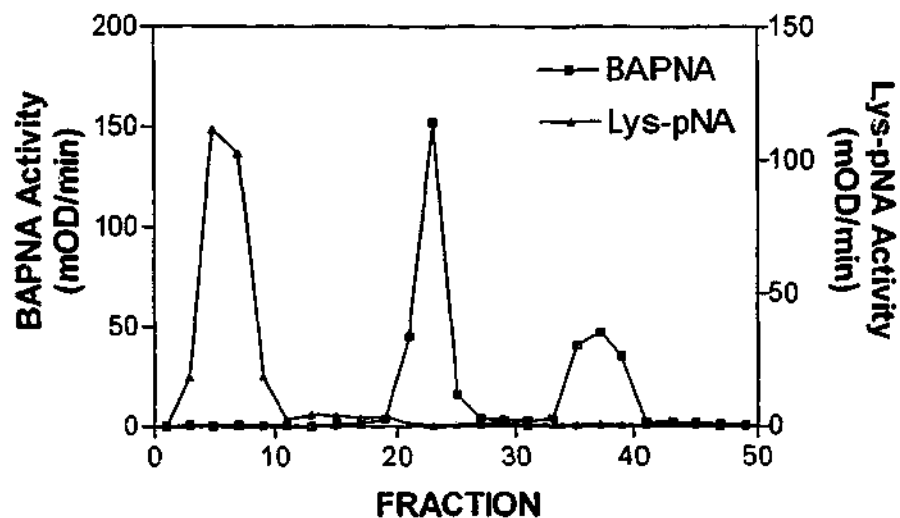


Figure 2.6. Chromatography of gingipains on Mono Q. Fractions from the void volume of the DE-52 cellulose column were chromatographed on Mono Q. A gradient of 0-200 mM NaCl was applied and three peaks were eluted. Fractions were assayed for activity against BAPNA and Z-L-Lys-pNA.

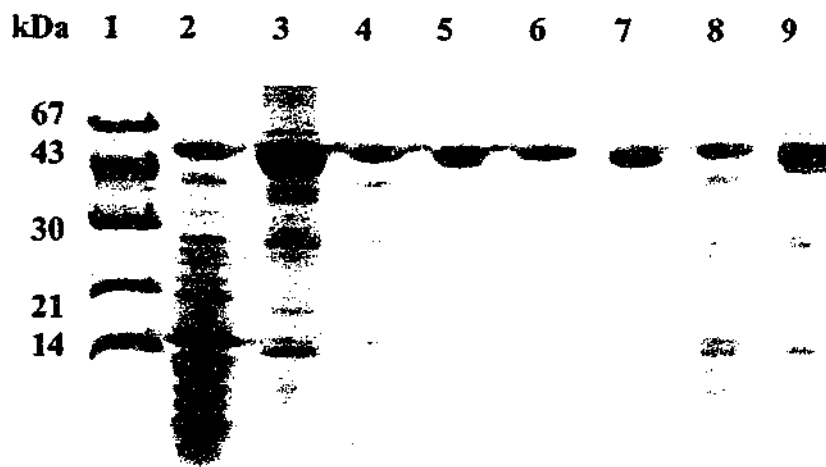


Figure 2.7. Tris-Tricine SDS-PAGE to monitor Purification of RgpA_{cat} and Kgp_{cat}. Aliquots were taken from pooled fractions of the void volume from the DE-52 column, and the three peaks eluted from the Mono Q column. Samples in lanes 1, 3, 5, 7 and 9 were run under non-reducing conditions and samples in lanes 2, 4, 6 and 8 were run under reducing conditions. Lanes (2) and (3), fraction from the void volume of De-52 column; (4) and (5), sample from peak 2 eluted off Mono Q column, containing RgpA_{cat}; (6) and (7), sample from peak 3 eluted off Mono Q column, containing RgpA_{cat}; (8) and (9), samples eluted in peak 1 from Mono Q column, containing Kgp_{cat}. Lane 1, molecular weight standard markers.

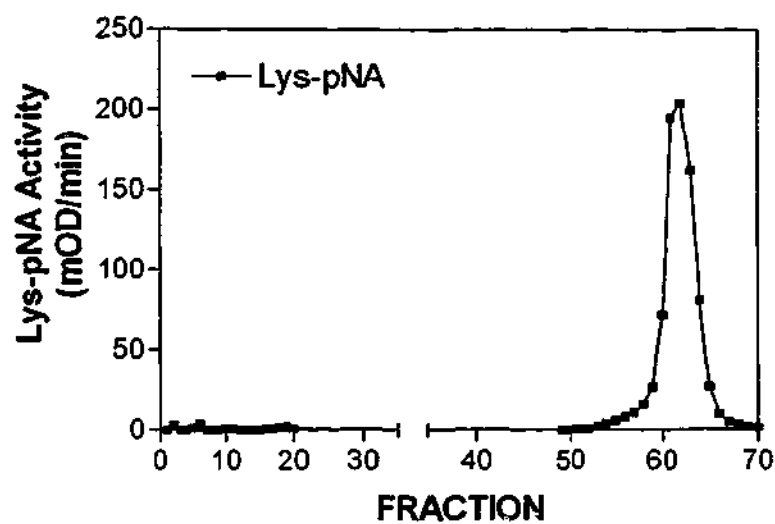


Figure 2.8. Anion exchange chromatography of Kgp_{cat} on Mono Q.

Pooled fractions containing Kgp_{cat} eluted from the Mono Q, were reapplied on the Mono Q column and eluted with a gradient of 0-200 mM NaCl. Fractions were assayed for Z-L-Lys-pNA activity.

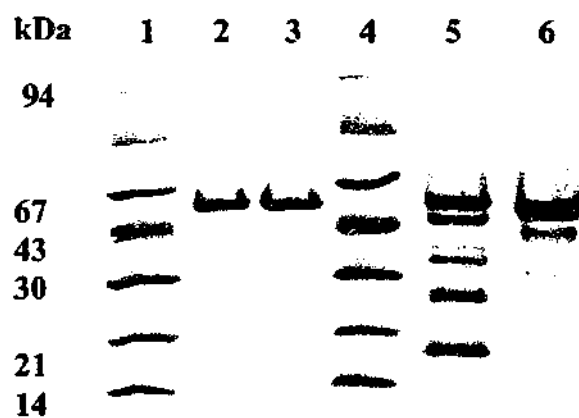


Figure 2.9. Tris-Tricine SDS-PAGE of RgpA_{cat} and Kgp_{cat}.

Purified samples of RgpA_{cat} and Kgp_{cat} were electrophoresed on a Tris-Tricine SDS-PAGE gel to monitor purity. Samples were run under reducing conditions. Lanes (1) and (4) Molecular weight markers; (2) and (3) RgpA_{cat} purified on the Mono Q column; (5) Kgp and (6) Kgp_{cat}.

2.3.3 Characterisation of Purified Enzymes

The purity of enzymes in each batch was checked using Tris-Tricine SDS-PAGE (Schägger and von Jagow, 1987). Both RgpB and RgpA_{cat} migrated as a single band with mobility equivalent to a molecular mass of 48 kDa and homogeneity greater than 95% as determined using laser densitometry scanning of the gel. HRgpA resolves into four major bands and one minor band on SDS-PAGE (Pike *et al.*, 1994). The identity of each protein band was confirmed by N-terminal sequence analysis as being derived from the RgpA polyprotein. Also, N-terminal sequence analysis was used to check for cross-contamination of RgpB and RgpA_{cat} preparations. In each case, only one sequence was obtained, which differed at only residue number 6, which was Glu and Gln in RgpB and RgpA_{cat}, respectively. Comparative analysis of amino acid derivative peaks of cycle eight of the Edman degradation for the 48 kDa band seen for RgpA_{cat} and RgpB, clearly indicated that any cross-contamination was below 10% of the major form of the gingipain-R being analysed.

2.3.4 Kinetic Characterisation of Proteases

The K_m values for cleavage of the substrate Z-Phe-Arg-AMC was determined for HRgpA, RgpA_{cat} and RgpB, while the K_m value for the cleavage of the substrate Z-Ala-Phe-Lys-AMC was determined for Kgp (Fig. 2.10). The K_m values for HRgpA and RgpA_{cat} were similar, 31.6 μ M and 34.6 μ M respectively, whereas the K_m value for RgpB (21.9 μ M) was lower. The K_m value for Kgp was 10.6 μ M and was the lowest of the K_m values determined for the gingipains.

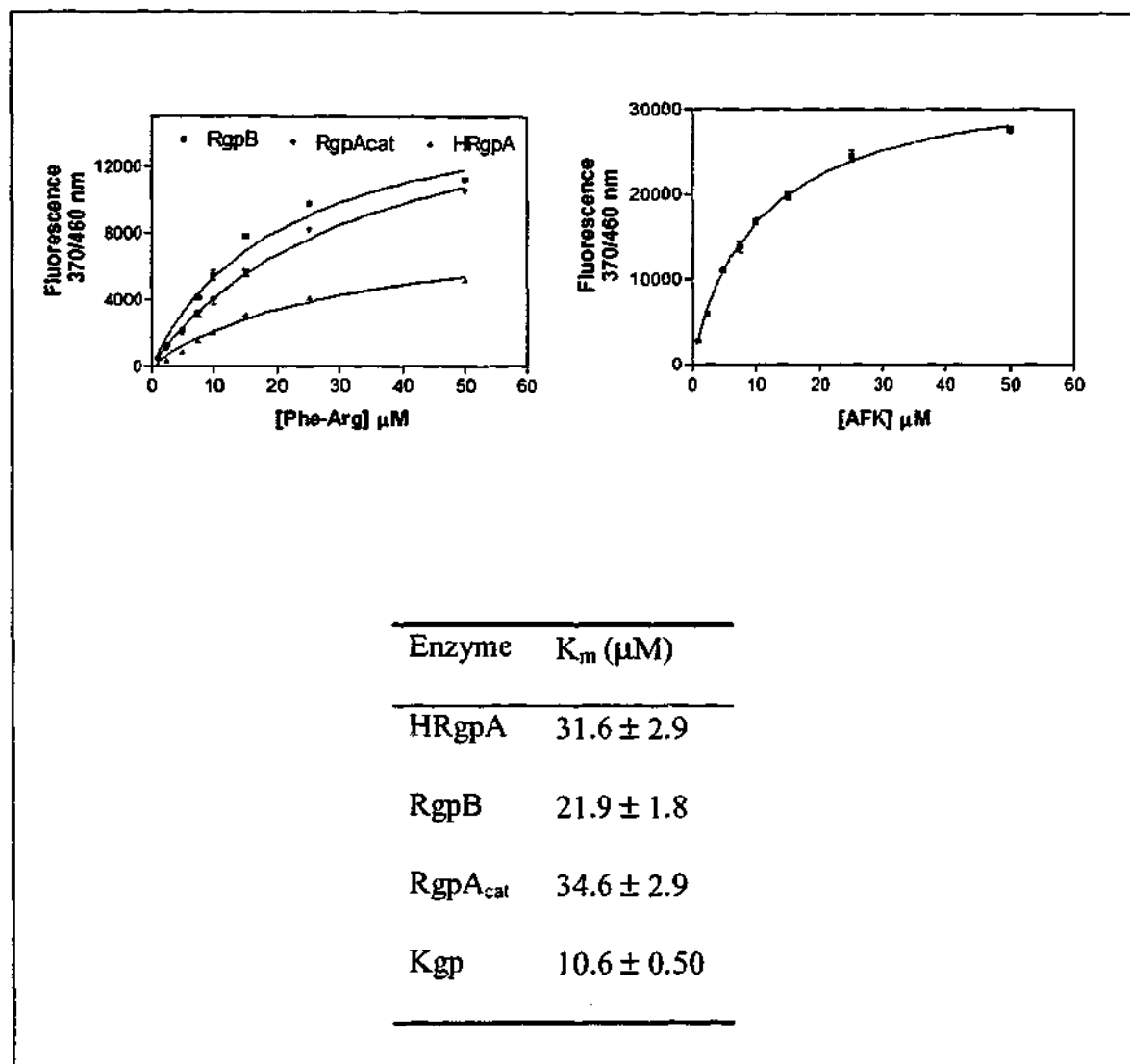


Figure 2.10. Kinetic analysis of HRgpA, RgpB, and RgpA_{cat} against Z-Phe-Arg-AMC [Phe-Arg] and for Kgp against Z-Ala-Phe-Lys-AMC [AFK]. Assays were carried out in triplicate and the means of the results had an error of 10% or less.

2.4 Discussion

All three gingipains, HRgpA, RgpB and Kgp, along with the catalytic domains RgpA_{cat} and Kgp_{cat} were at least highly purified in this study. The gingipain-R enzymes (HRgpA, RgpB and the catalytic domain RgpA_{cat}) were purified using methods previously described (Pike *et al.*, 1994; Potempa *et al.*, 1998), as was the gingipain-K, Kgp. This study was the first to describe a successful method for the purification of Kgp_{cat}, the catalytic domain of Kgp, from the culture supernatant of *P. gingivalis*.

Fujimura *et al.* (1998) apparently purified a lysine-specific enzyme from the membrane fraction of *P. gingivalis* strain ATCC 33277 with characteristics similar to that expected for Kgp_{cat} (monomeric form with a molecular weight on SDS-PAGE of 48 kDa). Thus it appears that these authors were the first to purify this form of Kgp. It should be noted, however, that the molecular weight of this enzyme was never shown by either gel filtration studies (as carried out here) or mass spectrometry. This leads to a level of doubt as to whether the enzyme purified by Fujimura *et al.* (1998) is really Kgp_{cat}, or simply Kgp in which the adhesin subunits were not apparent on SDS-PAGE.

The purification of Kgp_{cat}, the catalytic domain of Kgp, will help in future studies to establish the function and significance of the additional adhesin domains contained in Kgp. Specifically, specificity studies of Kgp and Kgp_{cat} will establish the influence of the adhesin subunits on the substrate specificity of Kgp. RgpA_{cat} purified in this chapter was used in the study in Chapter 3, to help determine the differences in substrate specificity between HRgpA and RgpB.

HRgpA and Kgp were purified from the culture supernatant of *P. gingivalis* and were purified with yields of 17% and 15%, respectively. The initial purification step of acetone precipitation was highly efficient and successful in that it retained the majority of the activity of HRgpA and Kgp, and had yields of 74% for gingipains-R and 68% for Kgp. The pH of the buffer used in the final purification step of HRgpA and Kgp on the arginine-Sepharose column was modified from 7.3 to 6.4 in this study. The use of buffer with a pH of 7.3 initially resulted in the purification of HRgpA and Kgp with very little or no activity at all. Optimisation of the pH led to the use of the pH 6.4 buffer to yield active forms of the gingipains.

Purification of RgpB was achieved using the method of purification previously described (Potempa *et al.*, 1998). The low molecular weight peak eluted from the Sephadex G-150 gel filtration column was used to further purify RgpB. The purification of Kgp_{cat} in its active form was a significant achievement, as the amount of catalytic domain in the culture fluid of the bacteria is very small to begin with. To date, it is unknown what results in the production of the catalytic domains of the gingipains. A possible reason underlying the production of the catalytic domains would be the loss of the additional adhesin domains from a small proportion of HRgpA and Kgp, either during synthesis by the bacteria or whilst the gingipains are in culture. The method of purification for RgpA_{cat} and Kgp_{cat} was initially optimised by the use of various chromatography columns including Mono P, Mono S, Phenyl-Superose and benzamidine-Sepharose, all of which did not separate the two catalytic domains. The method of purification established in this study will allow for the purification of Kgp_{cat} in the future. The purification of RgpA_{cat} and Kgp_{cat} did not have high yields when compared to those of HRgpA and RgpB.

The purification of HRgpA and Kgp in this study is comparable to the purification described by Pike *et al.* (1994), with a similar yield achieved for Kgp, 15% compared to an 18% yield by Pike *et al.* (1994). Although the yield of Kgp was similar to that described by Pike *et al.*, the amount of total protein was nearly half of that purified in the previous study 20 mg compared to 9.8 mg in this study.

The gingipains purified in this chapter will be used for the rest of the study to gain knowledge of the specificity of the enzymes. Gingipains have been shown to play an important role as virulence factors in the progression of adult periodontal disease by *P. gingivalis* and are thus studied extensively. The studies reported in the next chapter were carried out to determine the specificity of HRgpA and RgpB at the prime site positions, P2' and P3', and used RgpA_{cat} to help establish the reasons for the differences in specificity of the two proteinases. In the following chapter 4, an extensive study of the specificity of gingipains is carried out, in order to help develop a potential inhibitor.

CHAPTER THREE

CHARACTERISATION OF THE SPECIFICITY OF ARGININE-SPECIFIC GINGIPAINS FROM *PORPHYROMONAS* *GINGIVALIS* REVEALS ACTIVE SITE DIFFERENCES BETWEEN DIFFERENT FORMS OF THE ENZYMES

3.1 Introduction

Porphyromonas gingivalis is a major pathogen associated with the onset of adult periodontitis, one of the major causes of tooth loss today (Genco *et al.*, 1999). Periodontitis results from chronic inflammation of the gingival and periodontal tissue and has recently been associated with cardiovascular disease and pre-term delivery of low birth weight infants (Beck *et al.*, 1996; Genco, 1998; Offenbacher *et al.*, 1996). The disease is characterized by massive accumulation of neutrophils, bleeding on probing, bone resorption, formation of periodontal pockets and loss of tooth attachment. Approximately 15% of the population are known to suffer from the most severe forms of the disease, which, if left untreated, not only results in tooth loss, but also systemic complications (Beck *et al.*, 1996; Page, 1998).

P. gingivalis is a black pigmented, anaerobic, Gram-negative bacterium that produces a number of virulence factors, such as cysteine proteases, haemagglutinins, lipopolysaccharides and fimbriae, which enable the bacterium to colonise periodontal pockets (Cutler *et al.*, 1995). The proteolytic enzymes of the bacteria have been shown to play an important role in the pathogenesis of periodontitis (Kuramitsu, 1998; Holt *et al.*, 1999). The Arg-X specific and Lys-X specific proteases produced by the bacteria, referred to as gingipains-R and -K, comprise a major proportion of its total activity and are considered to be important virulence determinants ((Kuramitsu, 1998). Recent studies have revealed that null mutants of *P. gingivalis* for gingipain-R enzymes showed a marked decrease in virulence in *in vivo* models, and immunization with peptides corresponding to the N-terminal sequence of the catalytic domain of gingipains-R have also been shown to protect

against infection by the bacteria in mouse models (Genco *et al.*, 1998), indicating the overall importance of these enzymes in the pathogenesis of the disease by the bacterium.

The gingipains-R produced by *P. gingivalis* cleave peptide bonds exclusively after arginyl residues (Potempa and Travis, 1996) and are encoded by two genes, *rgpA* and *rgpB* (Curtis *et al.*, 1999). The major forms of gingipain-R derived from the *rgpA* gene are a 50 kDa catalytic domain (RgpA_{cat}) and a 95 kDa high molecular mass, non-covalent complex of catalytic and hemagglutinin/adhesin domains [HRgpA] (Curtis *et al.*, 1999), the former responsible for proteolytic activity and the latter for adhesion to extracellular matrix proteins and red blood cells. In comparison to *rgpA*, the *rgpB* gene lacks a sequence encoding the hemagglutinin/adhesin domains and its product occurs predominantly as the soluble 50-kDa gingipain-R [RgpB] (Mikolajczyk-Pawlinkska *et al.*, 1998). Gingipain-R enzymes have been shown to activate coagulation factors, degrade components of the complement pathway and several physiologically important proteins, contributing to the virulence of the pathogen (Imamura *et al.*, 1997; DiScipio *et al.*, 1996; Lantz *et al.*, 1991; Imamura *et al.*, 1994; Calkins *et al.*, 1998). In addition to causing destruction to the tissue supporting the teeth, gingipain-R enzymes play a major role in the deregulation of the inflammatory response and disruption of host defense mechanisms.

Analysis of the recently solved structure of RgpB indicates the molecule is composed of two distinct domains, an N-terminal catalytic domain with topological similarity to caspases and a C-terminal domain with an Ig-like structure (Eichinger *et al.*,

1999). The Ig-like domain of RgpB is thought to be involved in helping it bind to protein substrates or dock to endogenous proteins, other bacteria or host cell surfaces (Eichinger *et al.*, 1999). The catalytic domain of RgpB is almost identical to that of HRgpA (RgpA_{cat}) at the primary structure level, indicating that previously noted differences between HRgpA and RgpB in their ability to cleave protein substrates (Imamura *et al.*, 2000) are most likely due to the additional hemagglutinin/adhesin domains in HRgpA. This study initially aimed to determine the specificity of the two proteases towards substrate residues in the P₂'/P₃' region. Notable differences in specificity between HRgpA and RgpB led us to investigate whether the additional hemagglutinin/adhesin domains of HRgpA influence substrate specificity. Determination of the specificity of these proteases will aid in the design of drugs to combat periodontal disease.

3.2 Experimental Procedures

3.2.1 Materials

Bz-L-Arg-pNA, N α -p-Tosyl-L-lysine-chloromethyl ketone (TLCK) and leupeptin were purchased from Sigma (Sydney, Australia). Z-L-Lys-pNA was from Novabiochem (Darmstadt, Germany). An extract from the medicinal leech (*Hirudo medicinalis*) was a kind gift from Dr. Christian Sommerhof (Ludwig-Maximilian-University, Munich, Germany). The extract at 0.1 mg/ml totally inhibited 0.4 nmol α -thrombin amidolytic activity.

3.2.2 Fluorescence-Quenched Substrates

The fluorescent quenched substrates were synthesized as described previously (Le Bonniec *et al.*, 1996). Substrates were dissolved in DMF and the concentration of the stock solution was determined spectrophotometrically, assuming an absorption coefficient of $10^4 \text{ M}^{-1} \text{ cm}^{-1}$ at 360nm. Each substrate consisted of a 10-residue peptide with a 2-aminobenzoyl (Abz) group at the N-terminus and a penultimate 2,4-dinitrophenyl (Dnp) derivatized lysine. Peptides had the following general sequence: Abz-Val-Gly-Pro-Arg-Ser-X-X-Leu-Lys(Dnp)-Asp-OH, with the X denoting the variable amino acid positions at P₂' and P₃'. The P₂' specificity was determined using substrates with a leucine in the P₃' position, whereas the P₃' substrates contained a phenylalanine at the P₂' position.

3.2.3 Cultivation of the bacteria and purification of enzymes

P. gingivalis strain HG66 cells used as a source of the enzymes in this study were grown as described previously (Chen *et al.*, 1992). HRgpA and RgpB were purified from the HG66 strain culture fluid as described previously (Pike *et al.*, 1994). Briefly, HRgpA was purified using gel filtration and arginine-sepharose chromatography, while RgpB was purified using a combination of gel filtration and anion-exchange chromatography on Mono Q (Pike *et al.*, 1996). RgpA_{cat} was purified from the fractions containing RgpB that were eluted from a Sephadex G-150 gel filtration column (Potempa *et al.*, 1998). Briefly, fractions were pooled and loaded on to a DE-52 cellulose column, where RgpA_{cat} was eluted in the void volume using 50 mM Bis-Tris, 1 mM CaCl₂, pH 6.5. RgpA_{cat} was loaded on a Mono Q column, eluted with 1 M NaCl, 50 mM Bis-Tris, 1 mM CaCl₂, pH 6.5 buffer, and purified to homogeneity.

The purity of enzymes in each batch was checked using SDS-PAGE. Both RgpB and RgpA_{cat} migrated as a single band with mobility equivalent to a molecular mass of 48 kDa and homogeneity greater than 95% as determined using laser densitometry scanning of the gel. HRgpA resolves into four major bands and one minor band on SDS-PAGE (Pike *et al.*, 1994). The identity of each protein band was confirmed by N-terminal sequence analysis as being derived from the RgpA polypeptide. Also, N-terminal sequence analysis was used to check for cross-contamination of RgpB and RgpA_{cat} preparations. In each case, only one sequence was obtained, which differed at only residue number 8, which was Glu and Gln in RgpB and RgpA_{cat}, respectively. Comparative analysis of amino acid derivative peaks of cycle eight of

the Edman degradation for the 48 kDa band seen for RgpA_{cat} and RgpB, clearly indicated that any cross-contamination was below 10% of the major form of the gingipain-R being analysed.

3.2.4 Kinetic Studies

The k_{cat} and K_m values were measured at 37°C using substrates at concentrations ranging from 1-50 μ M, with a final concentration of active site titrated enzyme of 1.0 nM in 0.2 M Tris-HCl, 5 mM CaCl₂, 10 mM cysteine, 0.1 M NaCl, pH 7.6. The assay was performed in a total volume of 200 μ l in microplates and was carried out in triplicate. Enzyme solution (100 μ l) was added to 100 μ l of substrate solution and the initial velocity was recorded (usually over 10 min) at 7 different substrate concentrations at 330/420 nm on a fluorescent plate reader (Biolumin960, Molecular Dynamics). The initial velocities were plotted against substrate concentrations and the lines were fitted to a single site binding equation using non-linear regression analysis in the program Graph Pad Prism®. The K_m values were derived from the fitted line, while k_{cat} values were calculated from the V_{max} values by taking into account the amount of active enzyme used in the assays, the latter determined as described previously (Potempa *et al.*, 1997). Four substrates (P₂' His, P₂' Ser, P₃' Gly and P₃' Ala), towards which HRgpA and RgpB displayed a significant difference in activity, were assayed as above with the three gingipain-R enzymes, HRgpA, RgpB and RgpA_{cat}, on a fluorescent plate reader (FLUOstar *Galaxy*, BMG Labtechnologies).

3.2.5 Modelling

Molecular modeling was performed in collaboration with Dr James Whisstock. The X-ray crystal structure of RgpB (pdb identifier 1CVR; 20) was obtained from the protein data bank (Sali and Blundell, 1993). RgpB and RgpA are 90% identical and the sequences were aligned using the alignment package available in Quanta (Accelrys Inc, San Diego). The molecular model of RgpA was built using the program Modeler (Berman et al., 2000) and the X-ray crystal structure of RgpB as a template. A Ramachandran plot confirmed that all residues in the model of RgpA were in allowed conformations.

3.2.6 ELISA of gingipain binding to extracellular matrix proteins

To test the binding of the gingipain-R enzymes to different extracellular proteins, proteins to be tested were coated onto Nunc maxisorp ELISA plates at a concentration of 1 µg/ml in phosphate-buffered saline (PBS) at 4°C for 16 hrs. The wells were then blocked with 0.5% (w/v) BSA in PBS for 1 hr at 37°C. Every incubation was followed by three washes with 0.1% (v/v) Tween 20-PBS. Following blocking, the wells were incubated with serial dilutions of HRgpA, RgpB and RgpA_{cat}, all previously inactivated with TLCK, starting from 50 µg/ml in BSA-PBS for 2 hrs. The wells were then incubated with chicken anti-gingipain R (1 µg/ml) in BSA-PBS for 1 hr, followed by incubation with anti-chicken IgY-horseradish peroxidase conjugate (1 µg/ml) in BSA-PBS for 1 hr at 37°C. The plate was then washed and binding was detected by incubation with tetramethylbenzidine substrate solution. The reaction was terminated by adding 2 M H₂SO₄ and the product was read at 450nm.

3.2.7 Analysis of degradation of proteins by SDS-PAGE

Protein degradation was carried out at 37°C, in 0.2 M Tris-HCl, 1 mM CaCl₂ and 10 mM cysteine buffer. Aliquots were taken at various time points and enzyme activity was stopped by adding 1 mM TLCK. Aliquots containing the proteins and degradation products were electrophoresed on 10% Tris-Tricine (Shagger and van Jagow, 1987) sodium dodecyl sulfate-polyacrylamide gel electrophoresis (SDS-PAGE) gels and visualized by Coomassie blue R-250 staining. Fibrinogen cleaved by HRgpA was also blotted to a PVDF membrane following SDS-PAGE and bands were excised for N-terminal sequencing as previously described (Pike *et al.*, 1994).

3.2.8 Western Blot analysis of the degradation of human plasma fibrinogen by Arg-gingipains

Plasma was collected by mixing 9 ml of human blood with 1 ml of 3.2% (w/v) sodium citrate and centrifuging the mixture for 5 min at 2700 rpm. Plasma was depleted of albumin by mixing it with Cibacron Blue Sepharose equilibrated in PBS using 2 ml of the chromatography matrix per 1.5 ml plasma. After 30 min of gentle mixing at room temperature, the matrix was removed by centrifugation and the supernatant was used in further experiments. Plasma prepared in this way (50 µl) was made up to 100 µl using a buffer containing either 20 mM cysteine, 0.1 M Tris, pH 8.0, or the same buffer supplemented with 1 mg/ml of leech extract. To this mixture, 50 µl of activated gingipain-R was then added to yield a final enzyme concentration of 10 nM. The plasma mix was incubated at 37°C and 20 µl aliquots were transferred at 5, 10, and 15 min into 80 µl of 5 mM TLCK in

PBS to stop the reaction. Samples were boiled with SDS-PAGE reducing buffer for 10 minutes, electrophoresed on 10% Tris-Tricine (Shägger and van Jagow, 1987) SDS-PAGE gels and transferred onto nitrocellulose membrane overnight at 30 V. The membranes were blocked with 1% (w/v) low fat milk powder in Tris-Buffered saline (TBS) overnight. The membranes were washed in Tween-TBS and incubated with goat anti-human fibrinogen diluted 1:5,000 in 1% (w/v) bovine serum albumin in Tween-TBS for 1 hr. The membranes were washed and incubated for 1 hr with anti-goat-alkaline phosphatase diluted 1:100,000 in 1% (w/v) bovine serum albumin in Tween-TBS. Bound antibodies were detected using BCIP/NBT substrate.

3.3 Results

The specificity of HRgpA and RgpB at the P₂' position was determined using fluorescent quenched substrates with 18 different amino acids at this position, excluding substrates with an arginine or a cysteine residue. Substrates with a cysteine residue were not used, as oxidation of the cysteine residue would interfere with the activity of the enzymes. Similarly, cleavage of substrates containing an additional arginine residue would probably result in higher K_m and k_{cat}/K_m values due to secondary cleavage of the substrates. The specificity of the enzymes for the P₃' position was determined using substrates with 16 substitutions at this position, with cysteine, arginine, phenylalanine and glutamate excluded. Each substrate contained the following sequence of amino acids, (Abz)-Val-Gly-Pro-Arg-Ser-Xaa-Leu-Leu-Lys(Dnp)-Asp-OH, where Xaa is representative of any one of the 18 amino acids examined at the P₂' position in this example. The Lys(Dnp) group quenches the fluorescence of the N-terminal Abz group in an uncleaved substrate by resonance energy transfer. Cleavage of the substrate relieves quenching, resulting in an increase in fluorescence proportional to the concentration of the released fluorophore fragment, thus allowing the determination of the initial velocities of the enzymes in relation to substrate concentration and hence the kinetic parameters, K_m , V_{max} and k_{cat} . Values for k_{cat}/K_m were derived from the individual constants.

3.3.1. HRgpA Specificity at P₂' and P₃'

Phenylalanine is the most preferred amino acid at P₂' for cleavage by HRgpA, followed by leucine and tyrosine (Table 3.1). The k_{cat}/K_m value of the most preferred amino acid at P₂' for HRgpA, phenylalanine ($12.5 \mu\text{M}^{-1}\cdot\text{s}^{-1}$), was 11.4-fold greater than the k_{cat}/K_m value of the least preferred amino acid at P₂', which was proline ($1.1 \mu\text{M}^{-1}\cdot\text{s}^{-1}$). Leucine was the most preferred and isoleucine was the least preferred amino acid at the P₃' position (Table 3.2). The K_m values determined for HRgpA, which reflect the binding affinity of an enzyme for a substrate, indicate that HRgpA does not show an affinity for a particular group of amino acids (Table 3.1 and 3.2). HRgpA had the greatest affinity for the substrate with a positively charged lysine or a polar uncharged asparagine residue at P₂', with K_m values of $15.1 \mu\text{M}$ and $15.6 \mu\text{M}$, respectively. The K_m values for HRgpA at P₃' again reflect the lack of preference for any particular group of amino acids at this position, the K_m value for the substrate with a proline at P₃' ($6.2 \mu\text{M}$) was significantly lower than any other substrate (Table 3.2).

3.3.2 RgpB Specificity at P₂' and P₃'

Results obtained indicate that serine, a polar hydrophilic amino acid, was the most preferred residue at P₂' ($k_{cat}/K_m = 7.9 \mu\text{M}^{-1}\cdot\text{s}^{-1}$) for RgpB (Table 3.1). As with HRgpA, proline ($k_{cat}/K_m = 0.5 \mu\text{M}^{-1}\cdot\text{s}^{-1}$) was the least preferred amino acid at P₂' for RgpB. RgpB did not display a preference for any particular group of amino acid at P₃' (Table 3.2), with the k_{cat}/K_m value for lysine ($3.8 \mu\text{M}^{-1}\cdot\text{s}^{-1}$) the most preferred amino acid at P₃' only three fold greater than the value for threonine ($0.9 \mu\text{M}^{-1}\cdot\text{s}^{-1}$),

the least preferred amino acid at P₃'. The K_m values for RgpB indicate that it too does not show a preference towards a particular group of amino acids, although it has a broader range of K_m values, indicating a greater difference in its binding affinity towards substrates. RgpB had the highest affinity towards the substrate with an asparagine at the P₂' position ($K_m = 17.4 \mu\text{M}$). The substrate with a lysine at P₃' had a K_m value of $12.3 \mu\text{M}$, which was the lowest value overall for RgpB.

Table 3.1. Substrate Specificity of HRgpA and RgpB at P₂'.

Units for K_m are expressed in μM , k_{cat} were expressed in $\text{s}^{-1} \times 10$, k_{cat}/K_m were expressed in $\mu\text{M}^{-1} \cdot \text{s}^{-1}$.^a Assays were carried out in triplicate and values for K_m and k_{cat} had a standard error of less than or equal to 10%. Only residues from P₃ to P₃' are indicated and amino acids unique to each substrate are in bold. *nd* = not determined.

Substrate	HRgpA			RgpB		
	K_m	k_{cat}	k_{cat}/K_m	K_m	k_{cat}	k_{cat}/K_m
GPR-SFL	20.5	25.6	12.5	24.5	8.6	3.5
GPR-SLI	26.2	28.1	10.7	21.2	6.1	2.8
GPR-SYL	24.2	25	10.3	44.9	14.8	3.3
GPR-SQL	26.4	25.7	9.7	42.4	9.5	2.2
GPR-SGL	23.4	21.8	9.3	34.7	11.2	3.2
GPR-SWL	21.3	18.9	8.8	<i>nd</i>	<i>nd</i>	<i>nd</i>
GPR-STL	39.1	31.7	8.1	32.5	7.8	2.4
GPR-SSL	24.2	17.4	7.2	55.8	44.1	7.9
GPR-SHL	39.5	21.7	5.5	71.8	7.8	1.1
GPR-SNL	15.6	8.1	5.2	17.4	3.9	2.2
GPR-SVL	17.9	8.2	4.6	41.9	10.4	2.5
GPR-SDL	42.1	17.5	4.1	32.3	4.7	1.4
GPR-SKL	15.1	6.2	4.1	59.3	11.8	1.9
GPR-SAL	27.3	10.2	3.7	29.7	9.4	3.2
GPR-SIL	77.9	23.6	3.0	84.8	10.2	1.2
GPR-SML	20.4	4.9	2.4	38.9	13.4	3.4
GPR-SEL	22.8	5.3	2.3	25.2	4.0	1.6
GPR-SPL	21.2	2.3	1.1	49.4	1.9	0.5
Selectivity Factor			11.4			16

Table 3.2. Substrate Specificity of HRgpA and RgpB at P₃'.

Units for K_m are expressed in μM , k_{cat} were expressed in $\text{s}^{-1} \times 10^5$, k_{cat}/K_m were expressed in $\mu\text{M}^{-1} \cdot \text{s}^{-1}$. Assays were carried out in triplicate and values for K_m and k_{cat} had a standard error of less than or equal to 10%. Only residues from P₃ to P₃' are indicated and amino acids unique to each substrate are in bold.

Substrate	HRgpA			RgpB		
	K_m	k_{cat}	k_{cat}/K_m	K_m	k_{cat}	k_{cat}/K_m
GPR-SFL	20.5	25.6	12.5	24.5	8.6	3.5
GPR-SFN	23.1	27.0	11.7	46.5	12.5	2.7
GPR-SFG	27.8	2.9	10.4	53.3	18.8	3.5
GPR-SFD	17.8	15.4	8.4	41.5	11.5	2.7
GPR-SFP	6.2	4.3	6.9	18.7	5.5	2.9
GPR-SFH	35.6	24.7	6.9	47.9	14.4	3.0
GPR-SFK	20.9	13.2	6.3	12.3	4.7	3.8
GPR-SFS	19.4	11.9	6.1	19.7	4.8	2.4
GPR-SFY	24.8	15.2	6.1	15.8	3.2	2.0
GPR-SFA	13.1	7.8	5.9	31.6	7.2	2.2
GPR-SFT	23.7	14.1	5.9	36.9	3.3	0.9
GPR-SFW	17.8	9.9	5.5	25.1	7.8	3.1
GPR-SFV	64.0	29.7	4.6	30.4	11.1	3.6
GPR-SFQ	31.8	10.7	3.3	27.0	7.5	2.7
GPR-SFM	19.1	5.3	2.7	27.1	2.7	0.9
GPR-SFI	32.5	6.4	1.9	60.5	10.6	1.7
Selectivity Factor			6.6			4.3

3.3.3 Modelling of RgpA

RgpA and B share 90% sequence identity, with the majority of the substitutions mapping to the Ig like domain in the C-terminus. Only four substitutions (D281→N, Y283→S, P286→S and N331→K) map to the protease domain, all of which map to the region surrounding the active site (see Fig. 3.1).



Figure 3.1. The crystal structure of RgpB (Eichinger *et al.*, 1999). **A.** Overall structure of RgpB demonstrating the two domains making up the overall catalytic domain in red and green. The Ig domain is in yellow. The inhibitor, D-Phe-Phe-Arg-chloromethylketone, in the active site of RgpB is shown in purple, whilst substitutions in the active site of RgpB in relation to RgpA are shown in blue ball and stick. **B.** The electrostatic potential of the active site of RgpB (red equals electronegative, blue electropositive and white is neutral). **C.** Close up of the active site of RgpB, showing the substitutions relative to RgpA in blue ball and stick. The figure was produced using Quanta (Accelrys Inc.) and GRASP.

3.3.4 Comparison of the specificity of HRgpA, RgpB, and RgpA_{cat} at P₂' and P₃'

RgpA_{cat} was used to help determine if the differences in specificity between HRgpA and RgpB were due to the additional adhesin domains in HRgpA or due to the four amino acid substitutions in its active site compared to RgpB. The substrates to be used were selected on the basis of results obtained previously. One substrate each from the P₂' and P₃' range, for which HRgpA and RgpB had a high and a low K_m value, respectively, were selected. Values for K_m were determined for HRgpA, RgpB, and RgpA_{cat} towards substrates with a histidine or serine at the P₂', and a glycine or alanine at the P₃' position. The K_m values for HRgpA and RgpA_{cat} were similar, and differed from the values obtained for RgpB. Thus, for instance, the K_m value for RgpB towards the substrate with a serine at P₂' position was 55 μ M, whereas the values for HRgpA and RgpA_{cat} were 24 μ M and 30 μ M, respectively (Fig. 3.2). The K_m values for RgpB were nearly two-fold higher than the values for HRgpA and RgpA_{cat}, indicating that RgpB had a weaker affinity towards the substrates in comparison to HRgpA and RgpA_{cat}.

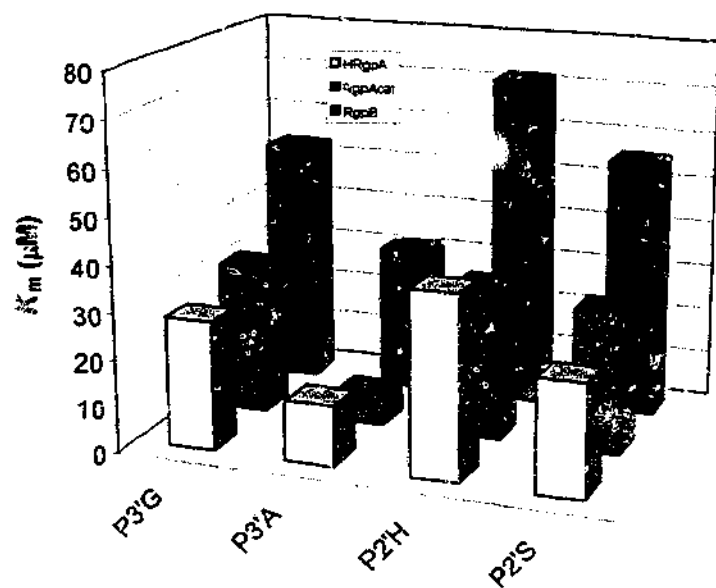


Figure 3.2. Comparison of the K_m values of HRgpA, RgpA_{cat} and RgpB towards fluorescent quenched substrates with a glycine or an alanine at P₃' and a histidine or a serine at P₂' position.

3.3.5 Binding of gingipains to fibrinogen, fibronectin and laminin

Results obtained in the specificity studies indicated that the adhesin domains are not responsible for the differences in specificity of HRgpA and RgpB towards peptide substrates. Since the binding activity of RgpA_{cat} had not previously been characterized, experiments were carried out to determine if the enzyme adhered to fibrinogen, fibronectin and laminin. HRgpA bound all three proteins, whereas RgpA_{cat} and RgpB showed very little or no binding activity towards the proteins [less than 10% of the value for HRgpA] (Fig. 3.3). The lack of binding activity for RgpB and RgpA_{cat} indicates that the gingipains require the additional adhesin domains found in HRgpA in order to bind proteins and that the catalytic or Ig-like domains of the smaller proteases do not possess any binding activity.

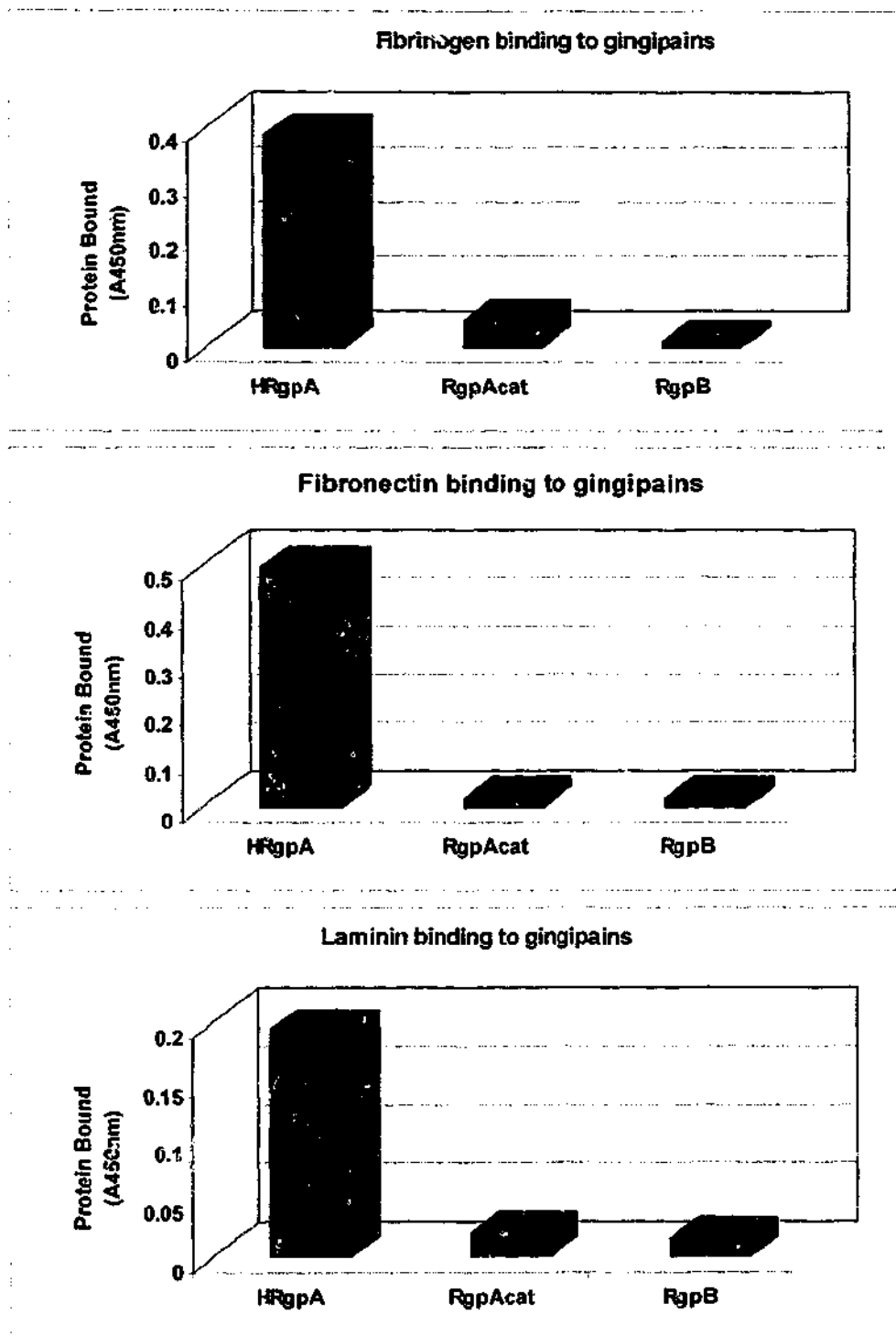


Figure 3.3. Binding of gingipains to (A) Fibrinogen, (B) Fibronectin and (C) Laminin. Values shown are an average of three experiments, using a 50 nM concentration of each proteinase. Proteins were coated at a concentration of 10nM.

3.3.6 Degradation of fibrinogen by the gingipains

Specificity studies using peptide substrates indicated that HRgpA and RgpA_{cat} are similar in their preferences for cleavage, and differ from RgpB. We wanted to determine if this was also so for a protein substrate, such as fibrinogen, which is cleaved by all of the gingipain-R forms under study. Thus the pattern of cleavage of fibrinogen was used to evaluate whether the pattern of cleavage of the protein and/or rate of cleavage was different for the individual gingipain-R enzymes. We examined cleavage of the protein in its purified form and in plasma, in order to evaluate whether there was a difference in the rate or position of cleavage in a complex milieu in comparison to the purified protein. Cleavage of the purified protein was followed directly using SDS-PAGE for the purified protein (Fig. 3.4) and by western blotting for the plasma protein (Fig. 3.5). It was apparent that all three forms of gingipain-R cleaved fibrinogen very similarly in terms of the kinetics of A α -chain degradation, which was most sensitive to cleavage. The A α -chain was cleaved at a number of positions, but for each enzyme isoform, a band of approximately 28kDa appeared and grew stronger over the period of the incubation. N-terminal sequencing of the approximately 28kDa band revealed that it was derived from the N-terminal portion of the A α -chain, having been cleaved at position 22 of the mature chain at the sequence VER¹HQS (arrow indicates cleavage position). In contrast to the situation with the A α -chain, HRgpA was significantly more efficient at cleaving the B β -chain than RgpB and RgpA_{cat}, leading to accumulation of a lower molecular mass cleavage product, which migrated just above the γ -chain. N-Terminal sequencing of this band revealed that it was indeed derived from the B β -chain and resulted from two

cleavages at positions 42 and 44 in the sequence GYR[↓]AR[↓]PAK (arrows indicate the position of cleavage).

The gingipain-R forms once again cleaved the A α -chain of fibrinogen in plasma with similar kinetics, although only HRgpA was able to generate the approximately 28kDa band derived from cleavage of the A α -chain in contrast to the situation with the pure protein (Fig. 3.5). Once again only HRgpA was able to cleave the B β -chain efficiently in the plasma context. The profile of cleavage of the α -chain and β -chain was the same in the absence or presence of leech extract (applied at a concentration that totally inhibited thrombin activity), indicating that cleavage of these chains was independent of thrombin. It should be noted that thrombin was apparently active in cleaving fibrinogen in the absence of leech extract to some extent, however, since a band corresponding to the γ -chain dimer was observed, which is not seen when the leech extract was present. This was only apparent for HRgpA treatment, indicating that HRgpA is more efficient at activating prothrombin than the other protease forms, as has been observed previously (Imamura *et al.*, 2001a). Once activated, thrombin would activate factor XIII to cause dimerisation of the γ -chains by transglutamination.

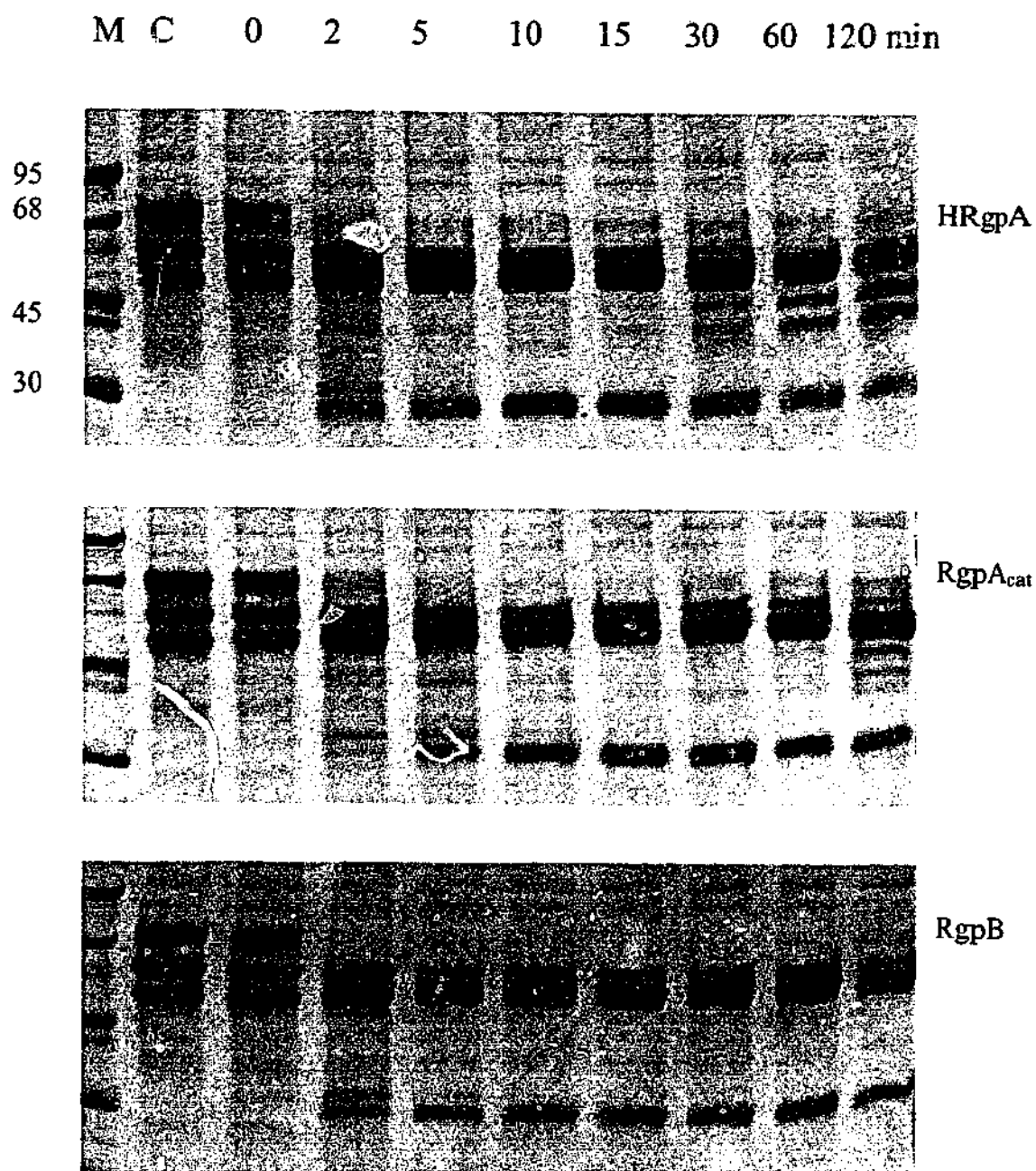


Figure 3.4. Degradation of fibrinogen by HRgpA, RgpA_{cat}, and RgpB at 0, 2, 5, 10, 15, 30, 60 and 120 min. A 10 nM concentration of enzyme was used for the assay. M designates the protein molecular weight markers (sizes indicated next to the markers for the HRgpA gel: 95 kDa, 68 kDa, 45 kDa and 30 kDa) and C designates control protein not incubated with enzyme. 10 μ g of protein was loaded per lane and electrophoresed on 10% Tris-Tricine SDS-PAGE gels.

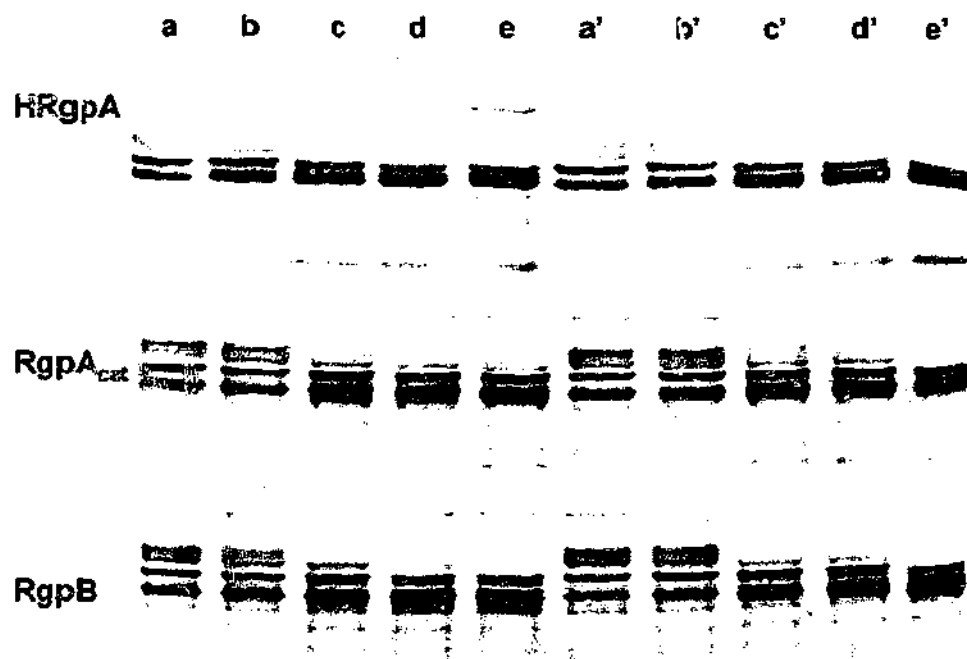


Figure 3.5. Cleavage of fibrinogen in plasma by gingipains. Samples of freshly collected human plasma depleted of albumin by absorption on the Cibacron Blue Sepharose alone (lanes a-e) or pretreated with a leech extract (lanes a'-e') were incubated with 10 nM of each form of gingipain for 0 min (lanes a and a'), 5 min (lanes b and b'), 10 min (lanes c and c'), 15 min (lanes d and d'), and 15 min (lanes e and e'). Lanes a and a', control plasma preincubated 15 min in the absence of gingipain. The reaction was stopped using TLCK (4 mM), samples were boiled in reducing treatment buffer, electrophoresed on 10% Tris-Tricine SDS-PAGE gels and then immunoblots were performed with fibrinogen being detected using a goat anti-human fibrinogen antibody.

3.4 Discussion

The initial focus of this study was to map the preferences of the gingipain-R enzymes for prime site amino acid residues in peptide substrates. A previous study (Potempa *et al.*, 1998) examined the specificity for residues in the non-prime sites and found that the gingipains were relatively non-specific for these residues and also that no marked difference in specificity could be found between different forms of the gingipains-R. This investigation therefore examined whether this was the case for the prime sites of substrates.

The two gingipain-R forms initially analysed, HRgpA and RgpB, were not very selective for substrate residues at the P₂' and P₃' sites, thus selectivity factors (or the ratio between top and bottom values for each kinetic term) ranged from 4.3 to 18.0. Both enzymes were most selective for substrate residues at the P₂' subsites, with RgpB somewhat more selective than HRgpA at P₂' and slightly less selective at P₃' (Tables 3.1 and 3.2). Overall, it appeared that the specificity constant for any given substrate, usually accepted to be the k_{cat}/K_m value, was mostly influenced by the k_{cat} value. In general, variation between K_m values was lower than for the k_{cat} values for any given subsite and enzyme. It was clear that HRgpA and RgpB were different in their specificity for different amino acids at the prime subsites and therefore it was of interest to know the underlying reasons for this.

Initial analysis of the difference in the specificity of the prime subsites led to the hypothesis that it was the additional adhesin domains of HRgpA, which might give rise to the differences in specificity. For this to be true, however, it would be

necessary for the active sites of the proteases to be identical. The catalytic domain of HRgpA (RgpA_{cat}) was therefore modeled upon the crystal structure of RgpB, in order to determine whether this was correct. The surface of the active-site and its surroundings are relatively flat, except for the S₁ pocket, which is a fairly narrow slot, bordered by in-plane hydrogen bond acceptors and covered by a hydrophobic lid (Fig. 3.1A). The active site is also characterized by a negative electrostatic potential, which may have an effect on the binding of substrates (Fig. 3.1B). There are four amino acid substitutions, D281→N, Y283→S, P286→S and N331→K, found in the active site of HRgpA compared to RgpB (Fig. 3.1C). Apart from these four substitutions, the active site of HRgpA and RgpB are identical. The amino acid substitutions could have a profound effect on the binding of substrates and subsequent cleavage, particularly P286S, since P285 and P286 form a double proline motif at the end of helix 9 in RgpB. These residues form one of the walls of the S₁ pocket and substitution of P286 with a serine may thus alter the accessibility to the S₁ pocket. These substitutions might change direct interactions with prime site substrate residues, but it is more likely that they cause a general change in the conformation of the prime site binding sites of the active site, thus giving rise to the differences in specificity noted.

In order to resolve whether it was the contribution of the active site substitutions or the additional adhesin domains that determined the differences in specificity between HRgpA and RgpB, the small quantity of RgpA_{cat} to be found in culture supernatants of *P. gingivalis* was purified. RgpA_{cat} is the catalytic domain of RgpA, analogous to RgpB, except that the 4 amino acid substitutions would be present at the active site.

It was shown that RgpA_{cat} was similar to HRgpA in terms of its kinetics of cleavage of four substrates containing P2' or P3' substitutions. Substrates were selected for analysis based on their having large differences in terms of their kinetics of cleavage by HRgpA and RgpB. Thus it appears that it is most likely that it is the active site substitutions in HRgpA versus RgpB that dictate their differences in specificity for prime site residues and not the additional adhesin domains found in HRgpA.

What then is the function of the additional adhesin domains in terms of the specificity of the proteases for cleavage of peptide or protein substrates? Previous work has attributed quite large differences in the cleavage of protein substrates by HRgpA versus RgpB to the additional adhesin subunits on HRgpA interacting with the protein substrates. The data generated in this study would indicate that the adhesin domains do not influence cleavage of peptide substrates, but is this also true for protein substrates to which the adhesin domains of the gingipains might bind? Firstly, there was a need to establish whether the catalytic domains of the gingipains could bind to proteins in the same way as HRgpA. Since the catalytic domains of the gingipains have an Ig-like domain, which might conceivably have adhesin activity, it was important to determine whether RgpA_{cat} or RgpB could bind to proteins. It has previously been shown that HRgpA binds to fibrinogen, fibronectin and laminin, but RgpB does not (Pike *et al.*, 1996). Work carried out here, showed that RgpA_{cat} also did not bind to these proteins (Fig. 3.3). This strongly indicates that the additional adhesin subunits in HRgpA mediate binding to the tested proteins.

The influence of binding to a protein substrate by HRgpA on cleavage was then tested. It was hypothesized that the binding event might influence the position of

cleavage within the substrate, and therefore the pattern of cleavage bands seen on SDS-PAGE, and/or the rate of cleavage of a protein substrate. To examine whether the adhesins have an influence on protein substrate cleavage, HRgpA, RgpA_{cat} and RgpB were tested to see if they differed in their cleavage of purified fibrinogen (Fig. 3.4). HRgpA, RgpA_{cat} and RgpB cleaved the A α -chain of fibrinogen with very similar kinetics. The γ -chain of fibrinogen was essentially not degraded, but differences were observed for cleavage of the B β -chain between the gingipain-R forms. HRgpA cleaved the B β -chain most efficiently, followed by RgpA_{cat}, then RgpB. This indicates that the additional adhesin domains of HRgpA may position the enzyme advantageously for cleavage of the B β -chain relative to RgpA_{cat}. The greater efficiency of both RgpA forms also indicates that the active site differences found between RgpA and RgpB forms have a strong effect in this context. The position of cleavage of the fibrinogen A α -chain and B β -chain would be predicted to preclude formation of the fibrinopeptides A and B, thus explaining why fibrinogen is rendered non-clottable by the gingipains-R and thus overall the anti-clotting effect that these enzymes have in plasma, despite their activation of procoagulant enzymes.

Cleavage of the protein in plasma was also tested in order to evaluate whether the adhesins served to target HRgpA to a substrate such as fibrinogen, resulting in faster cleavage (Fig. 3.5). It was shown that cleavage profiles in plasma were similar to those with purified fibrinogen in that all gingipain-R forms cleaved the A α -chain rapidly. However, there were some differences in the cleavage of the B β -chain, with only HRgpA cleaving this chain. This difference was not due to activation of the coagulation cascade (Imamura *et al.*, 1997; Imamura *et al.*, 2001), since the same

cleavage pattern was observed in the presence of the leech extract containing hirudin and other very effective inhibitors of proteases from coagulation cascade (Salzet, 2002; Baskova and Zavalova, 2001).

The results of this study strongly imply that the differences previously noted between different forms of gingipain-R in terms of their cleavage of isolated protein substrates are primarily due to differences at the active site of the enzymes, with the adhesin domains playing a minor role. However, cleavage in complex (patho)physiological fluids such as plasma may be affected by the presence of the competing proteins, since it has been noted that HRgpA is more efficient in a number of biological contexts than RgpB. This enhanced activity has often been attributed to the extra adhesin subunits found on HRgpA compared to RgpB and, indeed, it has been shown here that fibrinogen in plasma is cleaved in different way from purified fibrinogen. However, this difference is limited to the rate of β -chain degradation and accumulation of some cleavage products. Thus, it appears that the adhesin subunits of HRgpA play relatively little overall role in determining the cleavage rate of peptide or protein substrates in a complex physiological environment.

P. gingivalis is one of the major pathogens associated with adult periodontitis. Since periodontitis is one of the main causes of tooth loss today, and more recently has been linked to cardiovascular diseases, factors contributing to the virulence of the bacterium are attractive targets for the design of drugs or vaccines against the disease (Genco *et al*, 1999; Beck *et al.*, 1996; Genco, 1998). Gingipains-R are essential for the survival of *Porphyromonas gingivalis* and responsible for various intrinsic and

extrinsic factors associated with its virulence (Imamura *et al.*, 2000; Imamura *et al.*, 1997; DiScipiro *et al.*, 1996; Imamura *et al.*, 1994). Determination of the P₂' and P₃' specificity of the gingipain-R enzymes thus helps to define the properties of their active-site and improve our understanding of the specificity of these enzymes, which can be used further to develop selective synthetic inhibitors to combat periodontal disease.

CHAPTER FOUR

SPECIFICITY STUDIES OF GINGIPAINS REVEAL CO-OPERATIVITY IN BINDING OF SUBSTRATE RESIDUES TO THE ACTIVE SITES OF THE ENZYMES

4.1 Introduction

As elucidated in previous chapters, the gingipains-R and gingipain-K enzymes produced by *Porphyromonas gingivalis* are important and potent virulence factors in periodontal disease. The gingipains degrade constituents of the periodontal tissue, destroy host defence elements and dysregulate the kallikrein-kinin, coagulation and complement pathways (Potempa *et al.*, 1995a). The importance of these enzymes makes them an ideal target for development of specific potent therapeutic inhibitors.

This study follows on from the specificity studies in the previous chapter, where the P₂' and P₃' specificity of the gingipains-R was determined using a set of fluorescent quenched peptides. Results from the previous chapter showed a difference between the specificity of HRgpA and RgpB at P₂' and P₃', which was further investigated and found to be largely due to the four amino acid substitutions around the active site of HRgpA compared to RgpB. Here the specificity from P₃- P₃' was determined for HRgpA and RgpB, and gingipain-K (Kgp). Initially, a library of 6-mer peptides was constructed and screened as inhibitors against HRgpA, RgpB and Kgp. This strategy yielded a single inhibitory binding constant, in contrast to the K_m and k_{cat} data generated for the P₂' and P₃' positions for the gingipains-R, but this was sufficient to map the preferences of the active site binding pockets. This strategy allowed for faster screening of the many peptides produced for the three enzymes under study.

At the time of starting this work, no other similar studies had been carried out. Recent work by Curtis *et al.* showed Kgp to be an important factor for the virulence of *P. gingivalis* and a specific inhibitor for this enzyme to be a potential therapeutic agent in the control of the infections caused by the bacteria (Curtis *et al.*, 2002). This

publication briefly described the process whereby the specific inhibitor was identified, but did not describe the specificity of the enzyme. It did, however, serve to emphasize the importance of determining the specificity of Kgp and not just the gingipain-R enzymes.

In the present study, the specificity of both prime and non-prime sites was investigated. The peptide inhibitors being screened against the gingipain-R enzymes had an arginine at the P₁ position with a basic sequence of *G-G-R-G-G-G*, while inhibitors for Kgp contained a lysine at P₁ position and had the basic sequence of *G-G-K-G-G-G*. This initial strategy was selected to give more information about the actual site under investigation. The study in the previous chapter utilised a substrate library with the sequence GPRS in the P₃-P₁' positions. In particular, the Pro residue at the P₂ position might strongly influence binding of all other residues in the substrate, perhaps giving less clear information about the specificity of any site under investigation. This is unlikely to be the case with the Gly residues in the present substrate set and therefore it was expected that information gained in this study about individual subsites might be more defined. The comparison between the two studies should also be of considerable interest. Following screening of the first set of inhibitors, the results were used to construct a second library of peptides to study the key subsites identified in the first round screening in the context of supposedly favourable residues at the other sites. The ultimate aim was to gain information to aid development of potent, specific inhibitors for the gingipains.

4.2 Materials and Methods

4.2.1 Peptide Inhibitors for Primary screening

The peptide inhibitors were synthesized by Dr. Neil O'Brien-Simpson at the School of Dental Sciences, University of Melbourne. The peptide inhibitors were synthesized as 6-mers and the sequence of the inhibitors used for gingipains-R and -K are described below.

Gingipain-K	Gingipains-R
G-G-K-G-G-X	G-G-R-G-G-X*
G-G-K-G-X-G	G-G-R-G-X-G
G-G-K-X-G-G	G-G-R-X-G-G
G-X-K-G-G-G	G-X-R-G-G-G
X-G-K-G-G-G	X-G-R-G-G-G

Table 4.1: Structure of peptide inhibitors used to investigate the specificity of HRgpA, RgpB and Kgp in the first round of screening.

*The "X" in the peptides inhibitors indicates the position under investigation, in which 17 different amino acids were substituted. The amino acids, cysteine and glycine were not used in the study. Arginine residues were not substituted for gingipain-R enzymes and lysine residues were not substituted for gingipain-K.

4.2.2 Kinetic Studies

The K_i values were measured at 37°C using peptide inhibitor concentrations of 100 μ M, with a final concentration of active site titrated enzyme of 10 nM in 0.2 M

Tris-HCl, 5 mM CaCl₂, 10 mM cysteine, 0.1 M NaCl, pH 7.6 and a substrate concentration of 10 μM. The assay was performed in a total volume of 200 μl in microtitre plates. To 50 μl of peptide inhibitor, 50 μl of activated enzyme solution was added, followed immediately by the addition of 100 μl of 20 μM Z-Phe-Arg-AMC substrate for HRgpA and RgpB, and 20 μM Z-Ala-Lys-AMC substrate for Kgp. The initial turnover rate of the substrate was recorded at 370/460 nm on a fluorescent plate reader (FLUOstar *Galaxy*, BMG Labtechnologies, Australia). The K_i values were calculated using the formula below (Salvesen and Nagase, 1989):

$$K_i = \frac{[I]}{v_0/v_i} \times \frac{[S]}{K_m} + 1$$

Where [I] is the concentration of peptide inhibitor;

[S] is the concentration of substrate;

v_0 is the velocity of the enzyme in the absence of inhibitor;

v_i is the velocity of the enzyme in the presence of inhibitor.

K_m values determined in Chapter Two were used in the above equation for the respective gingipains. The K_m values were as follows: 31.6 μM for HRgpA, 21.9 μM for RgpB and 10.6 μM for Kgp.

4.2.3 Peptide inhibitors for secondary screening

A second set of peptide inhibitors was designed and produced based on the results from the screening of the first set of inhibitors. The gingipains generally showed the greatest selectivity at the P₁' and the P₃ positions (see results). To further determine the selectivity of the gingipains at these positions, new sets of peptide inhibitors, 9-mers, were constructed where the amino acids at P₂' and P₃' position with the lowest K_i values for the gingipains from the first round of screening were used and the two amino acids with the lowest K_i values at the P₂ position were substituted at this position. Table 4.2 below indicates the sequences of the peptide inhibitors screened against the gingipains.

<i>HRgpA</i>	<i>RgpB</i>	<i>Kgp</i>
<i>G-X-N-R-G-M-A-A-G</i>	<i>G-X-S-R-G-W-N-A-G</i>	<i>G-X-A-K-G-F-I-A-G</i>
<i>G-G-N-R-X-M-A-A-G</i>	<i>G-G-S-R-X-W-N-A-G</i>	<i>G-G-A-K-X-F-I-A-G</i>
<i>G-X-D-R-G-M-A-A-G</i>	<i>G-X-I-R-G-W-N-A-G</i>	<i>G-X-H-K-G-F-I-A-G</i>
<i>G-G-D-R-X-M-A-A-G</i>	<i>G-G-I-R-X-W-N-A-G</i>	<i>G-G-H-K-X-F-I-A-G</i>

Table 4.2. The general sequence of the second round of inhibitors used to screen the specificity of the gingipain enzymes.

4.3 Results

This study was designed to determine the specificity of HRgpA, RgpB and Kgp, in order to provide the basis for the design and development of a potential inhibitor for each gingipain. Initially, a library of 6-mer peptide inhibitors was designed and screened against the enzymes. The basic sequence of the inhibitors was G-G-K-G-G-G for Kgp and G-G-R-G-G-G for the gingipains-R. Due to the absolute specificity of the gingipains for the P₁ position (Lys residues for Kgp and Arg residues for HRgpA/RgpB), this strategy also obviated the need to check that the peptides were indeed being cleaved at the supposed P₁ position. The positions P₃, P₂, P₁' , P₂' and P₃' were investigated, with all the amino acids except cysteine and glycine substituted at each position for both gingipains-R and -K. It must be noted that Arg residues were omitted from any position other than P₁ for gingipains-R, and similarly Lys residues were omitted for Kgp. This eliminated potential secondary cleavage positions in the peptide molecules.

The screening method utilized a kinetic scheme in which the competitive inhibition by the inhibitory peptide was measured by comparing the velocity for cleavage of the substrate in the presence and absence of the inhibitor. It must be noted that only a single concentration of the inhibitory peptide was used in order to facilitate more rapid screening of the library, whereas the true K_i values require the comparison of the relative velocities over a number of inhibitor concentrations (Salvesen and Nagase, 1989). Thus, while the K_i values obtained are unlikely to be the true or real K_i values, the relative strength of each inhibitor will most likely be accurately revealed and thus the selectivity of a given subsite and its preference for binding of a

particular amino acid is likely to be accurately reflected by the kinetic scheme used. The competitive effect of the substrate was taken into account using the K_m value for the substrate and its concentration. It should be noted that the inhibitory peptide will in fact be cleaved by the enzymes and thus over the course of the assay, its concentration would be likely to change. Thus only initial velocities were used and during the study no deviations from linearity in the initial velocity plots was noted.

4.3.1 Primary Screening of gingipain specificity

4.3.1.1 Specificity of HRgpA

HRgpA showed highest affinity for peptides with a lysine residue at positions P_1' , P_3' , P_2 and P_3 (Table 4.3), as indicated by the lowest K_i values. The K_i values ranged from 0.2 μM for the peptide with a lysine at P_3 to 1.7 μM at the P_3' position. At P_2 and P_2' positions, HRgpA also displayed an affinity for the peptides with a methionine, with K_i values of 0.8 μM and 1.2 μM , respectively. Peptides with tyrosine and tryptophan residues had low affinity for HRgpA and thus had high K_i values. Similarly, peptides with a proline residue at the P_1' and P_3 positions had low affinity for the enzyme.

P_3 : HRgpA showed the highest selectivity (634) at this position. Most preferred were charged or polar amino acids, with Lys, Asn or Glu residues yielding the lowest K_i values. The substitution of a Thr residue resulted in the highest K_i for this position: it should be noted that this was a major influence on the high selectivity factor obtained. There did not seem to be great specificity for any particular group of amino acids at this position.

P_2 : This position generally showed much lower selectivity (6.6) than the P_3 position, substitution with Met or Lys residues yielding the highest affinity, while amino acids with ring structures in their side chains, such as His or Tyr had the highest K_i values.

P_1' : Similar to the P_2 position, much less selectivity (factor of 7.5) was displayed at the P_1' position. The most preferred residues were charged or polar, while the Pro

substituted peptide was the worst. HRgpA in general showed a preference for charged amino acids at P_1' position, with the least preferred amino acid being proline.

P_2' : At P_2' , HRgpA showed no particular preference towards any group of amino acids with a selectivity factor of 7.2, where methionine was the most preferred and tryptophan the least preferred amino acid.

P_3' : The selectivity factor of HRgpA at P_3' was 11.7. HRgpA preferred the positively charged lysine residue and showed a lesser affinity towards inhibitors with hydrophobic or aromatic side chains.

P ₃		P ₂		P ₁ '		P ₂ '		P ₃ '	
Residue	K _i	Residue	K _i	Residue	K _i	Residue	K _i	Residue	K _i
N	0.2	M	0.8	K	1.4	M	1.2	K	1.7
E	0.2	K	0.8	N	2.3	A	2.0	A	1.8
K	0.2	I	0.9	D	2.7	L	2.6	D	2.5
D	0.8	L	0.9	V	3.3	P	2.8	N	2.8
W	2.5	N	1.1	Y	3.7	V	2.8	T	3.4
F	2.7	E	1.3	H	3.9	N	2.9	P	3.4
H	4.1	S	1.4	M	4.4	F	3.0	E	3.5
M	5.8	F	1.6	E	4.5	Q	3.0	M	3.7
L	7.2	A	1.8	T	5.0	I	3.5	H	4.2
I	7.4	P	2.2	I	5.8	K	3.5	Q	4.3
A	7.8	D	2.4	Q	6.1	S	3.6	I	4.4
Y	7.8	T	2.5	L	6.1	H	3.8	L	4.6
S	13.1	V	3.2	F	6.1	E	3.8	F	4.7
Q	21.1	Q	3.5	A	8.1	T	4.2	V	5.3
V	22.3	W	4.4	S	8.2	D	5.7	S	5.6
P	29.2	H	5.1	W	10.5	Y	6.5	Y	6.9
T	164.9	Y	5.3	P	10.7	W	8.6	W	20.9
Selectivity Factor	634.2		6.6		7.5		7.2		11.7

Table 4.3. Inhibition constants (K_i) for HRgpA against peptide inhibitors with substitutions at P₁', P₂', P₃', P₂ and P₃. Units for K_i are expressed in μM . Assays were carried out in triplicate, with errors less than 10%.

4.3.1.2 Specificity of RgpB

In general, RgpB preferred positively charged amino acids, followed by negatively charged amino acids, with least preference towards hydrophobic amino acids. RgpB showed a high affinity for peptides with a lysine residue at the P₂, P₃, P₁' and, to a lesser extent, P₃' positions (Table 4.4).

P₃: At P₃, RgpB showed a preference for positively charged and hydrophilic amino acids. With a selectivity factor of 7.9, RgpB showed some selectivity at P₃, with least preference for bulky hydrophobic groups.

P₂: The non-polar, hydrophobic amino acid leucine was least preferred at P₂. With the lowest *K_i* value for the peptide with a lysine at P₂ of 3.4 μM, RgpB showed a preference for lysine and had a selectivity factor of 16.

P₁': At P₁', RgpB had a selectivity factor of 10.6 and showed a preference towards positively charged amino acids and a lesser preference for non-polar, hydrophobic amino acids.

P₂': The highest affinity of RgpB at P₂' was towards a peptide that contained a tryptophan residue (*K_i* of 1.28 μM), followed by peptides with positively charged amino acids. The selectivity factor at P₂' position was 25, with the least preference for negatively charged aspartate.

P_3' : With a selectivity factor of 3, RgpB did not show much selectivity at P_3' , although generally it preferred polar or positively charged amino acids and least preferred hydrophobic and negatively charged amino acids.

P ₃		P ₂		P ₁ '		P ₂ '		P ₃ '	
Residue	K _i	Residue	K _i	Residue	K _i	Residue	K _i	Residue	K _i
Q	11.7	K	3.4	H	12.6	W	1.28	N	7.3
K	14.7	S	5.4	K	16.1	H	4.3	A	9.6
T	16.5	I	6.9	S	21.7	I	4.7	K	10.7
S	16.6	P	8.7	N	35.6	K	6.9	P	11.9
D	19.4	F	8.8	V	36.8	S	7.1	M	12.0
H	25.6	V	10.1	T	39.8	F	7.6	L	12.2
V	27.7	M	11	D	42.5	V	8.1	H	12.6
E	28.2	A	11.1	E	48.2	L	8.5	F	13.8
F	30.1	T	11.2	Y	49.6	Q	9.1	V	14.6
P	34.3	N	12.6	A	54.2	T	9.7	S	14.7
A	36.0	D	13.6	I	59.7	Y	11.2	T	15.4
I	42.5	E	14.6	Q	61.8	M	11.5	Q	15.8
N	42.8	W	14.8	M	63.5	E	13.1	E	16.6
M	44.8	Q	22.1	F	85.3	A	13.4	Y	17.4
L	46.4	H	22.4	L	90.1	P	14.4	D	17.8
Y	87.8	Y	24.6	P	99.8	N	20.6	I	20.3
W	92.7	L	55.8	W	133.7	D	32.4	W	24.9
Selectivity Factor	7.9		16.4		10.6		25.3		3.4

Table 4.4. Inhibition constants (K_i) for RgpB against peptide inhibitors with substitutions at P₁', P₂', P₃', P₂ and P₃. Units for K_i are expressed in μM . Assays were carried out in triplicate, with errors less than 10%.

4.3.1.3 Specificity of Kgp

Kgp was inhibited more efficiently by peptides with substitutions at the non-prime sites than at the prime sites (Table 4.5). Overall, the selectivity at the non-prime sites was low.

P_3 : Peptides containing a histidine or a proline were the worst inhibitors at P_3 , whereas peptides with a phenylalanine or threonine were the best. The selectivity factor at this position was relatively low at nearly 5.

P_2 : At the P_2 position, Kgp was most efficiently inhibited by the peptide with an alanine residue at this position, followed by the peptides containing histidine or valine residues. The peptide with an alanine had a K_i of 1.58 μM and the peptide with a serine, which was the worst inhibitor, had a K_i of 13 μM . There was a slightly higher selectivity factor of 8 at this position.

P_1' : At the P_1' position, Kgp showed a preference for positively charged amino acids, with the peptide with an arginine at P_1' being the best inhibitor ($K_i = 12.3 \mu\text{M}$). With a selectivity factor of 15 and a K_i value of 190 μM for the peptide with a tyrosine at P_1' , Kgp showed least preference for peptides with amino acids with aromatic groups and negatively charged amino acids.

P_2' : Kgp showed greatest selectivity at the P_2' position with a selectivity factor of nearly 55, due to the low K_i value for the peptide with a phenylalanine ($K_i = 1.2 \mu\text{M}$) and the high K_i value of 66.4 μM for the substitution with a proline residue. At the

P_2' position, Kgp preferred amino acids with hydrophobic aromatic groups, thus peptides containing a phenylalanine and a tryptophan were the best inhibitors.

P_3' : Kgp showed a clear preference against amino acids with aromatic R groups, namely phenylalanine, tyrosine, tryptophan and histidine at P_3' . Kgp showed a preference for non-polar hydrophobic amino acids at P_3' and was best inhibited by peptides containing an isoleucine, alanine or serine at this position and had a selectivity factor of 7.2.

P ₃		P ₂		P ₁ '		P ₂ '		P ₃ '	
Residue	K _i	Residue	K _i	Residue	K _i	Residue	K _i	Residue	K _i
F	3.1	A	1.5	R	12.3	F	1.2	I	6.4
T	3.1	H	1.6	N	13.9	W	2.0	A	7.0
Q	4.7	V	1.8	P	15.4	N	11.3	S	8.1
A	5.2	W	3.4	F	16.0	S	12.0	V	9.2
I	5.2	P	3.7	M	16.2	R	13.7	E	9.4
E	5.5	I	5.3	S	16.8	I	14.7	Q	9.6
S	6.5	F	5.9	H	17.8	T	14.9	R	9.9
M	6.6	L	6.4	T	19.6	H	16.2	L	10.1
R	6.8	T	7.1	A	20.1	E	16.5	T	10.1
N	7.1	Q	7.3	L	21.0	D	17.0	P	11.2
D	7.5	N	7.6	I	27.8	V	17.9	M	11.5
W	8.3	D	8.4	Q	28.0	M	20.8	D	11.9
Y	9.4	E	9.1	V	33.4	Q	23.5	N	12.8
V	10.7	Y	11.6	D	40.0	A	26.4	H	13.5
L	12.4	R	11.7	W	40.9	Y	28.3	F	18.0
H	15.2	M	11.8	E	49.0	L	29.0	W	23.0
P	15.4	S	13.1	Y	190.4	P	66.4	Y	46.6
Selectivity Factor	4.9		8.3		15.4		54.8		7.2

Table 4.5. Inhibition constants (K_i) for Kgp against peptide inhibitors with substitutions at P₁', P₂', P₃', P₂ and P₃. Units for K_i are expressed in μM . Assays were carried out in triplicate, with errors less than 10%.

4.3.1.4 Comparison of HRgpA, RgpB and Kgp

A comparison of the specificity of the three gingipains HRgpA, RgpB and Kgp at the P₃- P₃' positions indicates the gingipains are fairly different. HRgpA displays the lowest K_i values overall, followed by RgpB and then Kgp. HRgpA showed the greatest selectivity towards peptide inhibitors at the P₃ position with a 630-fold difference between the best and worst inhibitor (Fig. 4.5). Kgp showed the lowest selectivity towards peptide inhibitors at the P₃ position with only a 5- fold difference between the best and worst peptide inhibitors. The K_i values for HRgpA towards peptide inhibitors at the P₂ position were very low ranging from 0.8 μM to 5.3 μM (Fig. 4.4). The selectivity of all three gingipains at the P₂ position was fairly low. At the P₁' position, Kgp showed the highest selectivity with a 15-fold difference between the best and worst inhibitor, followed by RgpB with a 10-fold difference and HRgpA with a 7-fold difference (Fig. 4.1). At the P₂' position, HRgpA did not show much selectivity, with only a 6-fold difference between the highest and lowest K_i value, whereas Kgp had a 55-fold difference between the K_i value of the best and worst inhibitor (Fig. 4.2). The specificity of Kgp and RgpB at P₃' was similar, with both gingipains having similar affinity towards the peptide inhibitors (Fig. 4.3).

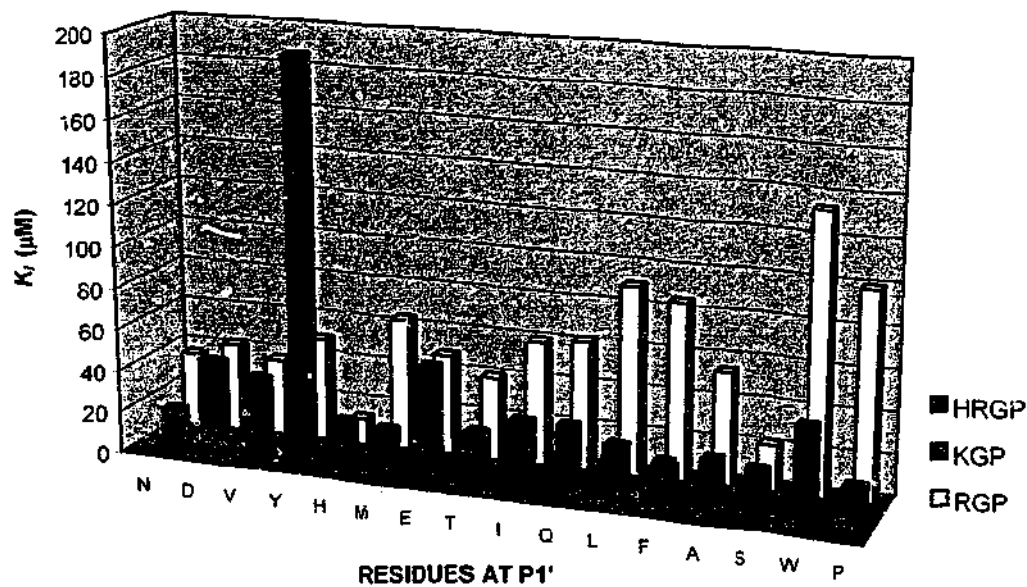


Figure 4.1. A comparison of inhibition constants of HRgpA, RgpB and Kgp towards peptides with varying amino acids at P₁'.

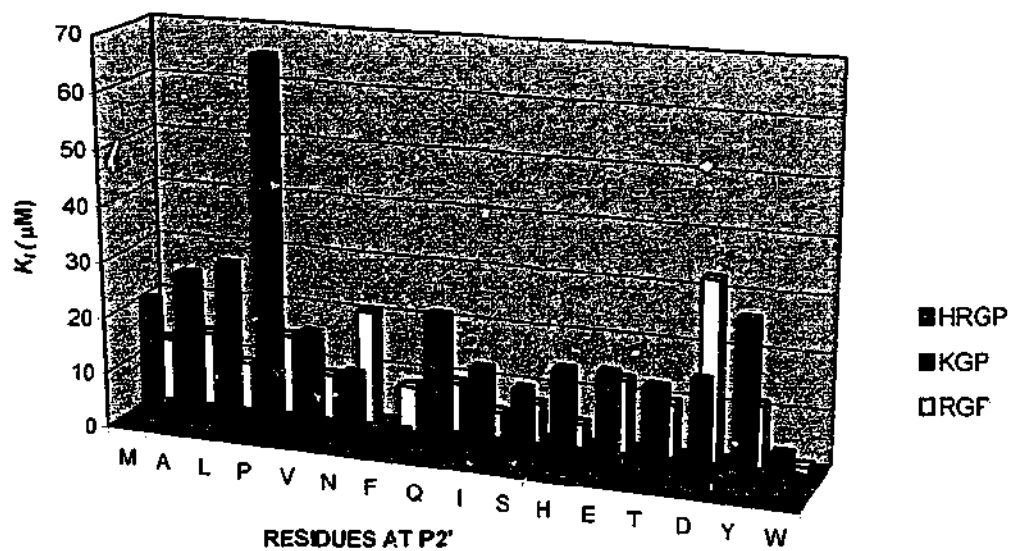


Figure 4.2. A comparison of inhibition constants of HRgpA, RgpB and Kgp towards peptides with varying amino acids at P₂'.

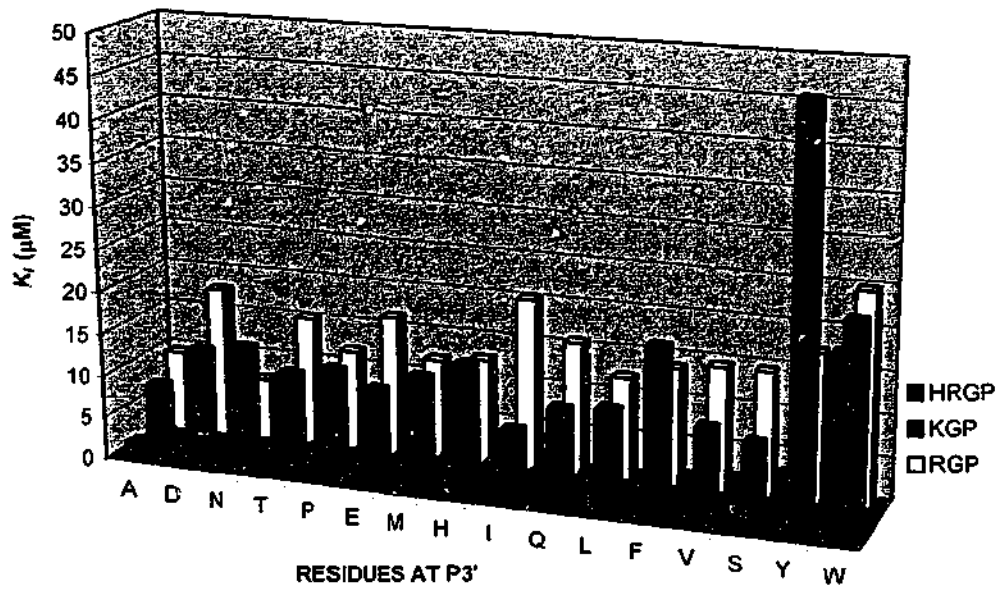


Figure 4.3. A comparison of inhibition constants of HRgpA, RgpB and Kgp towards peptides with varying amino acids at P₃'.

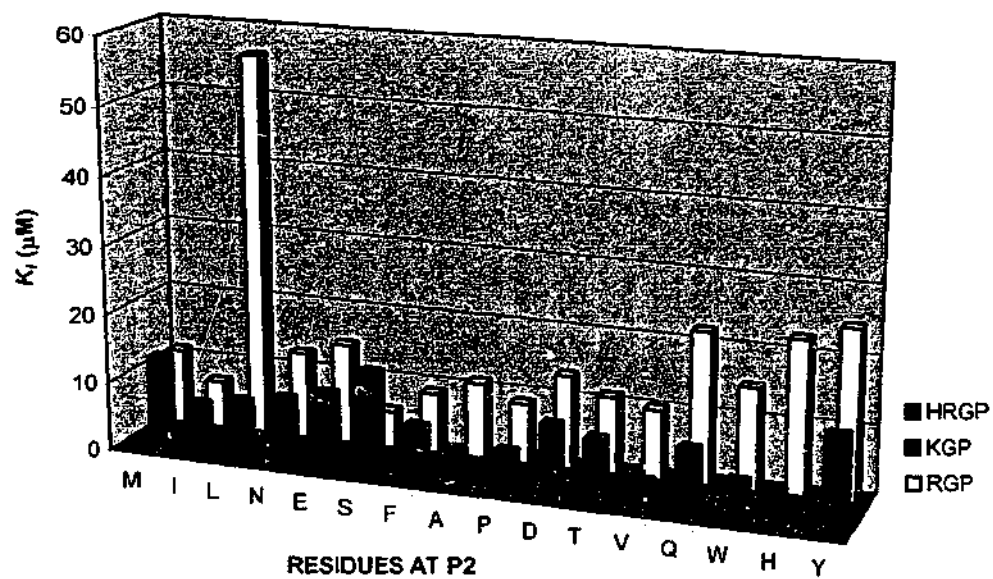


Figure 4.4. A comparison of inhibition constants of HRgpA, RgpB and Kgp towards peptides with varying amino acids at P₂.

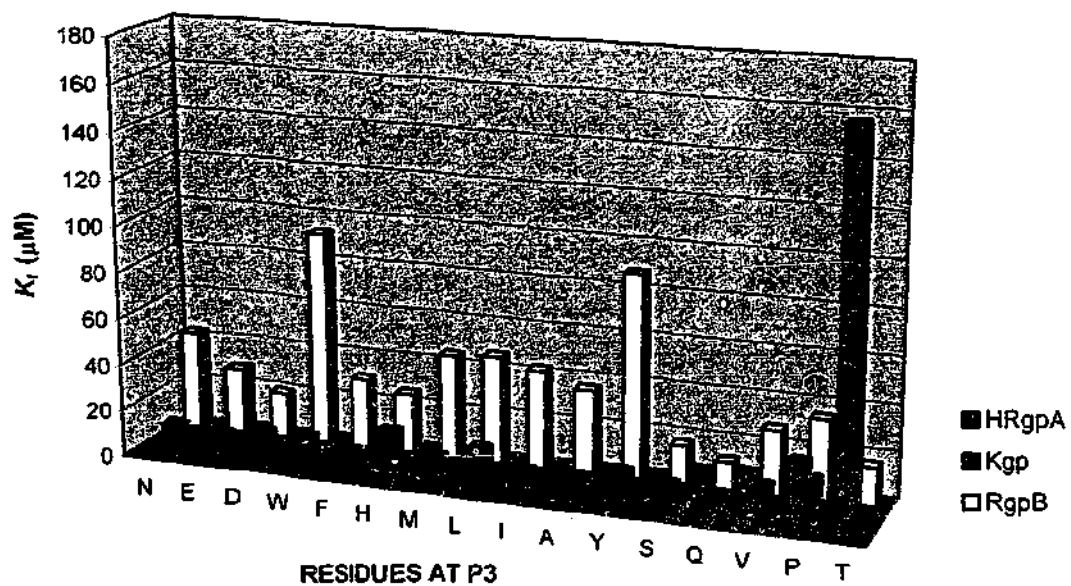


Figure 4.5. A comparison of inhibition constants of HRgpA, RgpB and Kgp towards peptides with varying amino acids at P₃.

4.3.2 Secondary screening of gingipain specificity

Following the first round of screening, a second set of peptide inhibitors was designed to further investigate the specificity of the respective gingipains based on the results from the screening of the first set of inhibitors. Since HRgpA was most efficiently inhibited at the P_3 position, with a selectivity factor of 634, the specificity at this position was further investigated for all enzymes. Also, since the P_1' position is an important position in a substrate/inhibitor, as the enzyme cleaves the peptide inhibitor between P_1 and P_1' position, the specificity at P_1' was also further investigated. Amino acids at P_2' and P_3' that were found to yield the lowest K_i values for the respective gingipains were placed at these positions and held constant. For example, the inhibitor with a methionine at the P_2' position and the inhibitor that contained an alanine at P_3' , were most efficient at inhibiting HRgpA. Thus, peptide inhibitors designed for HRgpA, contained a methionine residue at P_2' and an alanine residue at P_3' . At the P_2 position, two amino acids were substituted, both displaying good inhibition of HRgpA. For instance for HRgpA, the amino acids aspartate and asparagine were selected, yielding two separate sets of inhibitors. The sequence of inhibitors designed for each enzyme is described in Table 4.2. Thus, having selected the amino acids for positions P_2' , P_3' and P_2 , peptide inhibitors were designed and constructed for all three gingipains in the same manner, to further determine the specificity at P_1' and P_3 .

4.3.2.1 HRgpA Selectivity

Surprisingly, despite the amino acid substitutions yielding the most efficient inhibition being selected, generally K_i values were much higher for HRgpA in this round of screening, suggesting that despite the individual amino acids being good for binding to HRgpA, in combination the peptides did not bind efficiently.

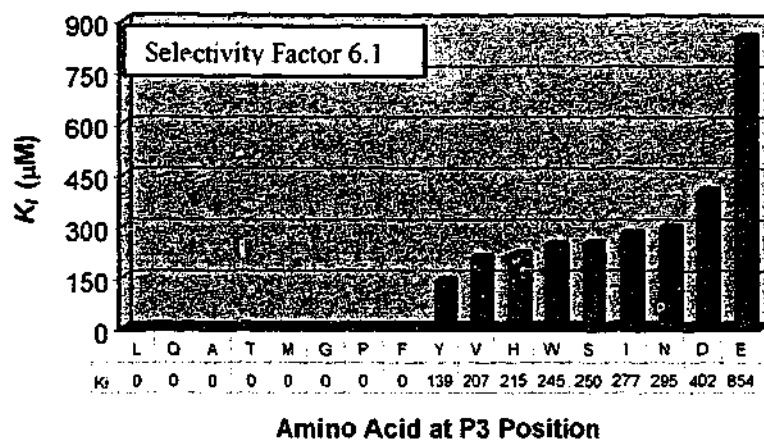
In the second round of screening for HRgpA, the peptides with an aspartate at the P_2 position and substitutions at P_1' showed the greatest selectivity. However, it must be noted that there was in fact considerable selectivity at P_3 when aspartate was at P_2 since a number of peptides did not inhibit HRgpA at all. For inhibitory peptides, there was a 26-fold difference between the lowest and highest K_i values (Fig. 4.7). The best peptide inhibitor had a tyrosine at P_1' and an asparagine residue at P_3 ($K_i=33 \mu\text{M}$), and the worst inhibitor in this series was the peptide with a proline at P_1' with a K_i of $886 \mu\text{M}$. Peptides with nonpolar, hydrophobic amino acids at P_1' were generally poor inhibitors.

The peptides with P_3 under investigation and an aspartate at P_2 showed the least selectivity with only a 6-fold difference between the best and worst peptide inhibitor. Peptides with a leucine, glutamine, alanine, threonine, methionine, glycine, proline or phenylalanine at P_3 did not inhibit HRgpA at all. HRgpA was most efficiently inhibited by the peptide containing a tyrosine at P_3 and was poorly inhibited by peptides containing negatively charged amino acids.

Peptides with an asparagine at P₂ and either P₃ or P₁' position under investigation, showed a selectivity of 11-fold and 16-fold, respectively (Fig. 4.6B and Fig. 4.7B). The *K_i* values for HRgpA were quite high, with the highest *K_i* value overall for the peptide with a methionine at P₁' and an asparagine at the P₂ position (1340 μM).

With an asparagine at P₂ and the P₃ position under investigation (Fig. 4.6B), HRgpA showed a preference for non-polar hydrophobic amino acids, the best inhibitor being that with a tryptophan at P₃. The peptide containing an aspartate residue at P₃ in this series was the worst inhibitor with a *K_i* of 642 μM. HRgpA showed no particular pattern of preference at P₁' when the peptides contained an asparagine at the P₂ position (Fig. 4.7B). There was 16-fold selectivity, with the peptides containing a serine, glutamine or isoleucine being the best inhibitors, while the peptide containing a methionine was the worst.

A



B

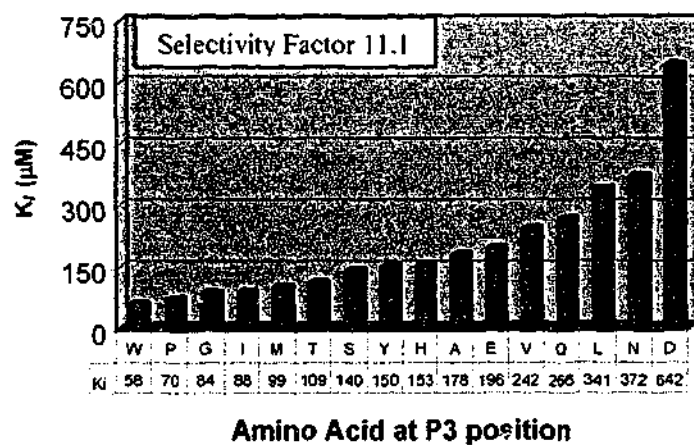
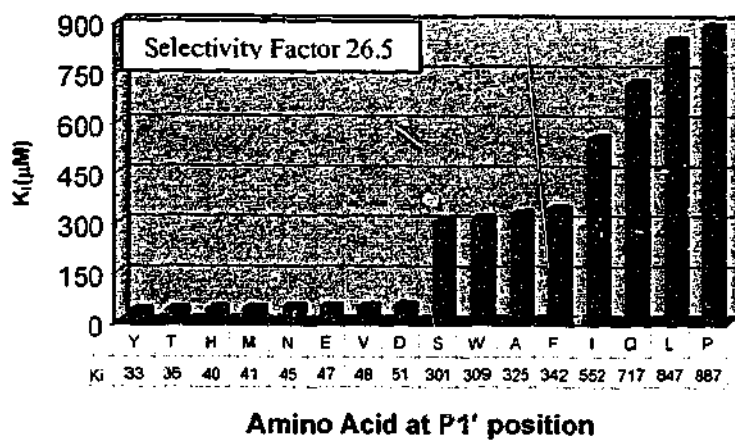


Figure 4.6. Inhibition constants (K_i) for HRgpA with the (A) P_2DP_3 and (B) P_2NP_3 series. K_i values are expressed in μM . All assays were carried out in triplicate and had errors of 10% or less. K_i value of zero (0) denotes no inhibition.

A



B

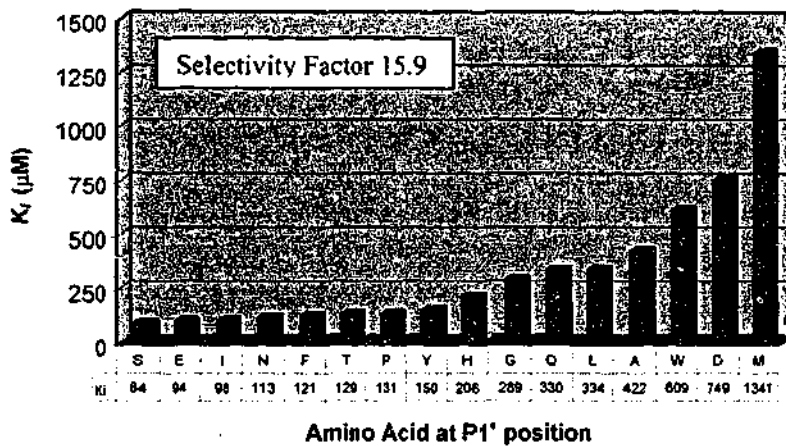


Figure 4.7. Inhibition constants (K_i) for HRgpA with the (A) P₂DP₁' and (B) P₂NP₁' series. K_i values are expressed in μM . All assays were carried out in triplicate and had errors of 10% or less.

4.3.2.2 RgpB Selectivity

The basic sequence for peptides screened against RgpB was *G-X-S-R-G-W-N-A-G*, with either a serine or an isoleucine at P₂ and the P₁' and P₃ positions under investigation.

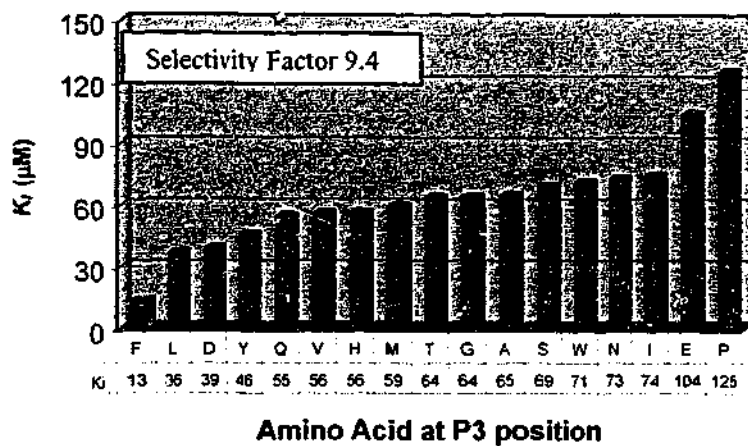
The best selectivity was achieved with peptide inhibitors containing a serine at P₂ and the P₁' position under investigation, with a selectivity factor of 168 (Fig. 4.9A). Neither of the peptides containing a proline at P₁' inhibited RgpB. RgpB was inhibited most efficiently by the peptide containing a histidine at the P₁' position and was poorly inhibited by peptides containing negatively charged amino acids, with the worst K_i value being 1111 μ M for aspartate.

The selectivity factor for peptides with a serine at the P₂ position and the P₃ position under investigation was 9 (Fig. 4.8A), with the lowest K_i value being for the peptide inhibitor containing a phenylalanine at P₃ (13 μ M) and the highest for the peptide inhibitor containing a proline at P₃ (125 μ M).

Peptides with an isoleucine at P₂ and the P₃ position under investigation had a selectivity of only 2.6 and thus did not show much selectivity (Fig. 4.8B). HRgpA showed a preference for peptides with non-polar hydrophobic groups at P₃, with peptides containing a proline, leucine or alanine being the best inhibitors. Peptides with negatively charged amino acids at P₃ were the worst inhibitors.

Peptides with an isoleucine at P_2 and the P_1' position under investigation also showed very little selectivity, with only a 3-fold difference between the best and worst inhibitor (Fig. 4.9B). The worst inhibitor was the peptide containing a phenylalanine at P_1' . The peptide containing a leucine at P_1' was the best inhibitor of RgpB.

A



B

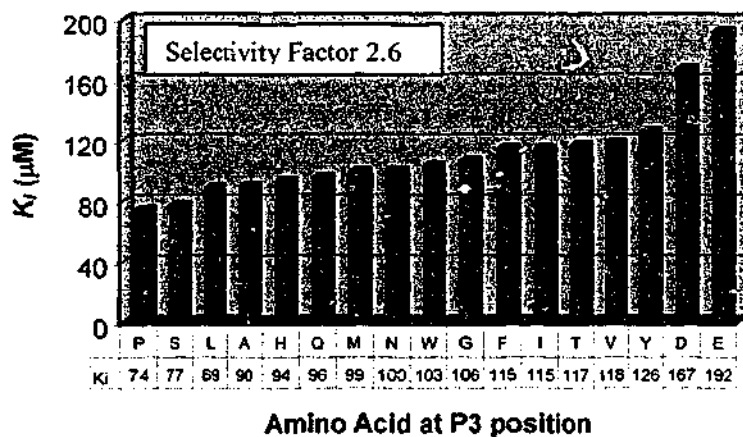
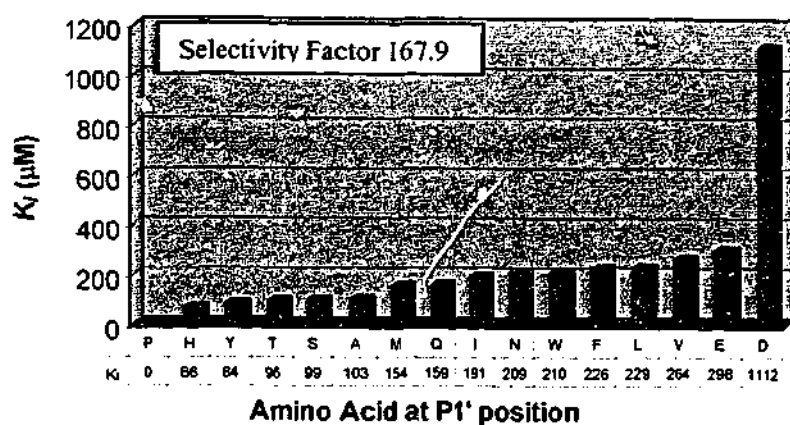


Figure 4.8. Inhibition constants (K_i) for RgpB with the (A) P₂SP₃ and (B) P₂I P₃ series. K_i values are expressed in μM . All assays were carried out in triplicate and had errors of 10% or less.

A



B

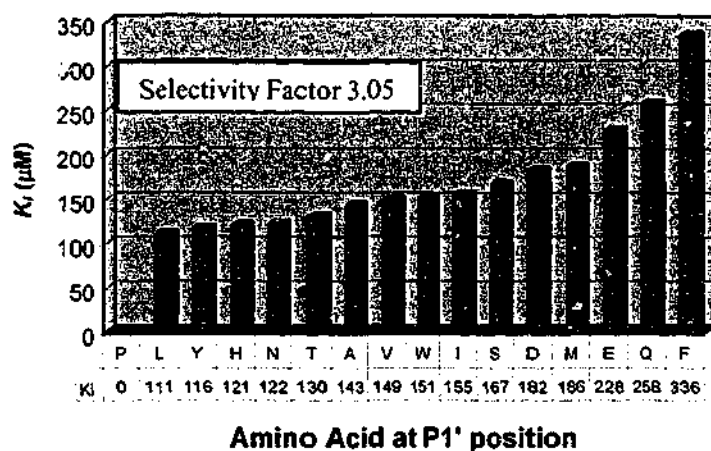


Figure 4.9. Inhibition constants (K_i) for RgpB with the (A) P_2SP_1' and (B) P_2IP_1' series. K_i values are expressed in μM . All assays were carried out in triplicate and had errors of 10% or less. K_i value of zero (0) denotes no inhibition.

4.3.2.3 Kgp Selectivity

Peptides screened against Kgp had the basic sequence *G-X-A-K-G-F-I-A-G*, with either an alanine or a histidine at P₂ and the P₃ and P₁' positions under investigation. The lowest *K_i* value for Kgp was with the peptides containing an alanine at P₂ and the P₃ position under investigation (Fig. 4.10A). Generally the series of peptide inhibitors with an Ala at P₂ showed much lower *K_i* values than the peptides containing a His at P₂. The peptide with an alanine at both the P₂ and P₃ positions had the lowest *K_i* value (0.6 μM).

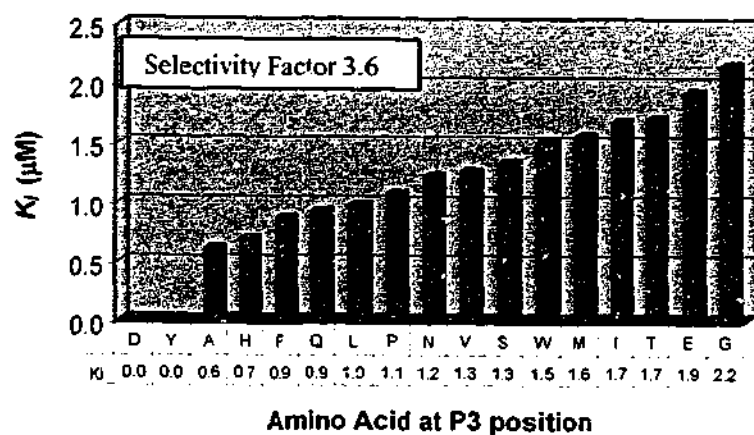
Kgp did not show much selectivity for peptides with an alanine at P₂ and the P₃ position under investigation (selectivity factor 12.5) [Fig. 4.10A]. Peptides with either an alanine or a histidine at P₃ had a *K_i* value of *ca.* 0.6 μM and were the best inhibitors. Peptides with either a glutamate or a glycine at P₃ position were the worst inhibitors. Kgp was not inhibited by peptides that contained an aspartate or a tyrosine at P₃. Peptides containing an alanine at P₂ with the P₁' position under investigation (Fig. 4.11A) had a selectivity factor of 12. The peptides with hydrophobic and negatively charged amino acids at P₁' were the worst inhibitors of Kgp, with the peptide containing a proline having a *K_i* value of 56 μM. Kgp was best inhibited by the peptide containing a tyrosine at P₁'.

With a histidine residue at P₂ and P₃ under investigation (Fig. 4.10B), Kgp showed a preference for peptides containing aromatic groups at the P₃ position, thus peptides containing a tyrosine, phenylalanine, histidine or tryptophan had the lowest *K_i*

values. Peptides containing isoleucine, valine or glycine residues at P₃ were not good inhibitors.

Kgp showed the highest selectivity towards peptides that contained a histidine at P₂ and the P₁' position under investigation, with a 22-fold difference between the best and worst peptide inhibitor (Fig. 4.11B). Peptides with a serine, isoleucine, alanine, leucine, phenylalanine, or glutamine at P₁' position did not inhibit Kgp at all. The lowest K_i value was towards the peptide that contained a proline at P₁' (21.8 μ M) and the highest K_i value was 476 μ M for the peptide that contained an aspartate at P₁'.

A



B

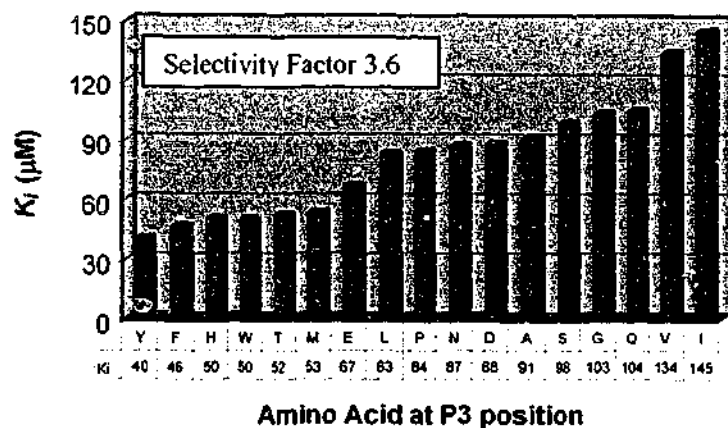
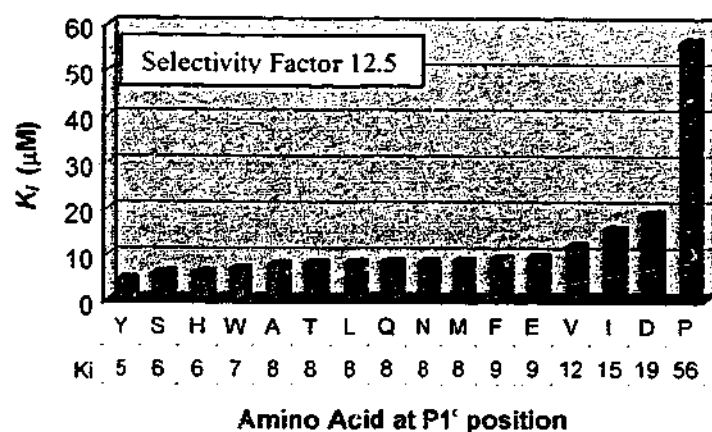


Figure 4.10. Inhibition constants (K_i) for Kgp with the (A) P_2AP_3 and (B) P_2HP_3 series. K_i values are expressed in μM . All assays were carried out in triplicate and had errors of 10% or less. K_i value of zero (0) denotes no inhibition.

A



B

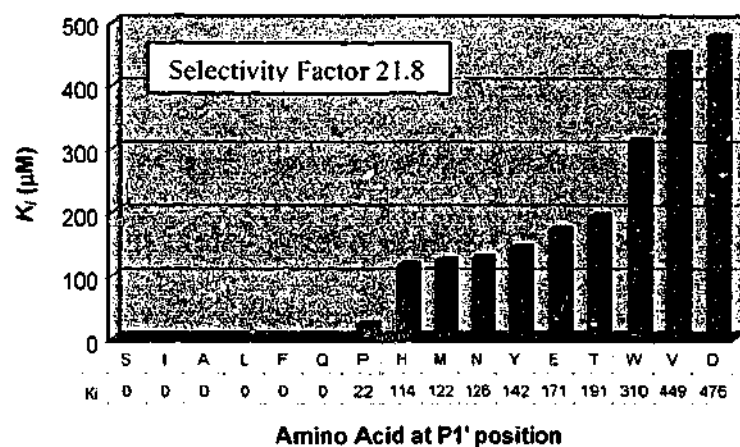


Figure 4.11. Inhibition constants (K_i) for Kgp with the (A) P_2AP_1' and (B) P_2HP_1' series. K_i values are expressed in μM . All assays were carried out in triplicate and had errors of 10% or less. K_i value of zero (0) denotes no inhibition.

4.4 Discussion

The study described in this chapter follows on from the study in chapter three where the specificity of the gingipain-R, enzymes was determined at P₂' and P₃' and the influence of the additional adhesin domains on the specificity of HRgpA was investigated. This study aimed to determine the P₃- P₃' specificity of three gingipain forms, HRgpA, RgpB and Kgp, in order to provide the information needed to develop a potential inhibitor for each of the gingipains. The specificity of the gingipains at P₁', P₂', P₃', P₂ and P₃ was determined by screening the gingipains against an initial library of peptide inhibitors. Following screening of the first set of peptides, a second set of peptide inhibitors was designed for each gingipain based on the results from the first set of peptides and further screening conducted.

HRgpA showed an affinity for peptides with a positively charged lysine residue at positions P₁', P₃', P₂ and P₃, with the lowest K_i values at these positions being towards the peptides with lysine in all of the above positions. These results are similar to the results in the previous chapter, where HRgpA was found to show the greatest affinity towards substrates with a polar asparagine residue at P₂' or a positively charged lysine residue. HRgpA showed the greatest selectivity at the P₃ position, with a 630-fold difference between the best and worst peptide inhibitor, indicating the potential importance of the P₃ position in the binding of a potential inhibitor. HRgpA generally had the lowest K_i values for the peptide, indicating a high affinity for the peptide substrate, similar to the results determined in the previous study where HRgpA was found to have a high affinity for the substrates. The active site of the catalytic domain of HRgpA (RgpA_{cat}) was modelled in the

previous chapter, based on the crystal structure of RgpB and was found to be relatively flat and characterized by a negative electrostatic surface. This overall negative electrostatic surface might be the reason for HRgpA's higher affinity towards positively charged or polar amino acids.

Similar to the specificity of HRgpA, RgpB too showed an affinity towards peptides with positively charged residues. RgpB showed a high affinity for peptides with a lysine residue at P₂, P₃, P₁' and P₃' with the lowest overall K_i value for the peptide with a lysine at P₂ position being 3.4 μM. This correlates to the crystal structure of RgpB, which contains a largely electronegative surface across the active site (Fig. 15). This explains the affinity of RgpB for positively charged residues. The K_i values for RgpB were not as low as those for HRgpA, but they were lower than the values for Kgp.

For Kgp, the peptide with a phenylalanine at the P₂' position had the lowest K_i value of 1.2 μM. There was a 55-fold difference between the peptide with the lowest and highest K_i value at P₂'. Although the crystal structure of Kgp has not been solved to date, the specificity of Kgp would indicate that the catalytic domain of Kgp would also most likely be negatively charged since in several instances, Kgp preferred positively charged residues.

This study was based on providing the information needed for rational design of peptide-based inhibitors for the gingipains, HRgpA, RgpB and Kgp. To gain maximal information, the specificity of each subsite from P₃-P₃' was determined for

each gingipain. Results from the first round of screening were used to select the 'best' residue for each subsite, i.e. the amino acid residue that generated the lowest K_i values. The overall concept was then to synthesize the "best" substrate for each enzyme, by synthesizing a peptide, which had each "best" residue at each subsite. Underlying this strategy is the principle of additivity in the binding of substrate residues to the enzymes, i.e. that each individual subsite interaction with the substrate would add to the overall interaction in an independent manner, such that the overall interaction was a simple sum of the interaction at each subsite. This is the assumption underlying most protease-substrate interactions, although not much literature exists to support or deny it. The other way in which individual amino acids might contribute to the overall binding of the substrate/inhibitor, is in a cooperative model. This model would imply that binding of each amino acid in the substrate at each subsite would affect binding of amino acids at other subsites. Such a model of binding is difficult to accommodate for a P_3 - P_3' substrate, as the number of interactive and cooperative effects which might be occurring would be enormous.

Before a "best" substrate/inhibitor was synthesized, it was decided to synthesize a further round of substrates/inhibitors for screening. This was to allow further investigation of two key subsites that were identified. The assumption at the outset of the second round of screening was that the P_3 and P_1' positions should be investigated with the other subsites occupied with the "best" amino acid residues. It was assumed that the synthesized molecules would have higher affinity than the first round of inhibitors overall, since three of the subsites, P_2 , P_2' and P_3' , would have the best substrate residues in this position. Since for each enzyme, there were two amino acid residues that could be regarded as the best residues at P_2 , two sets of

substrates/inhibitors were made for each position under investigation. This also gave rise to an excellent test for the additivity versus cooperativity models, since the additive model would suggest that the two substrate sets should yield very similar values because in the first round of screening, they yielded rather similar K_i values. Overall, the second round of synthesized molecules provided a test of the model of ideal substrate design, since lower K_i values in general should have been obtained.

Overall, the data from the second round screening provided very strong support for a cooperative model of binding of substrate residues to individual subsites in the case of the three gingipain forms tested here. Aside from the results obtained for Kgp with a P₂ Ala residue, all other sets of substrates gave much higher K_i values for the second round of substrates/inhibitors, despite supposedly having the best amino acids at all positions except the one under study. Even with the best amino acid at the position under study, as indicated by first round screening, the overall K_i was much higher. This indicated that cooperative interactions between the amino acids at each subsite in this case had disastrous consequences for the overall interaction compared to the first round of screening. It did usually result in increased selectivity, with many substrate/inhibitors no longer even inhibitory, but this effect on "selectivity" was not a desirable one in the context of trying to construct a potent, selective inhibitor for each enzyme.

Further support for the cooperative mode of substrate binding came from the data for each set of substrate/inhibitors with different residues only at P₂. Here again, the K_i values differed markedly between the two sets and the reaction of individual amino acid residues differed markedly dependent on which amino acid was at the P₂

position. This strongly implies that the P₂ residue strongly affects the binding of the adjacent P₃ residue, which is perhaps not that surprising, but it also strongly affected binding at P₁' , which is perhaps more surprising. This suggests that for the gingipain enzymes, the mechanism of binding substrates is highly cooperative. It was instructive to note that the best inhibitors for any of the enzymes were those with an Ala residue at the P₂ position for Kgp. Only these inhibitors actually had higher affinity than first round inhibitors.

Overall, therefore, the best substrate/inhibitors can be inferred from all of these studies, to at least serve as some kind of starting point for inhibitor design. It appears that for all enzymes, it would be better to have mainly small amino acids present at all sites except the P₁ residue (which would be Arg for the gingipains-R and Lys for gingipain-K) and perhaps one other site which was most selective for each enzyme. For HRgpA, this site would most likely be P₃ and the best K_i was recorded for this enzyme with Asn, Lys or Glu present at P₃ and Gly residues at all other positions except for the P₁ Arg residue. For RgpB, the best combination of affinity and selectivity was provided by the P₂' position, with a Trp residue at this position yielding the lowest K_i in this study and this position most selective in the first round of study. For Kgp, the substrate/inhibitor with the lowest K_i was yielded in the second round of screening (*G-A-A-K-G-F-I-A-G*), thus this might be an excellent starting point for this enzyme. It should be noted that even the best K_i values obtained in this study were in the micromolar range, however, which is far from ideal in terms of inhibitor potency. Thus the most objective viewpoint from outcomes of the present study is that rational inhibitor design for the gingipains is likely to be

very difficult indeed. The study by Curtis *et al.* (2002), in which they used random screening of large libraries of compounds and found a very specific, potent inhibitor of Kgp, indicates that this approach is very powerful. Taken together with the results from the present study, which indicates that rational design of inhibitors will most likely be very difficult, the outcome is a strong indication that the random screening approach may in fact be far more successful and efficient, despite the lack of information it actually provides about the active sites of the enzymes under study, which is the strength of the method employed here. The present study has provided some leads for further substrate design and, perhaps even more importantly, has strongly indicated which avenues not to follow in the further design and development of specific peptide-based inhibitors to help combat and stop the progression of periodontal disease.

CHAPTER FIVE

FINAL DISCUSSION

Proteolytic enzymes produced by bacteria are implicated in the onset and pathogenesis of several diseases. In most cases, the enzymes have a very important role to play in the pathogenesis and progression of the disease. The role of the enzymes varies from functions such as providing nutrients for the bacterium to destruction of host defense proteins.

Adult periodontitis is one of the major causes of tooth loss in populations around the world today. *Porphyromonas gingivalis* is a Gram-negative bacterium associated with the onset of the disease. Gingipains, a group of powerful cysteine proteinases produced by this bacterium, *P. gingivalis*, are enzymes that have been shown to be important factors in the pathogenesis of the disease (Kuramitsu, 1998; Holt *et al.*, 1999). The two main types of gingipains, gingipain-R and gingipain-K, have been shown to have a variety of different functions, some of which include degradation of components of the complement pathway and other important host defense proteins, activation of coagulation factors, and cleavage of matrix proteins to provide nutrients for the bacterium (Imamura *et al.*, 2000; Imamura *et al.*, 1997; Lantz *et al.*, 1991; DiScipio *et al.*, 1996), all of which have been shown to play an important role in the survival and growth of the bacteria, resulting in the progression of the disease. Studies have shown that null mutants of *P. gingivalis* for gingipain-R enzymes showed a marked decrease in virulence in *in vivo* models, and immunization with peptides corresponding to the N-terminal sequence of the catalytic domain of gingipains-R have also been shown to protect against infection by the bacteria in mouse models (Genco *et al.*, 1998), indicating the overall importance of these enzymes in the pathogenesis of the disease by the bacterium.

The importance of these enzymes makes them an ideal target for development of specific potent therapeutic inhibitors.

This study focused extensively on the specificity of the gingipains, gingipains-R, HRgpA and RgpB, and gingipain-K, Kgp, with a view to helping to develop inhibitors of the enzymes. A better understanding of the substrate specificity of the gingipains would aid in the development of an inhibitor that would specifically target the enzymes. The purification of the gingipains from the bacteria *P. gingivalis* (Chapter 2) was a crucial part of this study. Although, HRgpA, RgpB, and RgpA_{cat}, the catalytic domain of HRgpA, along with Kgp have been previously purified from the bacteria (Pike *et al.*, 1994; Potempa *et al.*, 1998), this study was the first to purify Kgp_{cat}, the catalytic domain of the lysine-specific gingipain, Kgp, from the culture supernatant of *P. gingivalis*. The purification of RgpA_{cat} was essential and was useful in Chapter 3, to help establish the reason for the differences in specificity at the P₂' and P₃' position between the two gingipains-R, HRgpA and RgpB. Although Kgp_{cat} was successfully purified, it was not used in any of the studies carried out as part of this thesis. Similar to the study carried out in Chapter 3, Kgp_{cat} could be used in the future to establish the role of the additional adhesin domains in the specificity of Kgp.

The specificity studies of HRgpA and RgpB at P₂' and P₃' in Chapter 3, determined that there is a difference in specificity between the two gingipains at the prime subsites. Although neither gingipain showed a preference for any particular group of amino acids at P₂' and P₃', there was a significant difference

noted in the K_m values of the gingipains towards the substrates at these positions. RgpB had a broader range of K_m values compared to HRgpA, indicating that RgpB had a greater difference in its binding affinity towards the substrates. The difference in the specificity of the two gingipains was thought to be due to the additional adhesin domains and this hypothesis was investigated by modeling the catalytic domain of HRgpA (RgpA_{cat}) on the crystal structure of RgpB. The active sites of the two gingipains were found to be identical except for four amino acid substitutions D281→N, Y283→S, P286→S and N331→K, found in the active site of HRgpA compared to RgpB.

To establish whether it was the amino acid substitutions or the additional adhesin domains that were responsible for the differences in specificity of the two enzymes, a limited specificity study was conducted on HRgpA, RgpB and RgpA_{cat}, the catalytic domain of HRgpA purified in Chapter 2. Although RgpA_{cat} lacked the additional adhesin domains present in HRgpA, the specificity of HRgpA and RgpA_{cat} was found to be similar, with both displaying similar K_m values. The K_m values obtained for RgpB differed from the values obtained for HRgpA and RgpA_{cat} and were nearly two-fold greater, indicating that RgpB has a weaker affinity towards the substrates.

Thus, the differences in specificity between HRgpA and RgpB are most likely due to the difference in the four amino acid substitutions in the active site of HRgpA compared to RgpB. The additional adhesin domains in HRgpA were found to play a minor role in cleavage of a protein or peptide substrate, reinforcing the previous finding that the four amino acid substitutions in the active site of the catalytic domain

are most likely responsible for the differences in specificity between HRgpA and RgpB. Results from the study in Chapter 3 led to the conclusion that the difference in specificity between HRgpA and RgpB is not due to the additional adhesin domains in HRgpA as described in previous studies, but is most likely due to the four amino acid substitution found in the active site of HRgpA as compared to RgpB. Although previous studies have attributed the differences in the cleavage of protein and peptide substrates between HRgpA and RgpB to the additional adhesin domains contained in HRgpA, the results from this study indicated that although the adhesin domains mediate binding of HRgpA to a protein substrate, they do not influence the cleavage of a substrate.

Following on from the results obtained in Chapter 3, an extensive and complete study of the specificity of the gingipains, HRgpA, RgpB and Kgp was carried out in Chapter 4. The specificity of gingipains was mapped for both prime and non-prime sites, from P₃- P₃' and single equilibrium inhibitory constants, K_i were generated using two sets of peptide libraries. Previous studies to determine the specificity of the gingipains have used commercially available peptide substrates. This study was unique and was one of the first of its kind, as it used the principle of rational drug design, to gain maximal information on the specificity of HRgpA, RgpB and Kgp, to design potential peptide inhibitors for the gingipains. The study included not only the gingipains-R, but also Kgp, as previous studies have shown it to be an important virulence factor for *P.gingivalis*, and more recently a study by Curtis *et al.* (2002), showed a specific inhibitor of Kgp to be a potential therapeutic agent in the control of the disease caused by the bacteria.

The results from the first set of screening of the peptide library showed a significant difference in the specificity of the three gingipains, with the exception of similar specificity towards the peptide inhibitor substrates between Kgp and RgpB at P₃'.

Results from the screening of the first set of peptides were used to select the 'best' residue for each subsite, i.e. the amino acid residue that generated the lowest K_i values, to design a second series of more specific peptide inhibitors for the gingipains. The principle of additivity was used to design the second series of peptides, whereby the substitution of the "best" residue at each subsite would result in the synthesis of the "best" substrate for each enzyme and each individual subsite interaction with the substrate would add to the interaction in an independent manner, resulting in an overall sum of interactions at each subsite. This is the assumption underlying most protease-substrate interactions, although not much literature exists to support or deny it. The other manner, in which individual amino acids might contribute to the overall binding of the substrate/inhibitor, is in a cooperative model. This model would imply that binding of each amino acid in the substrate at each subsite would affect binding of amino acids at other subsites. Such a model of binding is difficult to predict for a P₃-P₃' substrate, as the number of interactive and cooperative effects which might be occurring would be enormous.

Results obtained in Chapter 4, lead to the conclusion that the specificity of gingipains is cooperative rather than additive, the latter being the assumption generally used in the principle of rational design of inhibitors. These results lend strong support to a cooperative model of binding of substrate residues to individual subsites in the case

of all three gingipains. This further leads to the conclusion that the approach of rational design of inhibitors for gingipains is not a suitable one and will not lead to the construction of a selective and potent inhibitor for the enzymes.

The approach used by Curtis *et al.* (2002), in comparison to this study is a more suitable approach, where the screening of large random libraries of compounds resulted in the selection of a very potent and selective inhibitor for Kgp. Thus, the findings of this study have helped to conclude that the principle of rational design of inhibitors is not a suitable approach to use for gingipains, as the mode of specificity of these enzymes was found to be cooperative rather than additive. Although, this study only looked at the specificity of the gingipains and established the mode of selectivity of these enzymes towards substrates, it leads us to question the mechanism of specificity in other proteolytic enzymes and the approach used to design inhibitors. This finding might have to be taken into consideration when looking at using the approach of rational design of inhibitors for enzymes in future, as it may not be the most appropriate and efficient approach.

By narrowing down the specificity and providing an extensive knowledge of the selectivity of the gingipains, this study has helped lead us to a more appropriate approach of inhibitor design for gingipains, to be used in future studies. The emergence of bacterial pathogen resistance to common antibiotics strongly supports the necessity to develop alternative mechanisms for combating drug-resistant forms of infective bacteria (Travis and Potempa, 2000). The design and development of a selective and potent peptide-based inhibitor against gingipains will not only prove

valuable in retarding the growth and proliferation of *P.gingivalis*, but also lead to the use of this type of inhibitors against invasion by other infective organisms.

APPENDIX I

Expression of Protease-activated Receptor-2 by Osteoblasts

**Abraham, L.A., Chinni, C., Jenkins, A.L., Lourbakos, A., Ally, N., Pike, R.N.,
and Mackie, E.J.**

Bone 26: 7-14 (2000)

Expression of Protease-activated Receptor-2 by Osteoblasts

L. A. ABRAHAM,¹ C. CHINNI,¹ A. L. JENKINS,² A. LOURBAKOS,² N. ALLY,² R. N. PIKE,² and E. J. MACKIE¹

¹School of Veterinary Science, University of Melbourne, Parkville, Victoria, Australia

²Department of Biochemistry and Molecular Biology, Monash University, Clayton, Victoria, Australia

Osteoblasts express protease-activated receptor-1 (PAR-1), which is activated by thrombin or by synthetic peptides corresponding to the new "tethered ligand" N-terminus of PAR-1 created by receptor cleavage. Both thrombin and human PAR-1-activating peptide stimulate an elevation of $[Ca^{2+}]_i$ in the human SaOS-2 osteoblast-like cell line, but the peptide stimulates receptor-mediated Ca^{2+} entry, whereas thrombin does not. Stimulation of proliferation in rat primary osteoblast-like cells is greater in response to rat PAR-1-activating peptide than to thrombin. Because the PAR-1-activating peptides are now known to activate PAR-2, the current study was undertaken to investigate whether osteoblasts express this receptor and, if so, whether this could account for the observed discrepancies between responses of osteoblasts to thrombin and to PAR-1-activating peptides. Reverse transcriptase-polymerase chain reaction (RT-PCR) and immunocytochemical studies demonstrated expression of PAR-2 by primary cultures of rat calvarial osteoblast-like cells. In immunohistochemical studies of embryonic mouse bones, osteoblasts showed positive staining for the presence of PAR-2. Activators of PAR-2 include trypsin, mast cell tryptase, gingipain-R, and synthetic peptides corresponding to the PAR-2 tethered ligand sequence. Treatment of primary rat osteoblast-like cells with rat PAR-2-activating peptide (SLIGRL), or SaOS-2 cells with human PAR-2-activating peptide (SLIGKV), caused a dose-dependent increase in $[Ca^{2+}]_i$. Trypsin or gingipain-R also induced an increase in intracellular calcium concentration, and caused reciprocal cross desensitization. Activators of PAR-2 caused a sharp peak in $[Ca^{2+}]_i$ followed by a sustained plateau; $[Ca^{2+}]_i$ returned to baseline levels upon treatment with ethyleneglycol tetraacetic acid (EGTA). Treatment of rat osteoblast-like cells in vitro with SLIGRL did not affect thymidine incorporation or endogenous alkaline phosphatase activity. The results presented here demonstrate that osteoblasts express PAR-2, and that such expression is able to account for the observed discrepancies between thrombin and PAR-1-activating peptides in their ability to evoke calcium entry, but not proliferative responses. (Bone 26:7-14; 2000) © 2000 by Elsevier Science Inc. All rights reserved.

Address for correspondence and reprints: Dr. Eleanor J. Mackie, School of Veterinary Science, University of Melbourne, Parkville, Victoria 3052, Australia. E-mail: e.mackie@vet.unimelb.edu.au

L.A.A. and C.C. contributed equally to the present work.

Key Words: Protease-activated receptor (PAR); Osteoblast; Thrombin; Trypsin; Gingipain-R; SaOS-2 cells.

Introduction

The protease-activated receptor family (currently known to consist of four members) belongs to the larger group of G-protein-coupled, seven transmembrane domain receptors.^{14,18,27,33} Activation of the protease-activated receptors (PARs) occurs through proteolytic cleavage of the extracellular domain, resulting in generation of a new N-terminal "tethered ligand." For PARs-1, -2, and -4, peptides corresponding to the newly created N-terminus, are able to activate the relevant receptor in the absence of receptor cleavage.

PARs-1, -3, and -4 are activated by thrombin, whereas PAR-2 is known to be activated by trypsin and mast-cell tryptase.^{10,21,24,27} The bacterial protease, gingipain-R, which is produced by one of the causative agents of periodontal disease, *Porphyromonas gingivalis*, has also recently been shown to activate PAR-2 in human neutrophils.²¹

We have previously demonstrated that osteoblasts express PAR-1 in vitro and in vivo, and that thrombin-induced calcium responses in osteoblast-like cell lines are inhibited by antibodies to PAR-1.^{1,16} In a human osteoblast-like cell line (SaOS-2), however, the profile of the calcium response to thrombin differs from that to human PAR-1-activating peptide; cells treated with thrombin show a sharp transient increase in $[Ca^{2+}]_i$, whereas those treated with human PAR-1-activating peptide show a sharp peak followed by a sustained plateau due to Ca^{2+} entry.¹⁵ In addition, like thrombin, rat PAR-1-activating peptide stimulates proliferation of primary rat osteoblast cultures, but the maximal response to the peptide is greater than the maximal response to thrombin.² Because it has recently been shown that the PAR-1-activating peptides activate PAR-2 as well as PAR-1,⁶ it seemed likely that the differential responses to activators of PAR-1 in osteoblasts result from concurrent activation of PAR-2 by the peptides. Indeed, activation of PAR-2 stimulates Ca^{2+} entry in epithelial cells,⁷ and is known to stimulate proliferation of endothelial cells.²⁵ Expression of PAR-2 has been described in a number of tissues, including kidney, and in the epithelial and smooth muscle components of the gastrointestinal tract, respiratory tract, blood vessels, and skin, but expression in bone has not previously been characterized.^{4,8,10,11,27,30} The current study was undertaken to determine whether osteoblastic expression of PAR-2 could account for the differential responses of osteoblasts to thrombin and PAR-1-activating peptides.

Materials and Methods

Materials

Type III trypsin from bovine pancreas, bradykinin, and all other chemicals, unless stated otherwise, were purchased from Sigma-Aldrich. The peptides SLIGRL, SLIGKV, and SFFLRNPSENT-FELVPL (SFFL) were manufactured by Auspep (Parkville, Australia). Rabbit anti-PAR-2 antibody was a generous gift from the late Prof. S. R. Stone. This antibody was raised against a peptide corresponding to the region spanning the cleavage site of murine PAR-2 (SKGRSLIGRLETQPPITGK-NH₂), conjugated to keyhole limpet hemocyanin (KLH). The antibody was affinity purified on a column of the peptide used for the immunization, passed over a second column to remove anti-KLH antibody, and dialyzed against phosphate-buffered saline (PBS) at 4°C. Specificity of the antibody was confirmed by enzyme-linked immunosorbent assay (ELISA) against the immunogenic peptide and peptides corresponding to the cleavage sites of PAR-1 and PAR-3. Gingipain-R was purified and activated as described.²⁹

Culture of Osteoblast-like Cells

Calvarial osteoblasts were derived by sequential collagenase digestion of calvariae removed from neonatal hooded rats (bred at the School of Veterinary Science, Parkville). Calvariae were removed from neonates within 12 h of birth and stripped of periosteum prior to incubation for 20 min at 27°C in 3 mL of enzyme solution containing 0.1% collagenase (Boehringer Mannheim), 0.05% trypsin (Gibco BRL), and 4 mmol/L ethylene-diamine tetraacetic acid (EDTA) in calcium- and magnesium-free PBS (Gibco BRL). The digestion was repeated to obtain six cell populations. The cells released during each digest were collected by centrifugation in 3 mL of fetal calf serum (FCS; Gibco BRL), and resuspended in Dulbecco's modified Eagle's medium without phenol red (DMEM; Gibco BRL), supplemented with 10% FCS, L-glutamine (300 µg/mL; Gibco BRL), gentamicin (50 µg/mL), and amphotericin B (2.5 µg/mL) for plating into tissue culture flasks.²⁰ Medium was changed every second day and cultures maintained in a humidified atmosphere at 37°C under 5% CO₂ in air. Cells were cultured to confluence, then trypsinized and pooled prior to plating in appropriate vessels for further experiments.

SaOS-2 cells (human osteosarcoma-derived osteoblast-like cells; kindly provided by Dr. J. Moseley) were originally from the American Type Culture Collection. They were cultured in minimum essential medium (MEM; Gibco BRL) with additives as listed previously for primary cultures, and maintained as noted for primary cultures.

Immunocytochemistry

Primary osteoblast-like cells were cultured in the wells of eight-chamber slides for immunostaining. The monolayers were washed with Hanks balanced salt solution (HBSS; Gibco BRL) and fixed for 10 min in 4% paraformaldehyde in HBSS. The fixed cultures were treated with 20% acetic acid at 4°C for 30 sec to extinguish endogenous alkaline phosphatase activity. After the blocking of nonspecific binding sites with 1.5% normal goat serum, the anti-PAR-2 antibody (2.5 µg/mL) was applied and incubated for 30 min. An alkaline phosphatase detection system (Immunopure, ABC Alkaline Phosphatase Staining Kit; Pierce) and red chromogenic substrate (Alkaline Phosphatase Kit 1; Pierce) were employed to detect the primary antibody. Cells were counterstained with hematoxylin, dehydrated, and mounted in Aquamount (BDH).

For immunohistochemical studies, embryos were harvested from C57BL mice on embryonic day 17 (E17). Dissected hindlimbs were fixed and processed for cryomicrotomy as described.¹ Cryostat sections (10 µm) were collected onto 3-aminopropyl-triethoxysilane-coated slides and stored at -70°C prior to immunostaining to detect the presence of PAR-2. Tissue sections were fixed in 4% paraformaldehyde in PBS for 10 min at room temperature and washed in PBS. Endogenous peroxidase activity was inhibited by a 30-min incubation in methanol containing 0.3% v/v hydrogen peroxide. After blocking with 1% BSA in PBS for 30 min, the anti-PAR-2 antibody was applied (2.5 µg/mL) to the sections overnight at 4°C. Control sections were incubated in the absence of primary antibody or in PAR-2 antibody preincubated with immunogenic peptide (5 µg/mL) for 30 min at 4°C. Primary antibody was followed by the avidin-biotin-peroxidase complex (ABC) procedure (Immunopure ABC Peroxidase Staining Kit, Pierce) and peroxidase activity detected by diaminobenzidine (Sigmafast Peroxidase Substrate Tablet Set, Sigma) according to the manufacturers' instructions. Sections were counterstained with hematoxylin, dehydrated, and coverslipped in nonaqueous mountant. Control sections appeared identical, whether incubated in the absence of primary antibody or in the presence of PAR-2 antibody preincubated with immunogenic peptide.

Polymerase Chain Reaction

Osteoblast-like cells were grown in monolayer cultures and total RNA isolated using a commercially available RNA isolation reagent (Trizol, Gibco BRL). RNA was extracted by the same method from rat kidney for use as a positive control. First-strand cDNA was synthesized from 7 µg of RNA with Moloney Murine Leukemia Virus reverse transcriptase using oligo(dT) primer (Ready-To-Go You-Prime First-Strand Beads, Pharmacia Biotech). Using the entire first-strand reaction, PCR amplification was performed according to manufacturer's instructions with the following primer pairs: PAR-1 (intron-spanning): sense 5'-ATG GGG CCC CGG CGC TTG CTG-3', antisense 5'-CCC TAA GCT AGT AGC TTT TTG TAT ATG-3' (predicted fragment size 1290 bp); PAR-2: sense 5'-CAC CAC CTG TCA CGA TGT GTC-3', antisense 5'-CCC GGG CTC AGT AGG AGG TTT TAA CAC (predicted fragment size 472 bp). Reaction mixtures in which either RNA was omitted from the first-strand synthesis or specific primers were omitted from the amplification step served as negative controls. The samples were placed in a thermal cycler for 32 cycles of the following profile: denaturation at 95°C for 1 min; annealing at 55°C for 1 min; and polymerization at 72°C for 1 min. The PCR products were electrophoresed in 1.8% (w/v) agarose gels and labeled with ethidium bromide for photography.

Intracellular Calcium Measurement

Confluent monolayers of primary osteoblast-like cells were trypsinized and pooled 24 h prior to calcium measurement for replating at the same density to enable more complete dissociation with 2 mmol/L EDTA at the time of the assay. SaOS-2 cells were also passaged 24 h prior to being used in the calcium assay. The monolayers were washed with calcium- and magnesium-free PBS and dissociated for 10 min with 2 mmol/L EDTA in calcium- and magnesium-free PBS. Cells were then collected by centrifugation in 10 mL of serum-free DMEM (rat cells) or MEM (SaOS-2 cells) at 800 rpm for 5 min. Cells were washed three times and resuspended at a density of 0.5-1.0 × 10⁵/mL in an extracellular medium containing 121 mmol/L NaCl, 5.4 mmol/L KCl, 0.8 mmol/L MgCl₂, 1.8 mmol/L CaCl₂, 6 mmol/L

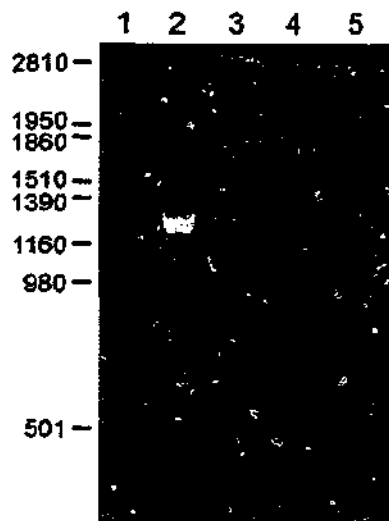


Figure 1. RT-PCR analysis of expression of protease-activated receptors by primary rat osteoblast-like cells. Lane 1: PAR-2 primers but no RNA. Lane 2: PAR-1 primers and osteoblast RNA. Lane 3: PAR-2 primers and osteoblast RNA. Lane 4: Osteoblast RNA but no primers. Lane 5: PAR-2 primers and rat kidney RNA.

NaHCO₃, 5.5 mmol/L glucose, 25 mmol/L HEPES, and 0.1% BSA (pH 7.3). The cells were loaded with 1 μ mol/L Fura-2/AM (Molecular Probes) for 30 min at room temperature. After centrifugation, cells were resuspended in extracellular medium and incubated for a further 30 min at room temperature to enable hydrolysis of the intracellular Fura-2/AM. Cells were centrifuged and resuspended in extracellular medium at a density of 0.5–1.0 $\times 10^5$ /mL for fluorescence measurements at 37°C in stirred cuvettes.¹⁶ For experiments involving giugipain-R, the final

resuspension was in extracellular medium without BSA. Calcium responses to different agonists were measured using a Perkin-Elmer LS 50B fluorimeter. The ratio of the fluorescence at 340 nm and 380 nm excitation and 510 nm emission was calculated. This ratio is proportional to the [Ca²⁺]_i.

Cell Proliferation

Osteoblast-like cell populations derived from the sequential calvarial collagenase digestions were dissociated after 7 days in culture and subcultured. The cells were resuspended at a density of 1 $\times 10^4$ per milliliter of medium for plating into 96 well tissue culture plates (100 μ L cell suspension per well). The cells approached confluence within 4–7 days and were deprived of serum, for a maximum of 24 h, prior to a 24 h incubation in the presence or absence of thrombin or SLIGRL, under standard conditions in serum-free medium containing 1 μ Ci/mL [³H]-thymidine (Amersham). Treatment of cells with 10% FCS served as a positive control. The cells were then washed twice with cold PBS and incubated at 37°C for 1 h in the presence of 80 μ L of trypsin (0.05%) and 0.53 mmol/L EDTA (Gibco BRL). Insoluble material from the dissociated cells was then harvested onto glass-fiber filters (ICN) using a cell harvester (Titertek Cell Harvester; ICN). The filters were dried at 37°C for 1 h and the filter disks transferred to 24 well microplate (Packard). After the addition of 300 μ L of scintillant (Microscint, MS-O; Packard), the plates were sealed for counting.³ The radioactivity (counts per minute [cpm]) of the samples within the plates was counted using a Packard Top Count microplate scintillation counter. Results are expressed as cpm and represent the means \pm values from ten replicate wells.

Alkaline Phosphatase Activity

Confluent calvarial osteoblast-like cell monolayer were trypsinized and plated in 24 well plates at a density of 2.0 $\times 10^4$

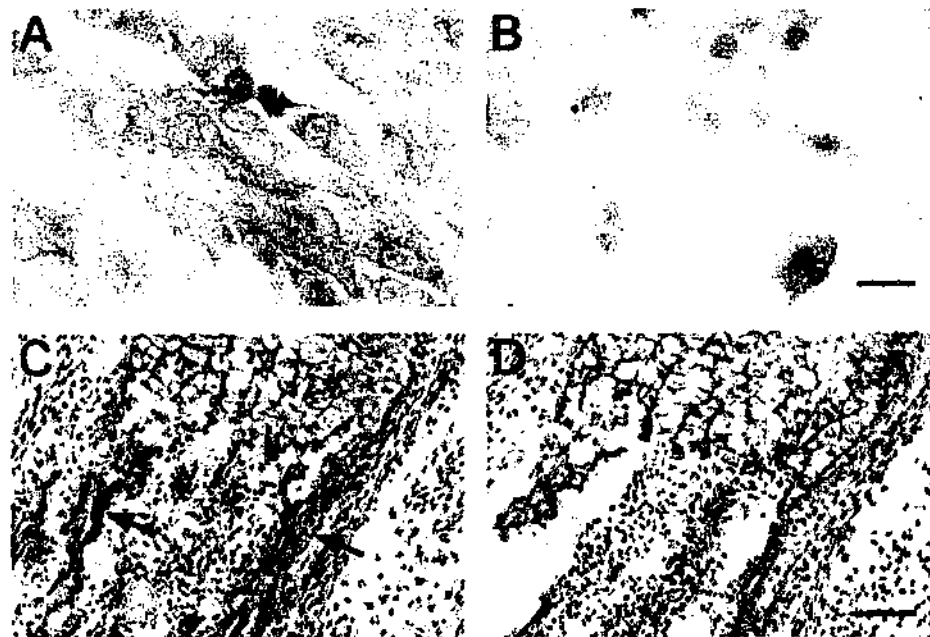


Figure 2. Expression of PAR-2 by osteoblasts in vitro and in vivo. (A,B) Monolayers of primary rat calvarial osteoblast-like cells were stained with anti-PAR-2 antibody (A) or antibody diluent (B). Staining was detected using alkaline phosphatase-labeled avidin-biotin complexes (red reaction product). The cells were counterstained with hematoxylin (bar = 25 μ m). (C,D) Sections of E17 mouse femur stained with anti-PAR-2 using peroxidase-labeled avidin-biotin complexes (brown reaction product) (C) or antibody diluent (D), and counterstained with hematoxylin. Arrows indicate specific PAR-2 staining of osteoblasts on the surfaces of spicules of primary spongiosa (bar = 100 μ m).

cells per well. Cells were cultured until subconfluent and deprived of serum for a maximum of 24 h prior to treatment for 24 h with thrombin (100 nmol/L) or SLIGRL (100 μ mol/L) in serum-free medium. Cells were washed in PBS and lysed by the addition of 100 μ L of PBS containing 0.5% Triton X-100. Two 40 μ L samples were removed from each well; the first sample was used to assay alkaline phosphatase activity and the second sample was assayed for total protein content. Both assays were performed in 96 well microtiter plates.

Aliquots of alkaline phosphatase substrate solution (60 μ L: 0.83 mol/L 2-amino-2-methyl-1-propanol, 3.3 mmol/L $MgCl_2$, 13.3 mmol/L *p*-nitrophenolphosphate [pH 10.0]) were added to the lysates (40 μ L) to achieve a final concentration of 8 mmol/L *p*-nitrophenolphosphate. For the generation of a standard curve, a serial dilution of a *p*-nitrophenol standard solution was prepared and 100 μ L of each concentration was included in each microtiter plate. Following incubation at 37°C for 30 min, 0.5N NaOH (100 μ L) was added to each well. The absorbance was read at 414 nm. The protein content of cell lysates was determined using the BCA assay (Pierce). Results of alkaline phosphatase assays are expressed as micromoles of *p*-nitrophenol per milligram of cellular protein and represent the means of values from four replicate wells.

Statistical Analysis

Data were analyzed using Microsoft EXCEL version 5 and results are expressed as the mean \pm SEM. The significance of differences between experimental groups was determined with Student's *t*-test.

Results

Expression of PAR-2 by Osteoblasts

The expression of PAR-2 by pooled primary calvarial osteoblast-like cells was investigated by RT-PCR and immunocytochemistry. PAR-2 primers detected a band of the appropriate size in RNA extracted from primary osteoblast cultures, as well as from kidney, which was used as a positive control (Figure 1, lanes 3 and 5). Intron-spanning PAR-1 primers detected only a single band of the predicted size for the appropriate region of mRNA, indicating the lack of detectable contamination of osteoblast RNA by genomic DNA (Figure 1, lane 2). Immunocytochemical staining of primary osteoblast-like cells revealed positive staining for PAR-2 expression (Figure 2A,B).

The expression of PAR-2 by osteoblasts *in vivo* was investigated by immunohistochemistry in embryonic mouse bones. Osteoblasts stained positively for PAR-2 expression. Figure 2C,D shows PAR-2 staining in osteoblasts forming the primary spongiosa of an E17 mouse femur.

Effects of Activators of PAR-2 on $[Ca^{2+}]_i$ in Osteoblast-like Cells

The ability of activators of PAR-2 (SLIGRL, trypsin, and ginsipain-R) to stimulate an increase in $[Ca^{2+}]_i$ was investigated in pooled rat calvarial osteoblast-like cells. Because the cells used are known to possess PAR-1,¹⁵ and because trypsin appears to activate PAR-1 in some cell types,²⁶ cross-desensitization studies between activators of PAR-1 and PAR-2 were also carried out. Bradykinin (1 μ mol/L) was added following specific activators to ensure that intracellular calcium pools had not been depleted. The rat PAR-2-activating peptide SLIGRL stimulated a dose-dependent increase in $[Ca^{2+}]_i$ with an EC_{50} of 2.4 μ mol/L (Figures 3 and 4A). The human PAR-2-activating peptide

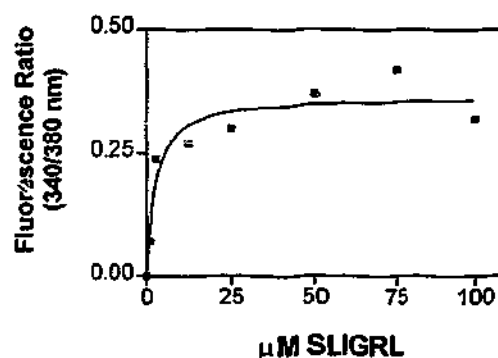


Figure 3. Intracellular calcium mobilization in Fura-2-loaded rat osteoblast-like cells treated with different concentrations of SLIGRL.

SLIGKV did not, however, elicit a response in rat cells (Figure 4B). Trypsin treatment also resulted in a transient rise in $[Ca^{2+}]_i$ (Figure 4 and Figure 5). Treatment of cells with trypsin abolished subsequent calcium responses to SLIGRL or thrombin but not to SFFL (Figure 5A,B). Neither SLIGRL nor thrombin, however, desensitized cells to trypsin (Figures 4A and 5C).

Following the initial calcium spike in response to SLIGRL or trypsin treatment of rat osteoblast-like cells, there was a sustained elevation above the resting level (Figures 4 and 5). Because similar traces had been obtained previously in the human SaOS-2 cell line with human PAR-1-activating peptide

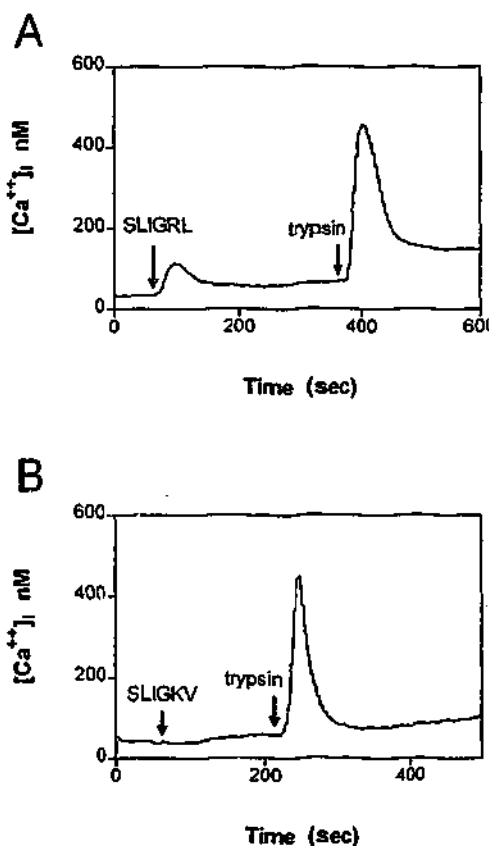


Figure 4. Species specificity of calcium responses by rat osteoblast-like cells to PAR-2-activating peptides. Calcium traces for Fura-2-loaded cells treated with the rat peptide (A) (SLIGRL, 100 μ mol/L), or the human peptide (B) (SLIGKV, 100 μ mol/L), followed by 200 nmol/L trypsin.

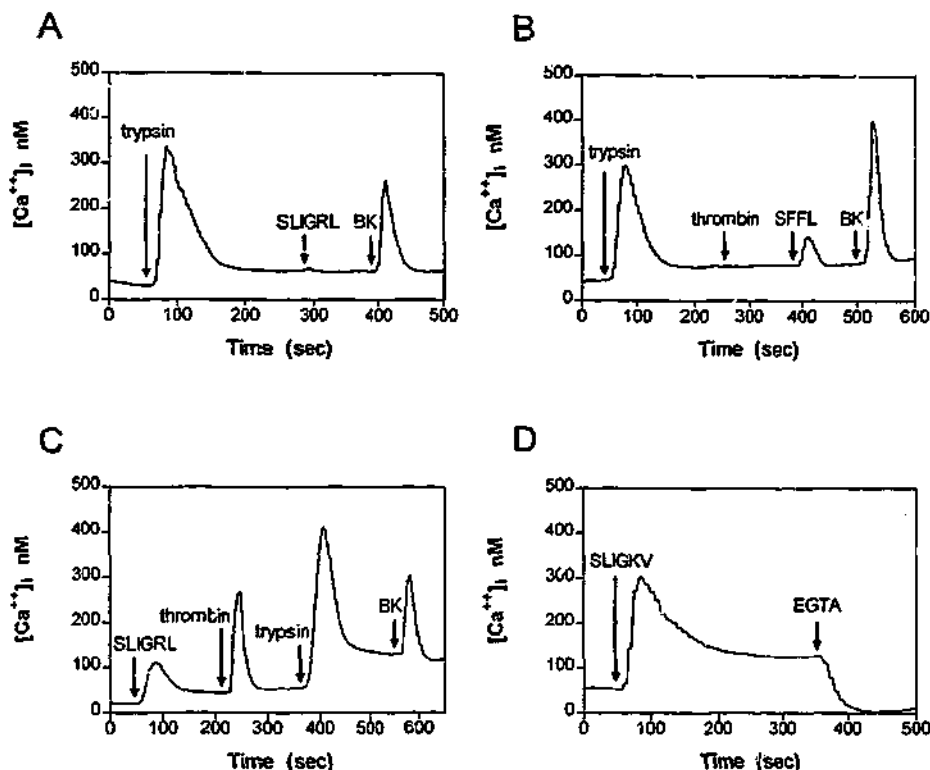


Figure 5. Intracellular calcium responses elicited by PAR-2 activation. Rat osteoblast-like cells (A-C) or SaOS-2 cells (D) were loaded with Fura-2 and treated with trypsin (200 nmol/L), SLIGRL (100 μ mol/L), bradykinin (BK; 1 μ mol/L), thrombin (100 nmol/L), SFLL (100 μ mol/L), SLIGKV (100 μ mol/L), or EGTA (5 mmol/L), as indicated on individual traces.

but not thrombin, we investigated responses of SaOS-2 cells to SLIGKV. SaOS-2 cells showed a dose-dependent increase in $[Ca^{2+}]_i$ in response to SLIGKV, with an EC_{50} of 15.97 μ mol/L. Like the rat primary osteoblast-like cells, SaOS-2 cells showed a sustained elevation of $[Ca^{2+}]_i$ following activation of PAR-2 (Figure 5D). This sustained increase was dependent on the presence of extracellular Ca^{2+} , as demonstrated by the fact that subsequent treatment with ethylene-glycol tetraacetic acid (EGTA) resulted in an immediate return to baseline levels (Figure 5D). The trace shown in Figure 5D is from SaOS-2 cells, but similar observations were made in rat primary osteoblast-like cells.

Gingipain-R stimulated $[Ca^{2+}]_i$ in osteoblast-like cells and abolished any response to a subsequent treatment with trypsin (Figure 6A). Similarly, trypsin caused complete desensitization of calcium mobilization to subsequent treatment with gingipain-R (Figure 6B).

Effect of Activators of PAR-2 on Proliferation and Differentiation of Osteoblast-like Cells

Experiments were carried out to investigate the possible role of PAR-2 in regulating proliferation and differentiation of primary osteoblast-like cells. Cells were treated with the PAR-2 activators trypsin and SLIGRL. Trypsin caused dissociation of cells from the tissue culture plastic when used at the same concentration as for the intracellular calcium responses, thus no data could be obtained for trypsin treatment. Both thrombin and SFLL have previously been shown to stimulate proliferation and to inhibit differentiation (as assessed by endogenous alkaline phosphatase activity) in primary osteoblast-like cells. We hypothesized that the enhanced proliferative response of osteoblast-like cells to

SFLL by comparison with thrombin may be due to the fact that SFLL activates PAR-2 as well as PAR-1. For this reason, thrombin was also included in the thymidine incorporation and alkaline phosphatase assays.

The specific activator of PAR-2, SLIGRL (100 μ mol/L), had no effect on alkaline phosphatase activity, whereas thrombin caused a significant decrease in activity (Figure 7A). Thymidine incorporation was unaffected by SLIGRL alone, but was significantly stimulated by thrombin (Figure 7B). Cells were also treated with thrombin and SLIGRL simultaneously to determine whether proliferation was indeed enhanced by the simultaneous activation of PAR-1 and PAR-2. Combined activation of PAR-1 and PAR-2 with thrombin and SLIGRL did not result in enhanced DNA incorporation above that produced by thrombin alone (Figure 7B).

Discussion

The experiments presented here were initiated to determine whether discrepancies between responses of osteoblast-like cells to two activators of PAR-1 (thrombin and PAR-1-activating peptides) could be accounted for by expression of PAR-2, which can also be activated by the peptides. The results of these experiments demonstrate that, indeed, osteoblast-like cells express PAR-2. Immunocytochemistry and RT-PCR of primary osteoblast-like cells were positive for PAR-2 expression. Moreover, expression of PAR-2 by osteoblasts in vivo was demonstrated in embryonic tissue by immunohistochemistry.

Activators of PAR-2 (trypsin, gingipain-R, and the specific peptide activator SLIGRL) were able to initiate transient increases in $[Ca^{2+}]_i$ in primary rat osteoblast-like cells, and treatment with trypsin caused desensitization to SLIGRL; these

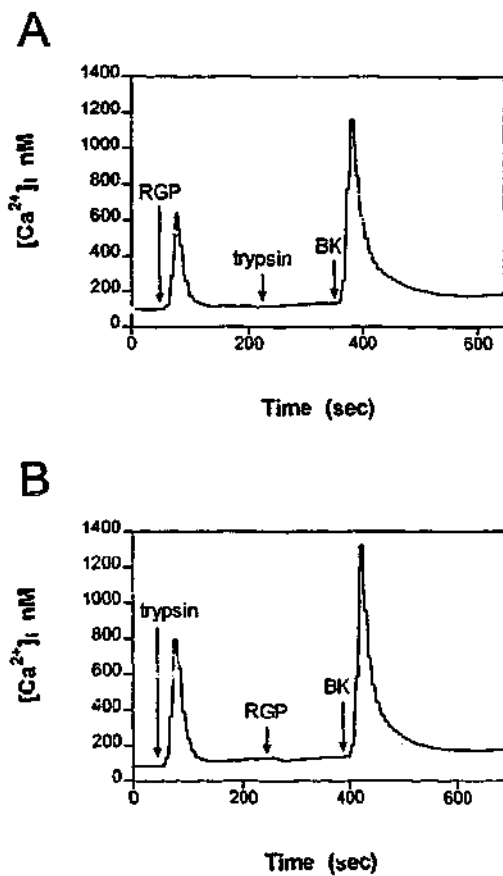


Figure 6. Intracellular calcium responses in osteoblast-like cells elicited by treatment with gingipain-R. Rat osteoblast-like cells were loaded with Fura-2 and treated with gingipain-R (RGP; 200 nmol/L), trypsin (200 nmol/L), or bradykinin (BK; 1 μ mol/L) as indicated.

observations confirm the presence of functional PAR-2 on osteoblasts. When protease-activated receptors are activated enzymatically, they are unable to respond to further enzymatic activation until mobilization of stored or newly synthesized receptors to the cell membrane.⁷ They can, however, under some circumstances still respond weakly to peptide activators for a short period until they are internalized. Desensitization studies with different combinations of activators of PAR-1 and PAR-2 in osteoblast-like cells showed similar results to those previously described for cells expressing both receptors.²⁶ The failure of SLIGKV (human PAR-2-activating peptide) to elicit a response in rat cells is worthy of some comment. This fact allowed us to consider SLIGKV as a negative control peptide in our studies of rat cells, but also highlights the fact that it cannot necessarily be expected that there is species cross reactivity of PAR-activating peptides.

Several years ago we demonstrated expression of PAR-1 by the human osteosarcoma-derived cell line, SaOS-2, and observed that treatment with the human PAR-1-activating peptide led to a sustained rise in $[Ca^{2+}]_i$, whereas thrombin caused a sharp peak followed by a rapid return to baseline.¹⁶ It was later determined that the plateau seen with the peptide was a result of Ca^{2+} entry, and it was assumed that the differential responses resulted from an inability of the peptide to cause full regulation of the receptor.¹⁵ Since these observations were made, PAR-2 was identified,²⁷ and it was subsequently demonstrated that PAR-1-activating peptides are able to activate PAR-2 as well as PAR-1.⁶

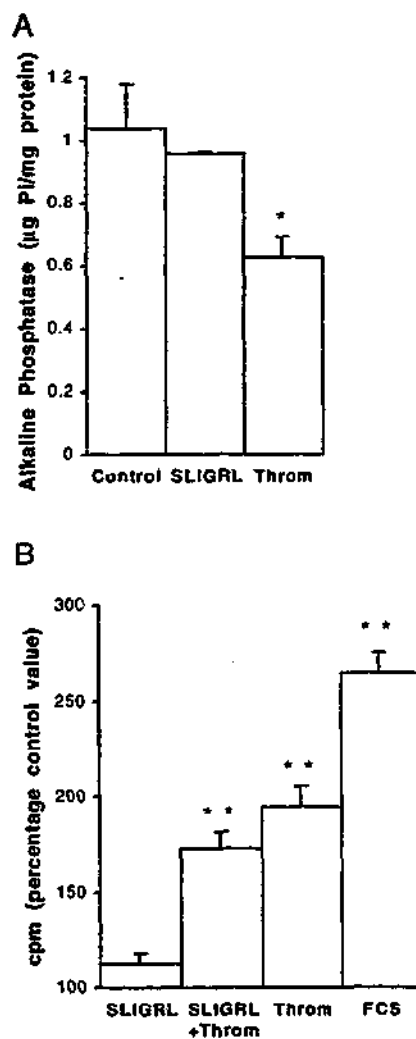


Figure 7. (A) Alkaline phosphatase activity in rat osteoblast-like cells treated with SLIGRL (100 μ mol/L) or thrombin (throm; 100 nmol/L). Results are expressed as alkaline phosphatase activity per milligram cellular protein (mean \pm SEM; n = 4). Alkaline phosphatase activity in SLIGRL-treated cells was not significantly different from that in untreated control cells, whereas thrombin caused a significant decrease in activity (asterisk denotes $p < 0.05$). (B) Thymidine incorporation in rat osteoblast-like cells treated with SLIGRL, SLIGRL and thrombin, thrombin, or FCS (10%). Results are expressed as a percentage of untreated control values for cpm (mean \pm SEM; n = 10). The value for SLIGRL treatment was not significantly different from the untreated control value, whereas all other treatments resulted in highly significant stimulation of proliferation (double asterisks denote $p < 10^{-6}$). The stimulation of proliferation by SLIGRL and thrombin in combination was not significantly different from that caused by thrombin alone.

One of the incentives for the current study was to determine whether the discrepancies observed between $[Ca^{2+}]_i$ responses to thrombin and to peptide activators of PAR-1 in SaOS-2 cells could be attributed to osteoblastic expression of PAR-2. In the current study, we demonstrate not only that osteoblasts express PAR-2, but that activation of PAR-2 leads to a sustained elevation of $[Ca^{2+}]_i$ that can be attributed to Ca^{2+} entry, because it is rapidly reversed by treatment with the extracellular calcium chelator EGTA. Thus, the observations described here can indeed account for the discrepancy in responses of SaOS-2 cells to thrombin and the human PAR-1-activating peptide.

Recently, we have also observed discrepancies between the proliferative responses of rat osteoblast-like cells to thrombin and to the rat PAR-1-activating peptide, SFFL.² Rat primary osteoblast-like cells proliferate in response to both activators of PAR-1, but the proliferative response to SFFL is greater than that to thrombin. As explained in our recent publication,² there are two possible explanations for this observation: (1) that osteoblasts express PAR-2 and concurrent activation of PAR-1 and PAR-2 (by SFFL) results in a greater proliferative response than that to PAR-1 alone; and (2) that osteoblasts express another thrombin receptor in addition to PAR-1, activation of which partially antagonizes the induction of proliferation by PAR-1. At the same time as we were conducting the experiments described here, we obtained some evidence that the second explanation is the correct one; in cells treated concurrently with thrombin and neutralizing antibodies to PAR-1, the proliferation rate was lower than in control cells, indicating that thrombin exerts two antagonistic effects on osteoblast proliferation through activation of PAR-1 and a second receptor.² The results presented here, indicating that SLIGRL is unable to exert any effect on proliferation of rat primary osteoblast-like cells, either alone or in combination with thrombin, rules out a role for PAR-2 in proliferation, and thus supports our conclusion that the discrepancy in proliferative responses can be explained by the presence of a second thrombin receptor. As mentioned in the *Introduction*, two additional thrombin receptors, PAR-3 and PAR-4, have been identified, but it is not yet known whether either of them is expressed by osteoblasts.

Alkaline phosphatase activity, another attribute influenced by thrombin activation of PAR-1, was also unaffected by PAR-2 activation. Thus, apart from calcium mobilization, no functional effects of PAR-2 activation in osteoblast-like cells have been identified. It is of some interest that activation of PAR-2, but not PAR-1, leads to Ca²⁺ entry in osteoblasts. This is a phenomenon associated with activation of many different receptors, including the parathyroid hormone receptor in osteoblasts.²⁰ Receptor-mediated influx of extracellular Ca²⁺ plays an important role in many physiological processes; not only does it replenish intracellular stores, but, in some cell types, also appears to be essential for processes including proliferation, and cytokine synthesis and secretion.²⁸ The significance of this phenomenon in responses of osteoblasts to activation of PAR-2 has yet to be determined.

Functions of PAR-2 in other cell types include stimulation of endothelial-cell proliferation, neutrophil activation, endothelium-dependent smooth muscle relaxation, neuronal toxicity, and prostaglandin release by enterocytes.^{13,19,25,30,31} PAR-2 activation of some cell types stimulates release of cytokines¹²; it is likely that PAR-2 has a similar role in osteoblasts.

Consideration of the activators of PAR-2 may also be useful in elucidating the role of PAR-2 in osteoblasts. None of the currently known enzymatic activators is likely to be a physiological activator of PAR-2 expressed by osteoblasts in normal bone tissue. Trypsin is likely to regulate enterocyte function *in vivo* through activation of PAR-2,¹⁹ and there is evidence that trypsin is a physiological activator of PAR-2 in the respiratory tract,⁹ but it is less likely to activate PAR-2 elsewhere in the body. Active tryptase is stored in mast-cell granules and is released upon degranulation. Therefore, osteoblasts are only likely to be exposed to tryptase in pathological conditions involving mast-cell degranulation. Such conditions include both generalized mastocytosis, which results in elevated plasma tryptase levels, and conditions leading to local accumulations of mast cells in or adjacent to bone. Skeletal manifestations of mastocytosis include osteoporosis, and mastocytosis may even present as "idiopathic" osteoporosis.^{5,17} High levels of tryptase

resulting from mast-cell degranulation are present locally in odontogenic cysts and may play a role in the associated bone resorption.³² Another activator of PAR-2, gingipain-R, is produced by *Porphyromonas gingivalis*, one of the causative agents of periodontal disease. This provides another example of an association between a known activator of PAR-2, and a condition involving excessive bone resorption. It is possible, therefore, that activation of PAR-2 stimulates osteoblast-mediated osteoclastic bone resorption. Whether osteoblastic PAR-2 plays a true physiological role in bone metabolism depends on the presence of as yet unidentified activators of PAR-2 in normal bone tissue.

Acknowledgments: This work was partly funded by Grants 970490 and 970498 awarded by the National Health and Medical Research Council of Australia to the late Prof. S. R. Stone. The authors thank M. De Niese for assistance with the cell culture.

References

1. Abraham, L. A., Jenkins, A. L., Stone, S. R., and Mackie, E. J. Expression of the thrombin receptor in developing bone and associated tissues. *J Bone Miner Res* 13:818-827; 1998.
2. Abraham, L. A. and Mackie, E. J. Modulation of osteoblast-like cell behaviour by activation of protease-activated receptor-1. *J Bone Miner Res* 14:1320-1329; 1999.
3. Ahern, T., Taylor, G. A., and Sanderson, C. J. An evaluation of an assay for DNA synthesis in lymphocytes with [³H] thymidine and harvesting on to glass fibre filter discs. *J Immunol Meth* 10:329-336; 1976.
4. al-Ani, B., Saifeddine, M., and Hollenberg, M. D. Detection of functional receptors for the proteinase-activated-receptor-2-activating polypeptide, SLIGRL-NH₂, in rat vascular and gastric smooth muscle. *Can J Physiol Pharmacol* 73:1203-1207; 1995.
5. Andrew, S. M. and Freemont, A. J. Skeletal mastocytosis. *J Clin Pathol* 46:1033-1035; 1993.
6. Blackhart, B. D., Emilsson, K., Nguyen, D., Teng, W., Martelli, A. J., Nystedt, S., Sundelin, J., and Scarborough, R. M. Ligand cross-reactivity within the protease-activated receptor family. *J Biol Chem* 271:16466-16471; 1996.
7. Bohm, S. K., Khitin, L. M., Grady, E. F., Aponte, G., Payan, D. G., and Bunnett, N. W. Mechanisms of desensitization and resensitization of proteinase-activated receptor-2. *J Biol Chem* 271:22003-22016; 1996.
8. Bohm, S. K., Kong, W., Bromme, D., Smeekens, S. P., Anderson, D. C., Connolly, A., Kahn, M., Nelken, N. A., Coughlin, S. R., Payan, D. G., and Bunnett, N. W. Molecular cloning, expression and potential functions of the human proteinase-activated receptor-2. *Biochem J* 314:1009-1016; 1996.
9. Cocks, T. M., Fong, B., Chow, J. M., Anderson, G. P., Frauman, A. G., Goldie, R. G., Henry, P. J., Cai, M. J., Hamilton, J. R., and Moffatt, J. D. A protective role for protease-activated receptors in the airways. *Nature* 398:156-160; 1998.
10. Corvera, C. U., Dery, O., McConalogue, K., Bohm, S. K., Khitin, L. M., Caughey, G. H., Payan, D. G., and Bunnett, N. W. Mast cell tryptase regulates rat colonic myocytes through proteinase-activated receptor 2. *J Clin Invest* 100:1383-1393; 1997.
11. D'Andrea, M. R., Derian, C. K., Leturcq, D., Baker, S. M., Brunmark, A., Ling, P., Darrow, A. L., Santulli, R. J., Brass, L. F., and Andrade-Gordon, P. Characterization of protease-activated receptor-2 immunoreactivity in normal human tissues. *J Histochem Cytochem* 46:157-164; 1998.
12. Hou, L., Kapas, S., Cruchley, A. T., Macey, M. G., Harriott, P., Chinni, C., Stone, S. R., and Howells, G. L. Immunolocalization of protease-activated receptor-2 in skin: Receptor activation stimulates interleukin-8 secretion by keratinocytes *in vitro*. *Immunology* 94:356-362; 1998.
13. Howells, G. L., Macey, M. G., Chinni, C., Hou, L., Fox, M. T., Harriott, P., and Stone, S. R. Proteinase-activated receptor-2: Expression by human neutrophils. *J Cell Sci* 110:881-887; 1997.
14. Ishihara, H., Connolly, A. J., Zeng, D., Kahn, M. L., Zheng, Y. W., Timmons, C., Tram, T., and Coughlin, S. R. Protease-activated receptor 3 is a second thrombin receptor in humans. *Nature* 386:502-506; 1997.
15. Jenkins, A. L., Bootman, M. D., Berridge, M. J., and Stone, S. R. Differences in intracellular calcium signaling after activation of the thrombin receptor by thrombin and agonist peptide in osteoblast-like cells. *J Biol Chem* 269:17104-17110; 1994.
16. Jenkins, A. L., Bootman, M. D., Taylor, C. W., Mackie, E. J., and Stone, S. R.

- Characterization of the receptor responsible for thrombin-induced intracellular calcium responses in osteoblast-like cells. *J Biol Chem* 268:21432-21437; 1993.
17. Johansson, C., Roupe, G., Lindstedt, G., and Mellstrom, D. Bone density, bone markers and bone radiological features in mastocytosis. *Age Ageing* 25:1-7; 1996.
18. Kahn, M. L., Zheng, Y. W., Huang, W., Bigornia, V., Zeng, D., Moff, S., Farese, R. V., Jr., Tam, C., and Coughlin, S. R. A dual thrombin receptor system for platelet activation. *Nature* 394:690-694; 1998.
19. Kong, W., McConalogue, K., Khitin, L. M., Hollenberg, M. D., Payan, D. G., Bohm, S. K., and Bunnett, N. W. Luminal trypsin may regulate enterocytes through proteinase-activated receptor 2. *Proc Natl Acad Sci USA* 94:8884-8889; 1997.
20. Lieberherr, M. Effects of vitamin D3 metabolites on cytosolic free calcium in confluent mouse osteoblasts. *J Biol Chem* 262:13168-13173; 1987.
21. Lourbakos, A., Chinni, C., Thompson, P., Potempa, J., Travis, J., Mackie, E. J., and Pike, R. N. Cleavage and activation of proteinase-activated receptor-2 on human neutrophils by gingipain-R from *Porphyromonas gingivalis*. *Fed Eur Bone Soc Lett* 435:45-48; 1998.
22. Marin, T. J., Ng, K. W., Partridge, N. C., and Livesey, S. A. Hormonal influences on bone cells. *Meth Enzymol* 145:324-336; 1987.
23. Mirza, H., Schmidt, V. A., Derian, C. K., Jesty, J., and Bahou, W. F. Mitogenic responses mediated through the proteinase-activated receptor-2 are induced by expressed forms of mast cell alpha- or beta-tryptases. *Blood* 90:3914-3922; 1997.
24. Molino, M., Barnathan, E. S., Numerof, R., Clark, J., Dreyer, M., Cumashi, A., Hoxie, J. A., Schechter, N., Woolkalis, M., and Brass, L. F. Interactions of mast cell tryptase with thrombin receptors and PAR-2. *J Biol Chem* 272:4043-4049; 1997.
25. Mirza, H., Yatsula, V., and Bahou, W. F. The proteinase activated receptor-2 (PAR-2) mediates mitogenic responses in human vascular endothelial cells. *J Clin Invest* 97:1705-1714; 1996.
26. Molino, M., Woolkalis, M. J., Reavey-Cantwell, J., Praico, D., Andrade-Gordon, P., Barnathan, E. S., and Brass, L. F. Endothelial cell thrombin receptors and PAR-2. Two protease-activated receptors located in a single cellular environment. *J Biol Chem* 272:11133-11141; 1997.
27. Nystedt, S., Emilsson, K., Wahlestedt, C., and Sundelin, J. Molecular cloning of a potential proteinase activated receptor [see comments]. *Proc Natl Acad Sci USA* 91:9208-9212; 1994.
28. Parakh, A. B. and Penner, R. Store depletion and calcium influx. *Physiol Rev* 77:901-930; 1997.
29. Potempa, J., Mikolajczyk-Pawlinska, J., Brassell, D., Nelson, D., Thøgersen, I. B., Enghild, J. J., and Travis, J. Comparative properties of two cysteine proteinases (gingipains R), the products of two related but individual genes of *Porphyromonas gingivalis*. *J Biol Chem* 273:21648-21657; 1998.
30. Saifeddine, M., al-Ani, B., Cheng, C. H., Wang, L., and Hollenberg, M. D. Rat proteinase-activated receptor-2 (PAR-2): cDNA sequence and activity of receptor-derived peptides in gastric and vascular tissue. *Br J Pharmacol* 118:521-530; 1996.
31. Smith-Swintosky, V. L., Cheo-Isaacs, C. T., D'Andrea, M. R., Santulli, R. J., Darrow, A. L., and Andrade-Gordon, P. Protease-activated receptor-2 (PAR-2) is present in the rat hippocampus and is associated with neurodegeneration. *J Neurochem* 69:1890-1896; 1997.
32. Teronen, O., Hietanen, T. O., Lindqvist, J., Salo, T., Sorsa, T., Eklund, K. K., Sommerhoff, C. P., Ylipaavalniemi, P., and Kontinen, Y. T. Mast cell-derived tryptase in odontogenic cysts. *J Oral Pathol* 25:376-381; 1996.
33. Vu, T. K., Hung, D. T., Wheaton, V. L., and Coughlin, S. R. Molecular cloning of a functional thrombin receptor reveals a novel proteolytic mechanism of receptor activation. *Cell* 64:1057-1068; 1991.

Date Received: April 30, 1999

Date Revised: August 20, 1999

Date Accepted: August 24, 1999

APPENDIX II

**A naturally occurring NAR variable domain binds the Kgp protease
from *Porphyromonas gingivalis***

**Nuttall, S.D., Krishnan, U.V., Doughty, L., Nathanielsz, A., Ally, N., Pike, R.N.,
Hudson, P.J., Kortt, A.A., and Irving R.**

FEBS Letters 516: 80-6 (2002)

A naturally occurring NAR variable domain binds the Kgp protease from *Porphyromonas gingivalis*

Stewart D. Nuttall^{a,b,*}, Usha V. Krishnan^{a,b}, Larissa Doughty^a, Anne Nathanielsz^{a,b}, Nafisa Ally^c, Robert N. Pike^c, Peter J. Hudson^{a,b}, Alexander A. Kortt^a, Robert A. Irving^{a,b}

^aCSIRO Health Sciences and Nutrition, 343 Royal Parade, Parkville, Vic. 3052, Australia

^bCRC for Diagnostics, 343 Royal Parade, Parkville, Vic. 3052, Australia

^cDepartment of Biochemistry and Molecular Biology, Monash University, Clayton, Vic. 3800, Australia

Received 25 January 2002; revised 18 February 2002; accepted 18 February 2002

First published online 6 March 2002

Edited by Gianni Cesareni

Abstract The new antigen receptor (NAR) from sharks consists of a single immunoglobulin variable domain attached to five constant domains, and is hypothesised to function as an antibody. Two closely related NARs with affinity for the Kgp (lysine-specific) gingipain protease from *Porphyromonas gingivalis* were selected by panning an NAR variable domain library. When produced in *Escherichia coli*, these recombinant NARs were stable, correctly folded, and specifically bound Kgp ($K_d = 1.31 \pm 0.26 \times 10^{-7}$ M). Binding localised to the Kgp adhesin domains, however without inhibiting adhesin activity. These naturally occurring proteins indicate an immune response to pathogenic bacteria and suggest that the NAR is a true antibody-like molecule. © 2002 Federation of European Biochemical Societies. Published by Elsevier Science B.V. All rights reserved.

Key words: Scaffold; Peptide display; V_H ; Variable domain; New antigen receptor; Lysine-specific gingipain protease from *Porphyromonas gingivalis*

1. Introduction

The immune systems of cartilaginous fish employ a diverse range of antibody and antibody-like proteins, including monomeric and pentameric IgM, IgX, and IgW [1,2]. These proteins are all of conventional antibody architecture, relying on the interaction of heavy (V_H) and light (V_L) domains to form an antigen-binding site comprising four to six variable CDR loops. In contrast, the new antigen receptors (NARs) from *Ginglymostoma cirratum* (nurse sharks, nNAR) and *Orectolobus maculatus* (wobbegong sharks, wNAR) encapsulate variability within two CDR loops of a single V_H domain. It is clear from immune electron microscopy that there is no associated light chain and that the variable domains do not associate together across a V_H/V_L -like interface [3]. Structurally, the intact NAR molecule consists of a disulphide-bonded dimer of two protein chains of five constant and one variable

immunoglobulin domains. This arrangement, and particularly the single variable domain, is very similar to the V_HH antibodies found in camelid species in a clear case of convergent evolution at the molecular level [3,4]. V_HH s are capable of binding a wide range of protein, hapten and peptide targets and represent a significant proportion of the camelid immune response [5,6]. While a similar function for the NAR in the shark immune response awaits formal proof, there is strong evidence that NARs are functional antibodies. For example, NARs show (i) protein variability that is almost exclusively encapsulated into the two major CDR loop regions, with maintenance of a conserved underlying immunoglobulin structural framework; and (ii) a pattern of hypermutation in the CDRs between secretory and transmembrane forms, analogous to the process of affinity maturation in mammalian IgG class molecules [7,8].

In a previous study, we showed that the individual wNAR variable domains could be expressed as soluble monomers in the *Escherichia coli* periplasm. An in vitro type II wNAR library was then designed with synthetic CDR3 loops, and successfully displayed on the surface of fd bacteriophages. Library panning using standard techniques against target proteins resulted in the isolation of NAR domains specific for proteins from *Porphyromonas gingivalis* [9]. *P. gingivalis* is an anaerobic bacterium strongly associated with human periodontal disease where virulence is mediated through a range of extracellular factors including the related gingipain cysteine proteases Kgp (specific for lysine residues) and HRgp (specific for arginine residues) [10]. Both proteases are high molecular weight complexes of a gingipain catalytic domain and have up to four haemagglutinin/adhesion subunits.

Here we report the results of further screening of NAR single variable domain libraries against Kgp, using an expanded library and screening techniques different to those previously reported. Surprisingly, we observed strong selection for two naturally occurring NAR proteins not derived from our synthetic CDR3 library. In this first description of antigen specificity in natural NARs, we analyse the binding characteristics of these antibody-like domains.

2. Material and methods

2.1. Equipment and reagents

Vent DNA polymerase and all restriction enzymes were purchased from New England Biolabs (Beverly, MA, USA) and used according to the manufacturer's instructions. T4 DNA ligase was from Biotech (Australia). DNA fragment recovery and purification was by QIA-

*Corresponding author. Fax: (61)-3-9662 7314.

E-mail address: stewart.nuttall@hsc.csiro.au (S.D. Nuttall).

Abbreviations: wNAR, new antigen receptor from wobbegong sharks; nNAR, new antigen receptor from nurse sharks; Kgp, lysine-specific gingipain protease from *Porphyromonas gingivalis*; HRgpA, high molecular weight arginine-specific gingipain protease from *Porphyromonas gingivalis*

quick Gel Extraction Kit, Qiagen (Germany). Small-scale preparations of DNA from *E. coli* were by QIAprep Spin Miniprep kit, Qiagen (Germany). Monoclonal anti-FLAG antibody was purified from hybridoma cell line KM5-1C7-8-5 (provided by Dr. N. Nicola, CRC for Cellular Growth Factors, WEHI, Australia) using rProtein A Sepharose fast flow resin from Amersham Pharmacia Biotech (Australia) according to the manufacturer's instructions. Purified anti-FLAG antibody was immobilised onto Mini-Leak[®] Low resin from Kem-En-Tec (Denmark) following the manufacturer's instructions, to generate anti-FLAG affinity resin. Goat anti-mouse IgG (Fc)-horseradish peroxidase (HRP) was from Pierce, BenchMark[®] Prestained Protein Ladder Cat. # 19748-010 was from Gibco BRL Life Technologies (Gaithersburg, MA, USA). Standard molecular biological techniques were performed as described [11]. HRgpA, RgpB and Kgp were purified from the H66 strain culture fluid as described previously [12].

2.2. *E. coli* strains

The cell line used for library propagation and selection and protein expression was *E. coli* TG1 (K12 *supE* Δ (*lac-proAB*) *thi hsdR5* *F'*(*traD36 proAB⁺ lacI^q lacZ* Δ M15)). *E. coli* transformants were maintained and grown in 2 \times YT broth supplemented with 100 μ g/ml (*w/v*) ampicillin +/– 2% (*w/v*) glucose. Solid media contained 2% (*w/v*) Bacto-agar. Transformation of *E. coli* was by standard procedures [11] performed using electro-competent cells.

2.3. Library construction and panning

DNA library cassettes encoding the wNAR were constructed from cDNA as described [9]. The total library size was $\sim 4.0 \times 10^8$ independent clones, consisting of $> 3 \times 10^8$ clones with synthetic CDR3 sequences, and $\sim 7.0 \times 10^6$ clones derived from natural cDNAs. Library contributions were normalised in proportion to their sizes prior to panning, and phagemid particles carrying the NAR-gene 3 protein were propagated and isolated by standard procedures [13]. For biopanning of the phagemid library, Kgp (2 μ g/ml in phosphate-buffered saline (PBS)) was coated onto Maxisorb Immunotubes and incubated at 4°C overnight. Immunotubes were rinsed (PBS), blocked with PBS/2% Blotto for 1 h at room temperature (RT), and incubated with freshly prepared phagemid particles (in PBS/2% Blotto) for 30 min at RT with gentle agitation, followed by 90 min without agitation. After incubation, immunotubes were washed (PBS/0.1% Tween 20; 7, 8, 10 washes for panning rounds 1–3), followed by an identical set of washes with PBS. Phagemid particles were eluted using 0.1 M HCl, pH 2.2/1 mg/ml bovine serum albumin, neutralised by the addition of 2 M Tris base, and either immediately reinfected into *E. coli* TG1 or stored at 4°C.

2.4. Nucleic acid isolation and cloning

Following final selection, phagemid particles were infected into *E. coli* TG1 and propagated as plasmids, followed by DNA extraction. The NAR cassette was extracted as a *NotI/SfiI* fragment and subcloned into the similarly restricted cloning/expression vector pGC [14]. DNA clones were sequenced on both strands using a BigDye terminator cycle sequencing kit (Applied Biosystems, USA) and a Perkin Elmer Sequenator. The nucleotide sequence of clones 12A-9 and 12A-14 associated with this study are deposited in the GenBank database under accession numbers AF466395 and AF466396.

2.5. Soluble expression of wNAR constructs from expression vector pGC

Recombinant proteins were expressed in the bacterial periplasm as described [9]. Briefly, *E. coli* TG1 starter cultures were grown overnight in 2 \times YT medium/ampicillin (100 μ g/ml)/glucose (2.0% *w/v*), diluted 1/100 into fresh 2 \times YT/100 μ g/ml ampicillin/glucose (0.1% *w/v*) and then grown at 37°C/200 rpm until $OD_{550\text{nm}} = 0.2\text{--}0.4$. Cultures were then induced with IPTG (1 mM final), grown for a further 16 h at 28°C and harvested by centrifugation (Beckman JA-14/6K/10 min/4°C). Periplasmic fractions were isolated by the method of Minsky [15] and either used as crude fractions or recombinant protein purified by affinity chromatography using an anti-FLAG antibody–Sepharose column (10 \times 1 cm). The affinity column was equilibrated in PBS, pH 7.4, and bound protein eluted with ImmunoPure[®] gentle elution buffer (Pierce). Eluted proteins were dialysed against two changes of PBS/0.02% sodium azide, concentrated by ultrafiltration over a 3000 Da cutoff membrane (YM3, Diaflo), and analysed by FPLC on a pre-calibrated Superdex75 column (Pharmacia) in PBS pH 7.4. Recombi-

nant proteins were analysed by SDS–polyacrylamide gel electrophoresis through 15% Tris/glycine gels.

2.6. Enzyme-linked immunosorbent assays

Protein antigens (0.5 μ g/well) in PBS were coated onto Maxisorb Immuno-plates (Nunc, Germany) and incubated at 4°C overnight. Plates were rinsed, blocked with PBS/5% Blotto for 1 h at RT, and incubated with periplasmic fractions or recombinant protein for 1 h at RT. Plates were rinsed with PBS, washed three times with PBS/0.05% Tween 20, and anti-FLAG antibody (1/1000 in PBS/5% Blotto) added. Plates were incubated and washed as above, and the HRP-conjugated secondary anti-mouse Fc antibody added (1/1000 in PBS/5% Blotto). Plates were washed again and developed using 2,2'-azino-di-(ethyl) benzothiazoline sulphonic acid (Boehringer Mannheim, Germany) and read at $OD_{405\text{nm}}$.

For localisation of Kgp binding, fibrinogen (10 nM) in PBS was coated as above, and the plates then rinsed, blocked with PBS/1% Blotto for 1 h at 37°C, and washed three times with PBS/0.1% Tween 20. Plates were then incubated with either 30 nM of gingipain alone or gingipain+3 μ M 12A-9 for 1 h at 37°C, washed as above, and incubated with 10 μ g/ml chicken anti-gingipain antibody for 1 h at 37°C before addition of a HRP-conjugated anti-chicken antibody (1/10000 in PBS/1% Blotto). Plates were washed again and developed using 3,3',5,5'-tetramethylbenzidine (Sigma, USA) and read at 450 nm.

2.7. Biosensor binding analysis

A BIAcore[®] 1000 biosensor (BIAcore AB, Uppsala, Sweden) was used to measure the interaction between wNAR proteins 12A-9 and 12A-14, and Kgp. Kgp at a concentration of 50 μ g/ml in 10 mM sodium acetate buffer, pH 4.5, was immobilised onto a CM5 sensor chip via amine groups using the Amine Coupling kit (BIAcore AB) [16]. The immobilisation was performed at 25°C and 5 μ l/min flow rate. Injection of 50 μ l of 50 μ g/ml Kgp coupled 2000RU to the surface. Binding experiments were performed in HBS buffer (10 mM HEPES, 0.15 M NaCl, 1 mM CaCl₂, 0.005% surfactant P20, pH 8.15) at 25°C and a constant flow rate of 5 μ l/min with a series of analyte concentrations (825–52.5 nM). Regeneration of the Kgp surface was achieved by running the dissociation reaction to completion before the next injection of analyte. The binding data was evaluated with BIA-evaluation 3.0.2 [17].

3. Results

3.1. Panning of an expanded wNAR variable domain library on Kgp

Previously we described the design and construction of a wNAR variable domain library with synthetic CDR3 loops. This library, although small ($\sim 3 \times 10^7$), was successfully displayed on the surface of fd bacteriophage and panned against Kgp displayed in the context of ELISA plate wells [9]. In order to isolate further antigen-specific NAR domains, the library was expanded to $\sim 4 \times 10^8$ independent clones by incorporation of both synthetic and naturally occurring (derived from cDNA) CDR3 sequences, followed by further transformations into *E. coli* TG1. Phagemid particles were then rescued and panned against the Kgp antigen immobilised on immunotubes. After three rounds of biopanning an ~ 100 -fold increase in bacteriophage titre was observed, with 100% of phagemid-transfected colonies positive for wNAR sequences suggesting that positive selection was occurring. Thus, wNAR variable domain cassettes were rescued from phagemids, cloned into the periplasmic expression vector pGC, and transformed into *E. coli* TG1.

Periplasmic fractions from recombinant clones were tested for binding to Kgp and to negative control antigens by ELISA (not shown). Over 50% of the clones tested showed significant binding above background. When sequenced, only two different sequences were present, represented by the clones designated 12A-9 and 12A-14. The primary and de-

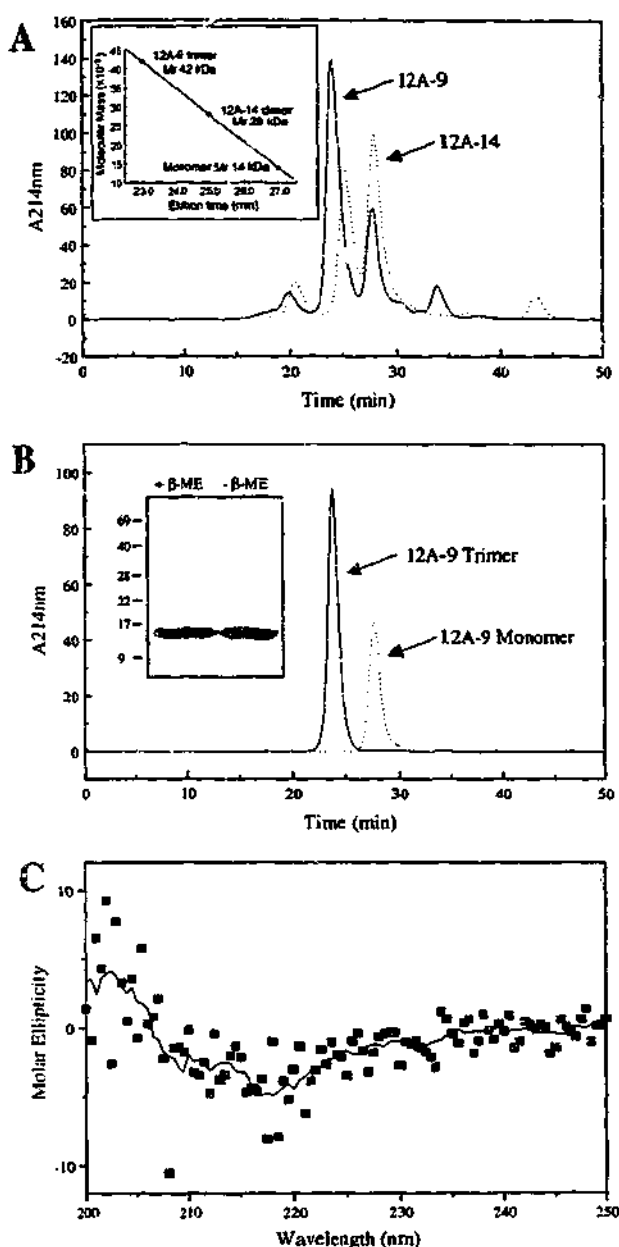


Fig. 2. Size exclusion chromatography and CD analysis of proteins 12A-9 and 12A-14. A: Elution profiles of affinity-purified 12A-9 and 12A-14 proteins on a calibrated Superdex75 HR10/30 column equilibrated in PBS, pH 7.4, and run at a flow rate of 0.5 ml/min. The 12A-14 and 12A-9 peaks eluting at 27 min are consistent with a monomeric domain (calculated M_r of 14 225 for 12A-14 and 14 122 for 12A-9). The 12A-14 peak eluting at 25 min is consistent with a dimer (M_r = 28 kDa) and the 12A-9 peak eluting at 23 min is consistent with a trimer (M_r = 42 kDa). The inset shows the relationship between molecular mass and elution time for this family of wNAR domains. The optical density at 214 nm is given in arbitrary units. B: Re-chromatography of isolated 12A-9 monomer and trimer peaks on Superdex75 column under the same conditions as for (A). The inset shows the wNAR 12A-9 trimer treated in the presence (+) or absence (-) of β -mercaptoethanol and analysed by SDS-polyacrylamide gel electrophoresis through a 15% (w/v) polyacrylamide Tris/glycine gel and stained with Coomassie brilliant blue. C: Circular dichroic spectrum of affinity-purified wNAR 12A-9 in 0.05 M sodium phosphate buffer, pH 7.4. The scatter plot shows data collected and the unbroken line represents an average of these data points.

ences scattered throughout both CDR and framework regions (Fig. 1B). It is notable that conserved cysteine residues are present in both CDR1 and -3 loops, and probably form stabilising inter-loop disulphide linkages [3,6,9].

3.2. Characterisation of recombinant 12A-9 and 12A-14 variable domains

To compare proteins 12A-9 and 12A-14 and to define their binding characteristics, recombinant proteins were isolated from the *E. coli* periplasm by affinity chromatography using an anti-FLAG antibody affinity resin and their oligomeric status analysed by size exclusion chromatography on a calibrated Superdex75 HR10/30 column. The elution profiles showed that both proteins contained two major oligomeric forms (Fig. 2A). The elution times indicated that 12A-14 consisted of a monomer (M_r ~ 14 kDa) and a dimer (M_r ~ 28 kDa), while 12A-9 consisted of a monomer and a trimer (~42 kDa) (Fig. 2A, inset). The presence of a dimer and trimer in affinity-purified fractions of 12A-14 and 12A-9, respectively, was confirmed by dynamic light scattering analysis (data not shown). As clone 12A-9 showed higher expression levels than clone 12A-14 (1 mg/l compared to 0.2 mg/l purified protein) and showed apparently higher binding activity (see next section), protein 12A-9 was chosen for further analysis.

The monomeric and trimeric peaks of 12A-9 were isolated by size exclusion chromatography and found to be stable with no evidence of re-equilibration (Fig. 2B). Furthermore, treatment of 12A-9 trimer in 8 M urea followed by size exclusion chromatography into PBS yielded back only trimer. The stability of the trimer was not due to disulfide bond linkages, as treatment of 12A-9 trimer with SDS in the absence of reducing agent produced a single protein band of ~14 kDa, expected for the monomer (Fig. 2B, inset). N-terminal amino acid sequencing of affinity-purified 12A-9 monomer/trimer mixture showed that only one protein species was present with the expected N-terminus (ARVDQTP-; Fig. 1A) indicating that the signal peptide had been correctly cleaved on secretion into the *E. coli* periplasm. Far ultraviolet CD spectra of aqueous solutions of protein 12A-9 trimer showed a profile with a negative band with λ_{max} at 217–219 nm (Fig. 2C). This spectrum is characteristic of β protein and not a disordered structure [18], confirming that the 12A-9 variable domain folds into a compact, β -sheet immunoglobulin fold in the *E. coli* periplasmic space.

3.3. Specificity and binding activity of recombinant protein 12A-9

The specificity of affinity-purified 12A-9 and 12A-14 proteins for Kgp was demonstrated by ELISA. Both proteins reacted specifically with Kgp but not the other antigens tested (Fig. 3A). Protein 12A-9 showed clearly superior binding characteristics with at least five-fold higher activity than protein 12A-14 (Fig. 3B). The binding kinetics of the monomeric 12A-9 and 12A-14 were also measured by BIAcore biosensor analysis with Kgp protein immobilised via amine coupling to the sensor surface. A comparison of the binding interactions of 12A-9 and 12A-14 binding to immobilised Kgp showed that ~10 times more 12A-14 was required to elicit a response similar to that obtained with 12A-9 (Fig. 4A), consistent with the result observed in the ELISA reaction. The apparent lower binding activity of 12A-14 can be attributed to either weaker binding (slow association rate and fast dissociation rate con-

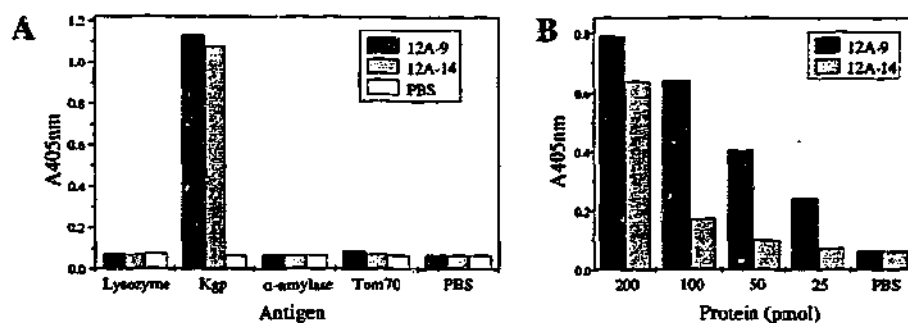


Fig. 3. Analysis of proteins 12A-9 and 12A-14 by ELISA. A: Proteins were purified from the periplasmic fraction of *E. coli* TG1 by affinity chromatography through an anti-FLAG M2 antibody column and tested for binding to lysozyme, Kgp, Tom70, and α -amylase. Results represent the average of triplicate wells. B: As for (A) except serial two-fold dilutions of equal amounts of 12A-9 and 12A-14 proteins were tested for binding to Kgp. Results represent the average of duplicate wells.

stants) or that only a small fraction ($\sim 5\%$) of the purified 12A-14 is active in binding immobilised Kgp. Interestingly, a comparison of the binding kinetics of affinity-purified 12A-9, 12A-9 monomer, and 12A-9 trimer, showed no difference in the dissociation rates between monomer and trimer (data not shown) suggesting that the 12A-9 trimer does not exhibit multivalent binding to immobilised Kgp. Whether the apparent inability of μ NAR 12A-9 trimer to exhibit multivalent binding is due to the orientation and accessibility of Kgp epitope on the sensor surface or to the steric orientation of the CDFs in the 12A-9 trimer remains to be resolved. Protein 12A-9 showed no binding to a blank surface (activated and then blocked with ethanolamine) in either its monomeric or trimeric form, indicating that there is no non-specific interaction with the sensor surface (Fig. 4A, inset; and not shown).

A series of sensorgrams for the binding of 12A-9 peak-purified monomer are shown in Fig. 4B. The binding data were fitted at each concentration to the 1:1 Langmuir binding model and the kinetic constants evaluated. The data showed a reasonably good fit to the 1:1 binding model, consistent with μ NAR 12A-9 monomer binding to a single epitope on Kgp, although some deviation from the binding model is apparent towards the end of the dissociation phase. The binding data gave a value for the k_a of $4.29 \pm 0.68 \times 10^4 \text{ M}^{-1} \text{ s}^{-1}$ and k_d of $7.81 \pm 1.30 \times 10^{-3} \text{ s}^{-1}$ to yield a dissociation constant (K_d) of $1.31 \pm 0.26 \times 10^{-7} \text{ M}$.

3.4. Mapping of the Kgp epitope

To determine the Kgp epitope targeted by protein 12A-9, different forms of gingipain were tested for binding. Protein 12A-9 bound both Kgp and the related arginine-specific gingipain, HRgpA, but not the lower molecular weight RgpB form that lacks most adhesin subunits (results not shown). This suggested that the adhesin domains formed at least part of the 12A-9 epitope. However, in a series of competition ELISA experiment, high concentrations of 12A-9 ($3 \mu\text{M}$, more than 10-fold above K_d) failed to inhibit binding of Kgp or HRgpA to immobilised fibrinogen and other proteins such as fibronectin (Fig. 5; and results not shown). Thus, either the 12A-9 epitope is removed from the adhesin regions involved in agglutination, or single μ NAR variable domains are of insufficient size to block the adhesin binding. Similarly, protein 12A-9 did not affect the enzyme activity of the gingipains, suggesting that it does not target the catalytic site of the enzymes.

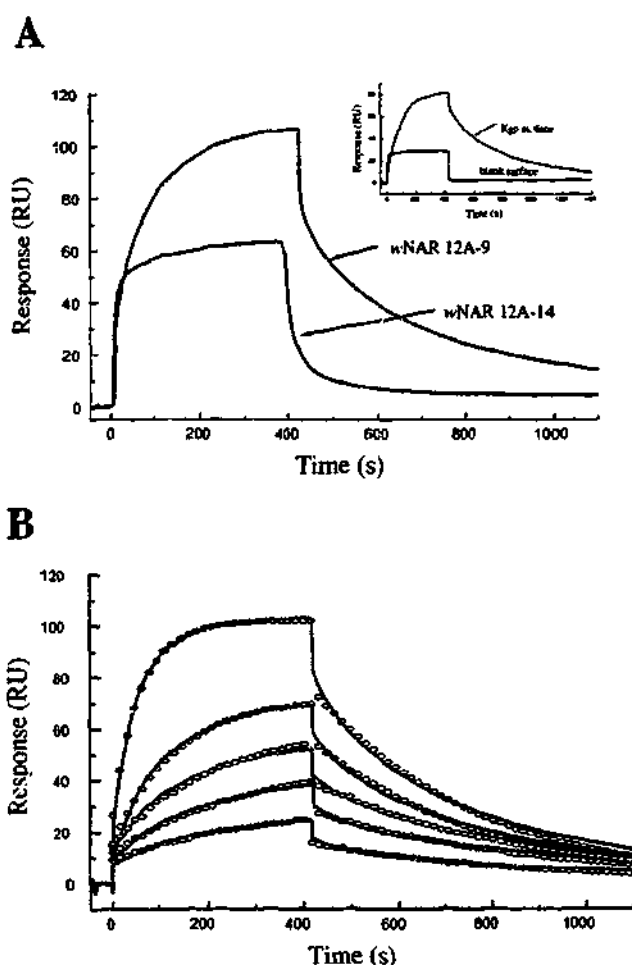


Fig. 4. Analysis of proteins 12A-9 and 12A-14 by BIAcore. Binding of μ NAR monomeric proteins to immobilised Kgp (2000RU) was measured at a constant flow rate of $5 \mu\text{l}/\text{min}$ with an injection volume of $35 \mu\text{l}$. Dissociation was continued with HBS buffer until the response returned to the initial value before injecting the next sample. A: Sensorgrams showing the binding of μ NAR monomeric proteins 12A-9 ($6 \mu\text{g}/\text{ml}$) and 12A-14 ($115 \mu\text{g}/\text{ml}$). The inset shows the binding profile of monomeric μ NAR protein 12A-9 ($6 \mu\text{g}/\text{ml}$) to immobilised Kgp and a blank surface (NHS/EDC activated and blocked with ethanolamine). B: Sensorgrams showing the binding of a series of concentrations of μ NAR 12A-9 protein (825, 413, 210, 105, 52.5 nM ; conditions as in A). The circles show the fit to the data obtained on analysis with the 1:1 Langmuir binding model for the evaluation of the kinetic rate constants.

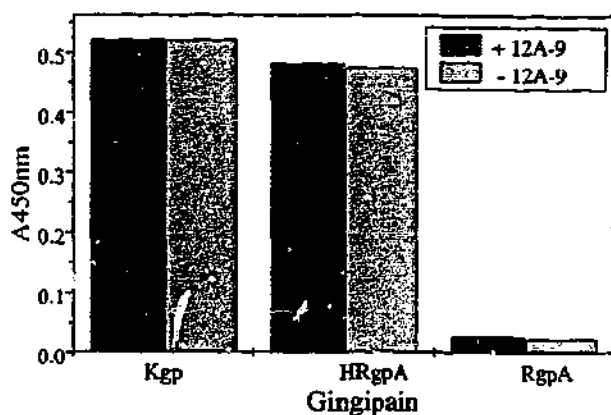


Fig. 5. rNAR protein 12A-9 does not inhibit the adhesin activity of Kgp and Rgp gingipains. Fibrinogen (10 nM) was coated onto ELISA wells and binding to this surface of Kgp and HRgpA gingipains tested in the presence or absence of 3 μ M 12A-9 protein. The lower molecular weight RgpA form, lacking adhesin domains, is shown for comparison.

4. Discussion

The isolation of two naturally occurring and antigen-specific NAR variable domains confirms the NAR from sharks as a functional antibody-like molecule. With an affinity for the target antigen of \sim 130 nM, these single domains have antigen specificity comparable to recombinant forms of the camelid V_H H single domain antibodies, where the affinity varies between 2 and 300 nM [5,6]. However, NARs encompass this affinity in two, rather than three CDR loops, as the CDR2 region is severely truncated [3,9]. The cysteine residues seen within many NAR (and camelid) CDR loops are conserved in both proteins 12A-9 and 12A-14, and probably contribute to the antigen-binding affinity by disulphide bond formation and structural stability.

Both the NAR variable domains reported here can be readily produced as recombinant proteins in *E. coli*. However, while a significant proportion of the 12A-9 and 12A-14 proteins are produced in monomeric form, multimers (dimer and trimer) also occur. Surprisingly, the isolated monomeric and multimeric species are remarkably stable, with no evidence of inter-conversion of peak purified proteins. The relationship between the 12A-9 monomer and trimer forms requires further investigation and may reflect non-covalent framework residue interactions peculiar to these proteins, as other NAR variable domains we have analysed do not show similar multimer formation and stability and are predominantly monomeric proteins. As a trimeric architecture is not expected to occur in native NAR molecules, where the variable domains are tethered to constant regions, it is possible that their existence here as trimeric variable domains is an unusual side-effect of recombinant expression. Ultimately, resolution of these questions will probably require X-ray crystallographic data to define the precise nature of the NAR solvent-exposed residues and surfaces.

The 12A-9 and 12A-14 NAR domains are clearly derived from functional shark cDNAs and show no similarity, beyond invariant regions in the underlying framework, to the anti-Kgp NARs isolated previously [9]. These earlier proteins have synthetic rather than naturally selected CDR3 loops

and were not affinity matured. Thus, it is likely that clones 12A-9 and 12A-14, introduced in the expanded library, efficiently out-competed any other Kgp-specific proteins. Alternatively, it is well documented that different selection matrices (immunotubes, this study; versus ELISA plates [9]) can produce radically different antibody selection solutions, even when screening is performed exactly in parallel [19]. The isolation of natural Kgp gingipain-specific NARs in sharks is perhaps surprising. However, while little is known about the oral microflora of sharks, one study reported isolation of *Vibrio*, *Staphylococcus*, and *Pseudomonas* species from the teeth of a great white shark [20]. Therefore, it is possible that wobbegong sharks carry *Porphyromonas* species and have mounted an immune response against the protease virulence determinants. The isolation of the two different but obviously closely related NAR proteins may also indicate the action of affinity maturation processes on an initial low-affinity NAR molecule. Indeed, clone 12A-14 could represent such a low-affinity progenitor, with subsequent 'maturation' to the 12A-9 form. If so, then both CDR loops and framework regions are being targeted, in what may be the shark equivalent of mammalian antibody somatic hypermutation.

With specific NAR binding molecules now isolated from both synthetic libraries generated using artificial loop sequences, and from the natural immune repertoire of sharks, it is clear that recombinant NAR variable domain libraries represent a valuable source of high-affinity single domain binding reagents. Future experimentation is clearly required to further compare their stability and structure with that of other antibody fragments, and such work is currently in progress.

Acknowledgements: We thank Dr. Kim Wark for advice and discussions, Dr. Terry Mulhern for performing the CD analysis, and Mr. Sony Fischer for assistance in obtaining wobbegong shark blood samples. We gratefully acknowledge the assistance of Mr. N. Bartone with oligonucleotide synthesis and Mr. P. Strike for the protein N-terminal sequencing.

References

- [1] Flajnik, M.F. (1996) *Vet. Immunol. Immunopathol.* 54, 145–150.
- [2] Marchalonis, J.J., Schluter, S.F., Bernstein, R.M. and Hohman, V.S. (1998) *Immunol. Rev.* 166, 103–122.
- [3] Roux, K.H., Greenberg, A.S., Greene, L., Strelets, L., Avila, D., McKinney, E.C. and Flajnik, M.F. (1998) *Proc. Natl. Acad. Sci. USA* 95, 11804–11809.
- [4] Nuttall, S.D., Irving, R.A. and Hudson, P.J. (2000) *Curr. Pharm. Biotechnol.* 1, 253–263.
- [5] Muyldermans, S. and Lauwereys, M. (1999) *J. Mol. Recognit.* 12, 131–140.
- [6] Muyldermans, S. (2001) *J. Biotechnol.* 74, 277–302.
- [7] Diaz, M., Greenberg, A.S. and Flajnik, M.F. (1998) *Proc. Natl. Acad. Sci. USA* 95, 14343–14348.
- [8] Diaz, M., Velez, J., Singh, M., Cerny, J. and Flajnik, M.F. (1999) *Int. Immunol.* 11, 825–833.
- [9] Nuttall, S.D., Krishnan, U.V., Hattarki, M., De Gori, R., Irving, R.A. and Hudson, P.J. (2001) *Mol. Immunol.* 38, 313–326.
- [10] O'Brien-Simpson, N.M., Paolini, R.A., Hoffmann, B., Slakeski, N., Dashper, S.G. and Reynolds, E.C. (2001) *Infect. Immunol.* 69, 7527–7534.
- [11] Ausubel, F.M., Brent, R., Kingston, R.E., Moore, D.D., Seidman, J.G., Smith, J.A. and Struhl, K. (1989) *Current Protocols in Molecular Biology*, John Wiley and Sons, New York.
- [12] Pike, R., McGraw, W., Potempa, J. and Travis, J. (1994) *J. Biol. Chem.* 269, 406–411.
- [13] Galanis, M., Irving, R.A. and Hudson, P.J. (1997) Bacteriophage library construction and selection of recombinant antibodies, in: *Current Protocols in Immunology* (Coligan, J.E., Kreisbeck,

- A.M., Margulies, D.H., Shevach, E.M. and Strober, W., Eds.), pp. 17.1.1–17.1.45, John Wiley and Sons, New York.
- [14] Coia, G., Ayres, A., Lilley, G.G., Hudson, P.J. and Irving, R.A. (1997) *Gene* 201, 203–209.
- [15] Minsky, A., Summers, R.G. and Knowles, J.R. (1986) *Proc. Natl. Acad. Sci. USA* 83, 4180–4184.
- [16] Gruen, L.C., Kortt, A.A. and Nice, E. (1993) *Eur. J. Biochem.* 217, 319–325.
- [17] Kortt, A.A., Nice, E. and Gruen, L.C. (1999) *Anal. Biochem.* 273, 133–141.
- [18] Brahms, S. and Brahms, J. (1980) *J. Mol. Biol.* 138, 149–178.
- [19] Lou, J., Marzari, R., Verzillo, V., Ferrero, F., Pak, D., Sheng, M., Yang, C., Sblattero, D. and Bradbury, A.J. (2001) *J. Immunol. Methods* 253, 233–242.
- [20] Buck, J.D., Spotts, S. and Gadbow Jr., J.J. (1984) *J. Clin. Microbiol.* 20, 849–851.

APPENDIX III

**Characterisation of the specificity of Arginine-Specific gingipains from
Porphyromonas gingivalis reveals active site differences between different forms
of the enzymes**

**Ally, N., Whisstock, J.C., Sieprawska-Lupa, M., Potempa, J., Le Bonniec, B.F.,
Travis, J. and Pike, R.N.**

Biochemistry 42:11693-700 (2003)

Characterization of the Specificity of Arginine-Specific Gingipains from *Porphyromonas gingivalis* Reveals Active Site Differences between Different Forms of the Enzymes[†]

Nafisa Ally,[‡] James C. Whisstock,^{‡,§} Magdalena Sieprawska-Lupa,^{||} Jan Potempa,^{||,‡} Bernard F. Le Bonniec,[#] James Travis,[‡] and Robert N. Pike^{*,‡}

Department of Biochemistry and Molecular Biology and Victorian Bioinformatics Consortium, Monash University, Clayton, Victoria 3800, Australia, Department of Microbiology, Faculty of Biotechnology, Jagiellonian University, 30-387 Kraków, Poland, Department of Biochemistry and Molecular Biology, University of Georgia, Athens, Georgia 30602, and Inserm, Unite 428, Universite Paris V, 75270 Paris Cedex 06, France

Received June 6, 2003; Revised Manuscript Received August 5, 2003

ABSTRACT: *Porphyromonas gingivalis* is a pathogen associated with periodontal disease, and arginine-specific proteases (gingipains-R) from the bacterium are important virulence factors. The specificity of two forms of gingipain-R, HRgpA and RgpB, for substrate positions C-terminal to the cleavage site was analyzed, and notable differences were observed between the enzymes. Molecular modeling of the HRgpA catalytic domain, based on the structure of RgpB, revealed that there are four amino acid substitutions around the active site of HRgpA relative to RgpB that may explain their different specificity. Previously, differences in the ability of these two gingipain-R forms to cleave a number of proteins were attributed to additional adhesins on HRgpA mediating increased interaction with the substrates. Here, purified RgpA_{cat}, the catalytic domain of HRgpA, which like RgpB also lacks adhesin subunits, was used to show that the differences between HRgpA and RgpB are probably due to the amino acid substitutions at the active site. The kinetics of cleavage of fibrinogen, a typical protein substrate for the gingipain-R enzymes, which is bound by HRgpA but not RgpA_{cat} or RgpB, were evaluated, and it was shown that there was no difference in the cleavage of the fibrinogen A α -chain between the different enzyme forms. HRgpA degraded the fibrinogen B β -chain more efficiently, generating distinct cleavage products. This indicates that while the adhesin domain(s) play(s) a minor role in the cleavage of protein substrates, the major effect is still provided by the amino acid substitutions at the active site of *rgpA* gene products versus those of the *rgpB* gene.

Porphyromonas gingivalis is a major pathogen associated with the onset of adult periodontitis, one of the major causes of tooth loss today (1). Periodontitis results from chronic inflammation of the gingival and periodontal tissue and has recently been associated with cardiovascular disease and preterm delivery of low birth weight infants (2–4). The disease is characterized by massive accumulation of neutrophils, bleeding on probing, bone resorption, formation of periodontal pockets, and loss of tooth attachment. Approximately 15% of the population are known to suffer from the most severe forms of the disease, which, if left untreated, results not only in tooth loss but also in systemic complications (2, 5).

P. gingivalis is a black pigmented, anaerobic, Gram-negative bacterium that produces a number of virulence factors, such as cysteine proteases, haemagglutinins, lipopolysaccharides, and fimbriae, which enable the bacterium to colonize periodontal pockets (6). The proteolytic enzymes of the bacteria have been shown to play an important role in the pathogenesis of periodontitis (7, 8). The Arg-X-specific and Lys-X-specific proteases produced by the bacteria, referred to as gingipains-R and -K, comprise a major proportion of its total activity and are considered to be important virulence determinants (7). Recent studies have revealed that null mutants of *P. gingivalis* for gingipain-R enzymes showed a marked decrease in virulence in in vivo models, and immunization with peptides corresponding to the N-terminal sequence of the catalytic domain of gingipains-R has also been shown to protect against infection by the bacteria in mouse models (9), indicating the overall importance of these enzymes in the pathogenesis of the disease by the bacterium.

The gingipains-R produced by *P. gingivalis* cleave peptide bonds exclusively after arginyl residues (10) and are encoded by two genes, *rgpA* and *rgpB* (11). The major forms of gingipain-R derived from the *rgpA* gene are a 50 kDa catalytic domain (RgpA_{cat})¹ and a 95 kDa high molecular mass, noncovalent complex of catalytic and hemagglutinin/

[†] This work was supported by National Health and Medical Research Council (Australia) Grant 990199 (to R.N.P.), Grant 3 PO4A 003 24 from the Committee of Scientific Research (KBN, Poland) (to J.P.), and National Institutes of Health Grant DE 09761 (to J.T.). J.C.W. is a Logan Fellow of Monash University and a Senior Research Fellow of the NHMRC.

^{*} To whom correspondence should be addressed. Telephone: 61-3-9905 3923. Fax: 61-3-9905 4699. E-mail: rob.pike@med.monash.edu.au.

[‡] Department of Biochemistry and Molecular Biology, Monash University.

[§] Victorian Bioinformatics Consortium, Monash University.

^{||} Jagiellonian University.

^{||} University of Georgia.

[#] Inserm, Unite 428, Universite Paris V.

adhesin domains (HRgpA) (12), the former responsible for proteolytic activity and the latter for adhesion to extracellular matrix proteins and red blood cells. In comparison to *rgpA*, the *rgpB* gene lacks a sequence encoding the hemagglutinin/adhesin domains, and its product occurs predominantly as the soluble 50 kDa gingipain-R (RgpB) (13). Gingipain-R enzymes have been shown to activate coagulation factors and degrade components of the complement pathway and several physiologically important proteins, contributing to the virulence of the pathogen (14–19). In addition to causing destruction to the tissue supporting the teeth, gingipain-R enzymes play a major role in the deregulation of the inflammatory response and disruption of host defense mechanisms.

Analysis of the recently solved structure of RgpB indicates that the molecule is composed of two distinct domains, an N-terminal catalytic domain with topological similarity to caspases and a C-terminal domain with an Ig-like structure (20). The Ig-like domain of RgpB is thought to be involved in helping it bind to protein substrates or dock to endogenous proteins, other bacteria, or host cell surfaces (20). The catalytic domain of RgpB is almost identical to that of HRgpA (RgpA_{cat}) at the primary structure level, indicating that previously noted differences between HRgpA and RgpB in their ability to cleave protein substrates (14) are most likely due to the additional hemagglutinin/adhesin domains in HRgpA. This study initially aimed to determine the specificity of the two proteases toward substrate residues in the P₂'/P₃' region. Notable differences in specificity between HRgpA and RgpB led us to investigate whether the additional hemagglutinin/adhesin domains of HRgpA influence substrate specificity. Determination of the specificity of these proteases will aid in the design of drugs to control periodontal disease.

EXPERIMENTAL PROCEDURES

Materials. Bz-L-Arg-pNA, N^α-p-tosyl-L-lysine chloromethyl ketone (TLCK), and leupeptin were purchased from Sigma (Sydney, Australia). Z-L-Lys-pNA was from Novabiochem (Darmstadt, Germany). An extract from the medicinal leech (*Hirudo medicinalis*) was a kind gift from Dr. Christian Sommerhof (Ludwig Maximilian University, Munich, Germany). The extract at 0.1 mg/mL totally inhibited 0.4 nmol of α-thrombin amidolytic activity.

Fluorescence-Quenched Substrates. The fluorescence-quenched substrates were synthesized as described previously (21). Substrates were dissolved in DMF, and the concentration of the stock solution was determined spectrophotometrically, assuming an absorption coefficient of 10⁴ M⁻¹ cm⁻¹ at 360 nm. Each substrate consisted of a 10-residue peptide with a 2-aminobenzoyl (Abz) group at the N-terminus and a penultimate 2,4-dinitrophenyl- (Dnp-) derivatized lysine.

Peptides had the following general sequence: Abz-Val-Gly-Pro-Arg-Ser-X-X-Leu-Lys(Dnp)-Asp-OH, with the X denoting the variable amino acid positions at P₂' and P₃'. The P₂' specificity was determined using substrates with a leucine in the P₃' position, whereas the P₃' substrates contained a phenylalanine at the P₂' position.

Cultivation of the Bacteria and Purification of Enzymes. *P. gingivalis* strain HG66 cells used as a source of the enzymes in this study were grown as described previously (22). HRgpA and RgpB were purified from the HG66 strain culture fluid as described previously (23). Briefly, HRgpA was purified using gel filtration and arginine-Sepharose chromatography, while RgpB was purified using a combination of gel filtration and anion-exchange chromatography on Mono Q (24). RgpA_{cat} was purified from the fractions containing RgpB that were eluted from a Sephadex G-150 gel filtration column (25). Briefly, fractions were pooled and loaded onto a DE-52 cellulose column, where RgpA_{cat} was eluted in the void volume using 50 mM Bis-Tris and 1 mM CaCl₂, pH 6.5. RgpA_{cat} was loaded on a Mono Q column, eluted with 1 M NaCl, 50 mM Bis-Tris, and 1 mM CaCl₂, pH 6.5, buffer, and purified to homogeneity.

The purity of enzymes in each batch was checked using SDS-PAGE. Both RgpB and RgpA_{cat} migrated as a single band with mobility equivalent to a molecular mass of 48 kDa and homogeneity greater than 95% as determined using laser densitometry scanning of the gel. HRgpA resolves into four major bands and one minor band on SDS-PAGE (23). The identity of each protein band was confirmed by N-terminal sequence analysis as being derived from the RgpA polypeptide. Also, N-terminal sequence analysis was used to check for cross-contamination of RgpB and RgpA_{cat} preparations. In each case, only one sequence was obtained, which differed at only residue 8, which was Glu and Gln in RgpB and RgpA_{cat}, respectively. Comparative analysis of amino acid derivative peaks of cycle 8 of the Edman degradation for the 48 kDa band seen for RgpA_{cat} and RgpB clearly indicated that any cross-contamination was below 10% of the major form of the gingipain-R being analyzed.

Kinetic Studies. The *k*_{cat} and *K*_m values were measured at 37 °C using substrates at concentrations ranging from 1 to 50 μM, with a final concentration of active site titrated enzyme of 1.0 nM in 0.2 M Tris-HCl, 5 mM CaCl₂, 10 mM cysteine, and 0.1 M NaCl, pH 7.6. The assay was performed in a total volume of 200 μL in microplates and was carried out in triplicate. Enzyme solution (100 μL) was added to 100 μL of substrate solution, and the initial velocity was recorded (usually over 10 min) at seven different substrate concentrations at 330/420 nm on a fluorescent plate reader (Biolumin960, Molecular Dynamics). The initial velocities were plotted against substrate concentrations, and the lines were fitted to a single site binding equation using nonlinear regression analysis in the program GraphPad Prism. The *K*_m values were derived from the fitted line, while *k*_{cat} values were calculated from the *V*_{max} values by taking into account the amount of active enzyme used in the assays, the latter determined as described previously (26). Four substrates (P₂' His, P₂' Ser, P₃' Gly, and P₃' Ala), toward which HRgpA and RgpB displayed a significant difference in activity, were assayed as above with the three gingipain-R enzymes, HRgpA, RgpB, and RgpA_{cat}, on a fluorescent plate reader (Fluostar Galaxy, BMG Technologies).

¹ Abbreviations: RgpA_{cat}, catalytic domain derived from the *rgpA* gene; HRgpA, 95 kDa form of arginine-specific gingipain derived from the *rgpA* gene; RgpB, 50 kDa form of arginine-specific gingipain derived from the *rgpB* gene; Ig, immunoglobulin; Bz or Z, benzoyl-carbonyl; TLCK, N^α-p-tosyl-L-lysine chloromethyl ketone; DMF, dimethylformamide; Dnp, dinitrophenyl; Abz, o-aminobenzoic acid. The residues of a peptide substrate are designated P_n, ..., P₂, P₁, P₁', ..., P_n' and interact with corresponding subsites in the protease designated S_n, ..., S₂, S₁, S₁', ..., S_n'; cleavage occurs by definition between the P₁ and P₁' positions.

Modeling. The X-ray crystal structure of RgpB (PDB identifier ICVR; 20) was obtained from the Protein Data Bank (27). RgpB and RgpA are 90% identical, and the sequences were aligned using the alignment package available in Quanta (Accelrys Inc., San Diego). The molecular model of RgpA was built using the program Modeler (28) and the X-ray crystal structure of RgpB as a template. A Ramachandran plot confirmed that all residues in the model of RgpA were in allowed conformations.

ELISA of Gingipain Binding to Extracellular Matrix Proteins. To test the binding of the gingipain-R enzymes to different extracellular proteins, proteins to be tested were coated onto Nunc maxisorp ELISA plates at a concentration of 1 $\mu\text{g}/\text{mL}$ in phosphate-buffered saline (PBS) at 4 °C for 16 h. The wells were then blocked with 0.5% (w/v) BSA in PBS for 1 h at 37 °C. Every incubation was followed by three washes with 0.1% (v/v) Tween 20-PBS. Following blocking, the wells were incubated with serial dilutions of HRgpA, RgpB, and RgpA_{cat}, all previously inactivated with TLCK, starting from 50 $\mu\text{g}/\text{mL}$ in BSA-PBS for 2 h. The wells were then incubated with chicken anti-gingipain-R (1 $\mu\text{g}/\text{mL}$) in BSA-PBS for 1 h, followed by incubation with anti-chicken IgY-horseradish peroxidase conjugate (1 $\mu\text{g}/\text{mL}$) in BSA-PBS for 1 h at 37 °C. The plate was then washed, and binding was detected by incubation with tetramethylbenzidine substrate solution. The reaction was terminated by adding 2 M H₂SO₄, and the product was read at 450 nm.

Analysis of Degradation of Proteins by SDS-PAGE. Protein degradation was carried out at 37 °C in 0.2 M Tris-HCl, 1 mM CaCl₂, and 10 mM cysteine buffer. Aliquots were taken at various time points, and enzyme activity was stopped by adding 1 mM TLCK. Aliquots containing the proteins and degradation products were electrophoresed on 10% Tris-Tricine (29) sodium dodecyl sulfate-polyacrylamide gel electrophoresis (SDS-PAGE) gels and visualized by Coomassie blue R-250 staining. Fibrinogen cleaved by HRgpA was also blotted to a PVDF membrane following SDS-PAGE, and bands were excised for N-terminal sequencing as previously described (23).

Western Blot Analysis of the Degradation of Human Plasma Fibrinogen by Arg-Gingipains. Plasma was collected by mixing 9 mL of human blood with 1 mL of 3.2% (w/v) sodium citrate and centrifuging the mixture for 5 min at 2700 rpm. Plasma was depleted of albumin by mixing it with Cibacron Blue-Sepharose equilibrated in PBS using 2 mL of the chromatography matrix per 1.5 mL of plasma. After 30 min of gentle mixing at room temperature, the matrix was removed by centrifugation, and the supernatant was used in further experiments. Plasma prepared in this way (50 μL) was made up to 100 μL using a buffer containing either 20 mM cysteine and 0.1 M Tris, pH 8.0, or the same buffer supplemented with 1 mg/mL leech extract. To this mixture was then added 50 μL of activated gingipain-R to yield a final enzyme concentration of 10 nM. The plasma mix was incubated at 37 °C, and 20 μL aliquots were transferred at 5, 10, and 15 min into 80 μL of 5 mM TLCK in PBS to stop the reaction. Samples were boiled with SDS-PAGE reducing buffer for 10 min, electrophoresed on 10% Tris-Tricine (29) SDS-PAGE gels, and transferred onto nitrocellulose membrane overnight at 30 V. The membranes were blocked with 1% (w/v) low fat milk powder in Tris-buffered

saline (TBS) overnight. The membranes were washed in Tween-TBS and incubated with goat anti-human fibrinogen diluted 1:5000 in 1% (w/v) bovine serum albumin in Tween-TBS for 1 h. The membranes were washed and incubated for 1 h with anti-goat alkaline phosphatase diluted 1:100000 in 1% (w/v) bovine serum albumin in Tween-TBS. Bound antibodies were detected using BCIP/NBT substrate.

RESULTS

The specificity of HRgpA and RgpB at the P₂' position was determined using fluorescence-quenched substrates with 18 different amino acids at this position, excluding substrates with an arginine or a cysteine residue. Substrates with a cysteine residue were not used, as oxidation of the cysteine residue would interfere with the activity of the enzymes. Similarly, cleavage of substrates containing an additional arginine residue would probably result in higher K_m and k_{cat}/K_m values due to secondary cleavage of the substrates. The specificity of the enzymes for the P₃' position was determined using substrates with 16 substitutions at this position, with cysteine, arginine, phenylalanine, and glutamate excluded. Each substrate contained the following sequence of amino acids, (Abz)-Val-Gly-Pro-Arg-Ser-Xaa-Leu-Leu-Lys(Dnp)-Asp-OH, where Xaa is representative of any one of the 18 amino acids examined at the P₂' position in this example. The Lys(Dnp) group quenches the fluorescence of the N-terminal Abz group in an uncleaved substrate by resonance energy transfer. Cleavage of the substrate relieves quenching, resulting in an increase in fluorescence proportional to the concentration of the released fluorophore fragment, thus allowing the determination of the initial velocities of the enzymes in relation to substrate concentration and hence the kinetic parameters, K_m , V_{max} , and k_{cat} . Values for k_{cat}/K_m were derived from the individual constants.

HRgpA Specificity at P₂' and P₃'. Phenylalanine is the most preferred amino acid at P₂' for cleavage by HRgpA, followed by leucine and tyrosine (Table 1). The k_{cat}/K_m value of the most preferred amino acid at P₂' for HRgpA, phenylalanine (12.5 $\mu\text{M}^{-1}\cdot\text{s}^{-1}$), was 11.4-fold greater than the k_{cat}/K_m value of the least preferred amino acid at P₂', which was proline (1.1 $\mu\text{M}^{-1}\cdot\text{s}^{-1}$). Leucine was the most preferred and isoleucine was the least preferred amino acid at the P₃' position (Table 2). The K_m values determined for HRgpA, which reflect the binding affinity of an enzyme for a substrate, indicate that HRgpA does not show an affinity for a particular group of amino acids (Tables 1 and 2). HRgpA had the greatest affinity for the substrate with a positively charged lysine or a polar uncharged asparagine residue at P₂', with K_m values of 15.1 and 15.6 μM , respectively. The K_m values for HRgpA at P₃' again reflect the lack of preference for any particular group of amino acids at this position; the K_m value for the substrate with a proline at P₃' (6.2 μM) was significantly lower than any other substrate (Table 2).

RgpB Specificity at P₂' and P₃'. Results obtained indicate that serine, a polar hydrophilic amino acid, was the most preferred residue at P₂' ($k_{cat}/K_m = 7.9 \mu\text{M}^{-1}\cdot\text{s}^{-1}$) for RgpB (Table 1). As with HRgpA, proline ($k_{cat}/K_m = 0.5 \mu\text{M}^{-1}\cdot\text{s}^{-1}$) was the least preferred amino acid at P₂' for RgpB. RgpB did not display a preference for any particular group of amino acids at P₃' (Table 2), with the k_{cat}/K_m value for lysine (3.8

Table 1: Substrate Specificity of HRgpA and RgpB at P₂'^a

substrate	HRgpA			RgpB		
	<i>K_m</i>	<i>k_{cat}</i>	<i>k_{cat}/K_m</i>	<i>K_m</i>	<i>k_{cat}</i>	<i>k_{cat}/K_m</i>
GPR-SFL	20.5	25.6	12.5	24.5	8.6	3.5
GPR-SLL	26.2	28.1	10.7	21.2	6.1	2.8
GPR-SYL	24.2	25	10.3	44.9	14.8	3.3
GPR-SQL	26.4	25.7	9.7	42.4	9.5	2.2
GPR-SGL	23.4	21.8	9.3	34.7	11.2	3.2
GPR-SWL	21.3	18.9	8.8	nd	nd	nd
GPR-STL	39.1	31.7	8.1	32.5	7.8	2.4
GPR-SSL	24.2	17.4	7.2	55.8	44.1	7.9
GPR-SHL	39.5	21.7	5.5	71.8	7.8	1.1
GPR-SNL	15.6	8.1	5.2	17.4	3.9	2.2
GPR-SVL	17.9	8.2	4.6	41.9	10.4	2.5
GPR-SDL	42.1	17.5	4.1	32.3	4.7	1.4
GPR-SKL	15.1	6.2	4.1	59.3	11.8	1.9
GPR-SAL	27.3	10.2	3.7	29.7	9.4	3.2
GPR-SIL	77.9	23.6	3.0	84.8	10.2	1.2
GPR-SML	20.4	4.9	2.4	38.9	13.4	3.4
GPR-SEL	22.8	5.3	2.3	25.2	4.0	1.6
GPR-SPL	21.2	2.3	1.1	49.4	1.9	0.5
selectivity factor			11.4			16

^a Units for *K_m* are expressed in μM , *k_{cat}* were expressed in $\text{s}^{-1} \times 10^3$, and *k_{cat}/K_m* were expressed in $\mu\text{M}^{-1}\text{s}^{-1}$. Assays were carried out in triplicate, and values for *K_m* and *k_{cat}* had a standard error of less than or equal to 10%. Only residues from P₃ to P₃' are indicated, and amino acids unique to each substrate are in bold. nd = not determined.

Table 2: Substrate Specificity of HRgpA and RgpB at P₃'^a

substrate	HRgpA			RgpB		
	<i>K_m</i>	<i>k_{cat}</i>	<i>k_{cat}/K_m</i>	<i>K_m</i>	<i>k_{cat}</i>	<i>k_{cat}/K_m</i>
GPR-SFL	20.5	25.6	12.5	24.5	8.6	3.5
GPR-SFN	23.1	27.0	11.7	46.5	12.5	2.7
GPR-SFG	27.8	2.9	10.4	53.3	18.8	3.5
GPR-SFD	17.8	15.4	8.4	41.5	11.5	2.7
GPR-SFP	6.2	4.3	6.9	18.7	5.5	2.9
GPR-SFH	35.6	24.7	6.9	47.9	14.4	3.0
GPR-SFK	20.9	13.2	6.3	12.3	4.7	3.8
GPR-SFS	19.4	11.9	6.1	19.7	4.8	2.4
GPR-SFY	24.8	15.2	6.1	15.8	3.2	2.0
GPR-SFA	13.1	7.8	5.9	31.6	7.2	2.2
GPR-SFT	23.7	14.1	5.9	36.9	3.3	0.9
GPR-SFW	17.8	9.9	5.5	25.1	7.8	3.1
GPR-SFV	64.0	29.7	4.6	30.4	11.1	3.6
GPR-SFQ	31.8	10.7	3.3	27.0	7.5	2.7
GPR-SFM	19.1	5.3	2.7	27.1	2.7	0.9
GPR-SFI	32.5	6.4	1.9	60.6	10.6	1.7
selectivity factor			6.6			4.3

^a Units for *K_m* are expressed in μM , *k_{cat}* were expressed in $\text{s}^{-1} \times 10^3$, and *k_{cat}/K_m* were expressed in $\mu\text{M}^{-1}\text{s}^{-1}$. Assays were carried out in triplicate, and values for *K_m* and *k_{cat}* had a standard error of less than or equal to 10%. Only residues from P₃ to P₃' are indicated, and amino acids unique to each substrate are in bold.

$\mu\text{M}^{-1}\text{s}^{-1}$), the most preferred amino acid at P₃', only 4.3-fold greater than the value for threonine ($0.9 \mu\text{M}^{-1}\text{s}^{-1}$), the least preferred amino acid at P₃'. The *K_m* values for RgpB indicate that it too does not show a preference toward a particular group of amino acids, although it has a broader range of *K_m* values, indicating a greater difference in its binding affinity toward substrates. RgpB had the highest affinity toward the substrate with an asparagine at the P₂' position (*K_m* = 17.4 μM). The substrate with a lysine at P₃' had a *K_m* value of 12.3 μM , which was the lowest value overall for RgpB.

Modeling of RgpA. RgpA and RgpB share 90% sequence identity, with the majority of the substitutions mapping to the Ig-like domain in the C-terminus. Only four substitutions



FIGURE 1: Crystal structure of RgpB (20). (A, top) Overall structure of RgpB demonstrating the two domains making up the overall catalytic domain in red and green. The Ig domain is in yellow. The inhibitor, D-Phe-Phe-Arg chloromethyl ketone, in the active site of RgpB is shown in purple, while substitutions in the active site of RgpB in relation to RgpA are shown in blue ball-and-stick representation. (B, bottom left) Electrostatic potential of the active site of RgpB (red equals electronegative, blue is electropositive, and white is neutral). (C, bottom right) Close-up of the active site of RgpB, showing the substitutions relative to RgpA in blue ball-and-stick representation. The figure was produced using Quanta (Accelrys Inc.) and GRASP.

(D281 → N, Y283 → S, P286 → S, and N331 → K) map to the protease domain, all of which map to the region surrounding the active site (see Figure 1).

Comparison of the Specificity of HRgpA, RgpB, and RgpA_{cat} at P₂' and P₃'. RgpA_{cat} was used to help to determine if the differences in specificity between HRgpA and RgpB were due to the additional adhesin domains in HRgpA or due to the four amino acid substitutions in its active site compared to RgpB. The substrates to be used were selected on the basis of results obtained previously. One substrate each from the P₂' and P₃' range, for which HRgpA and RgpB had a high and a low *K_m* value, respectively, was selected. Values for *K_m* were determined for HRgpA, RgpB, and RgpA_{cat} toward substrates with a histidine or serine at the P₂' and a glycine or alanine at the P₃' position. The *K_m* values for HRgpA and RgpA_{cat} were similar and differed from the values obtained for RgpB. Thus, for instance, the *K_m* value for RgpB toward the substrate with a serine at the P₂' position was 55 μM , whereas the values for HRgpA and RgpA_{cat} were 24 and 30 μM , respectively (Figure 2). The *K_m* values for RgpB were nearly 2-fold higher than the values for HRgpA

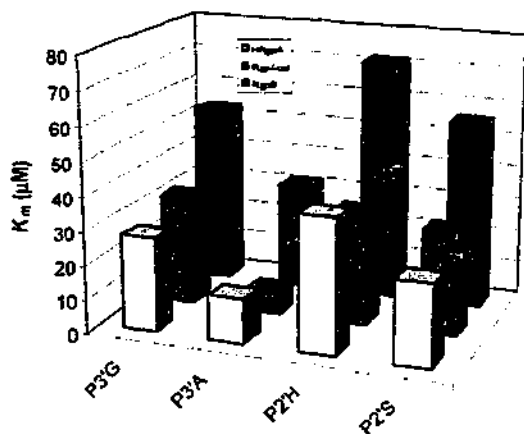


FIGURE 2: Comparison of the K_m values of HRgpA, RgpA_{cat}, and RgpB toward fluorescence-quenched substrates with a glycine or an alanine at the P₃' and a histidine or a serine at the P₂' position.

and RgpA_{cat}, indicating that RgpB had a weaker affinity toward the substrates in comparison to HRgpA and RgpA_{cat}.

Binding of Gingipains to Fibrinogen, Fibronectin, and Laminin. Results obtained in the specificity studies indicated that the adhesin domains are not responsible for the differences in specificity of HRgpA and RgpB toward peptide substrates. Since the binding activity of RgpA_{cat} had not previously been characterized, experiments were carried out to determine if the enzyme adhered to fibrinogen, fibronectin, and laminin. HRgpA bound all three proteins, whereas RgpA_{cat} and RgpB showed very little or no binding activity toward the proteins (less than 10% of the value for HRgpA) (results not shown). The lack of binding activity for RgpB and RgpA_{cat} indicates that the gingipains require the additional adhesin domains found in HRgpA in order to bind proteins and that the catalytic or Ig-like domains of the smaller proteases do not possess any binding activity.

Degradation of Fibrinogen by the Gingipains. Specificity studies using peptide substrates indicated that HRgpA and RgpA_{cat} are similar in their preferences for cleavage and differ from RgpB. We wanted to determine if this was also so for a protein substrate, such as fibrinogen, which is cleaved by all of the gingipain-R forms under study. Thus the pattern of cleavage of fibrinogen was used to evaluate whether the pattern of cleavage of the protein and/or rate of cleavage was different for the individual gingipain-R enzymes. We examined cleavage of the protein in its purified form and in plasma to evaluate whether there was a difference in the rate or position of cleavage in a complex milieu in comparison to the purified protein. Cleavage of the purified protein was followed directly using SDS-PAGE for the purified protein (Figure 3) and by western blotting for the plasma protein (Figure 4). It was apparent that all three forms of gingipain-R cleaved fibrinogen very similarly in terms of the kinetics of α -chain degradation, which was most sensitive to cleavage. The α -chain was cleaved at a number of positions, but for each enzyme isoform, a band of approximately 28 kDa appeared and grew stronger over the period of the incubation. N-Terminal sequencing of the approximately 28 kDa band revealed that it was derived from the N-terminal portion of the α -chain, having been cleaved at position 22 of the mature chain at the sequence VERIHQS (arrow indicates cleavage position). In contrast to the situation with the α -chain, HRgpA was significantly more efficient at cleaving

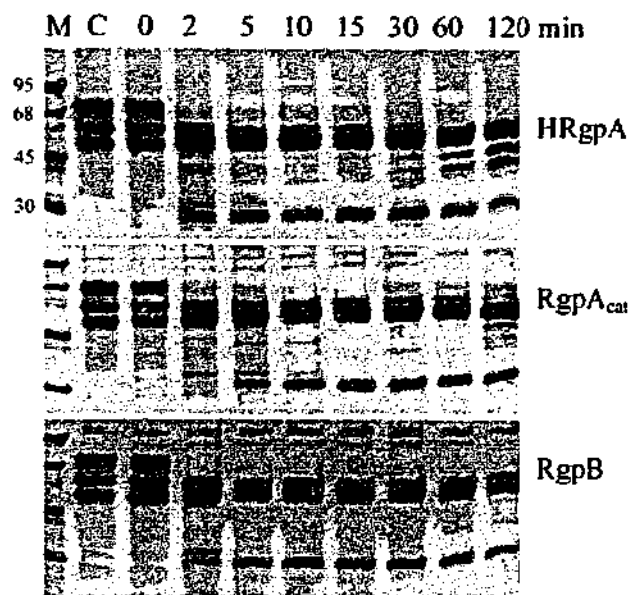


FIGURE 3: Degradation of fibrinogen by HRgpA, RgpA_{cat}, and RgpB at 0, 2, 5, 10, 15, 30, 60, and 120 min. A 10 nM concentration of enzyme was used for the assay. M designates the protein molecular mass markers (sizes indicated next to the markers for the HRgpA gel: 95, 68, 45, and 30 kDa), and C designates control protein not incubated with enzyme. 10 μ g of protein was loaded per lane and electrophoresed on 10% Tris-Tricine SDS-PAGE gels.

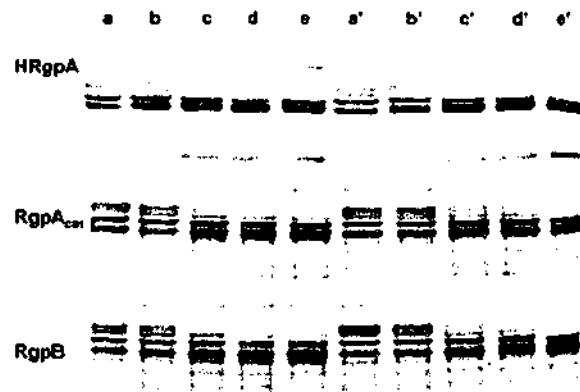


FIGURE 4: Cleavage of fibrinogen in plasma by gingipains. Samples of freshly collected human plasma depleted of albumin by absorption on the Cibacron Blue Sepharose alone (lanes a–e) or pretreated with a leech extract (lanes a'–e') were incubated with 10 nM gingipain (each form) for 0 min (lanes b and b'), 5 min (lanes c and c'), 10 min (lanes d and d'), and 15 min (lanes e and e'). Lanes a and a' are control plasma preincubated for 15 min in the absence of gingipain. The reaction was stopped using TLCK (4 mM), samples were boiled in reducing treatment buffer and electrophoresed on 10% Tricine SDS-PAGE gels, and then immunoblots were performed with fibrinogen being detected using a goat anti-human fibrinogen antibody.

the β -chain than RgpB and RgpA_{cat}, leading to accumulation of a lower molecular mass cleavage product which migrated just above the γ -chain. N-Terminal sequencing of this band revealed that it was indeed derived from the β -chain and resulted from two cleavages at positions 42 and 44 in the sequence GYRIARIPAK (arrows indicate the position of cleavage).

The gingipain-R forms once again cleaved the α -chain of fibrinogen in plasma with similar kinetics, although only

HRgpA was able to generate the approximately 28 kDa band derived from cleavage of the A α -chain in contrast to the situation with the pure protein (Figure 4). Once again, only HRgpA was able to cleave the B β -chain efficiently in the plasma context. The profile of cleavage of the α -chain and β -chain was the same in the absence or presence of leech extract (applied at a concentration that totally inhibited thrombin activity), indicating that cleavage of these chains was independent of thrombin. It should be noted that thrombin was apparently active in cleaving fibrinogen in the absence of leech extract to some extent, however, since a band corresponding to the γ -chain dimer was observed, which is not seen when the leech extract was present. This was only apparent for HRgpA treatment, indicating that HRgpA is more efficient at activating prothrombin than the other protease forms, as has been observed previously (30). Once activated, thrombin would activate factor XIII to cause dimerization of the γ -chains by transglutamination.

DISCUSSION

The initial focus of the present study was to map the preferences of the gingipain-R enzymes for prime site amino acid residues in peptide substrates. A previous study (25) examined the specificity for residues in the nonprime sites and found that the gingipains were relatively nonspecific for these residues and also that no marked difference in specificity could be found between different forms of the gingipains-R. Our investigation therefore examined whether this was the case for the prime sites of substrates.

The two gingipain-R forms initially analyzed, HRgpA and RgpB, were not very selective for substrate residues at the P $_2'$ and P $_3'$ sites; thus selectivity factors (or the ratio between top and bottom values for each kinetic term) ranged from 4.3 to 18.0. Both enzymes were most selective for substrate residues at the P $_2'$ subsites, with RgpB somewhat more selective than HRgpA at P $_2'$ and slightly less selective at P $_3'$ (Tables 1 and 2). Overall, it appeared that the specificity constant for any given substrate, usually accepted to be the k_{cat}/K_m value, was mostly influenced by the k_{cat} value. In general, variation between K_m values was lower than for the k_{cat} values for any given subsite and enzyme. It was clear that HRgpA and RgpB were different in their specificity for different amino acids at the prime subsites. We therefore were interested to know the underlying reasons for this.

Initial analysis of the difference in the specificity of the prime subsites led us to hypothesize that it was the additional adhesin domains of HRgpA which might give rise to the differences in specificity. For this to be true, however, it would be necessary for the active sites of the proteases to be identical. We therefore modeled the catalytic domain of HRgpA (RgpA $_{cat}$) upon the crystal structure of RgpB to determine whether this was correct. The surface of the active site and its surroundings are relatively flat, except for the S $_1$ pocket, which is a fairly narrow slot, bordered by in-plane hydrogen bond acceptors and covered by a hydrophobic lid (Figure 1A). The active site is also characterized by a negative electrostatic potential, which may have an effect on the binding of substrates (Figure 1B). There are four amino acid substitutions, D281 \rightarrow N, Y283 \rightarrow S, P286 \rightarrow S, and N331 \rightarrow K, found in the active site of HRgpA compared to RgpB (Figure 1C). Apart from these four substitutions, the active sites of HRgpA and RgpB are

identical. The amino acid substitutions could have a profound effect on the binding of substrates and subsequent cleavage, particularly P286S, since P285 and P286 form a double proline motif at the end of helix 9 in RgpB. These residues form one of the walls of the S $_1$ pocket, and substitution of P286 with a serine may thus alter the accessibility to the S $_1$ pocket. These substitutions might change direct interactions with prime site substrate residues, but it is more likely that they cause a general change in the conformation of the prime site binding sites of the active site, thus giving rise to the differences in specificity noted.

To resolve whether it was the contribution of the active site substitutions or the additional adhesin domains that determined the differences in specificity between HRgpA and RgpB, we purified the small quantity of RgpA $_{cat}$ to be found in culture supernatants of *P. gingivalis*. RgpA $_{cat}$ is the catalytic domain of RgpA, analogous to RgpB, except that the four amino acid substitutions would be present at the active site. We showed that RgpA $_{cat}$ was similar to HRgpA in terms of its kinetics of cleavage of four substrates containing P2' or P3' substitutions. We selected the substrates analyzed on the basis of their having large differences in terms of their kinetics of cleavage by HRgpA and RgpB. Thus it appears that it is most likely that it is the active site substitutions in HRgpA versus RgpB that dictate their differences in specificity for prime site residues and not the additional adhesin domains in HRgpA.

What then is the function of the additional adhesin domains in terms of the specificity of the proteases for cleavage of peptide or protein substrates? Previous work has attributed quite large differences in the cleavage of protein substrates by HRgpA versus RgpB to the additional adhesin subunits on HRgpA interacting with the protein substrates. Our data would indicate that the adhesin domains do not influence cleavage of peptide substrates, but is this also true for protein substrates to which the adhesin domains of the gingipains might bind? We first needed to establish whether the catalytic domains of the gingipains could bind to proteins in the same way as HRgpA. Since the catalytic domains of the gingipains have an Ig-like domain, which might conceivably have adhesin activity, it was important to determine whether RgpA $_{cat}$ or RgpB could bind to proteins. We have previously shown that HRgpA binds to fibrinogen, fibronectin, and laminin, but RgpB does not (24). Work carried out here showed that RgpA $_{cat}$ also did not bind to these proteins. This strongly indicates that the additional adhesin subunits in HRgpA mediate binding to the tested proteins.

We then tested whether binding to a protein substrate by HRgpA influences cleavage. We hypothesized that the binding event might influence the position of cleavage within the substrate, and therefore the pattern of cleavage bands seen on SDS-PAGE, and/or the rate of cleavage of a protein substrate. To test whether the adhesins have an influence on protein substrate cleavage, we examined whether HRgpA, RgpA $_{cat}$, and RgpB differed in their cleavage of purified fibrinogen (Figure 3). HRgpA, RgpA $_{cat}$, and RgpB cleaved the A α -chain of fibrinogen with very similar kinetics. The γ -chain of fibrinogen was essentially not degraded, but differences were observed for cleavage of the B β -chain between the gingipain-R forms. HRgpA cleaved the B β -chain most efficiently, followed by RgpA $_{cat}$ and then RgpB. This indicates that the additional adhesin domains of HRgpA may

position the enzyme advantageously for cleavage of the B β -chain relative to RgpA_{cat}. The greater efficiency of both RgpA forms also indicates that the active site differences found between RgpA and RgpB forms have a strong effect in this context. The position of cleavage of the fibrinogen A α -chain and B β -chain would be predicted to preclude formation of the fibrinopeptides A and B, thus explaining why fibrinogen is rendered nonclottable by the gingipains-R and thus overall the anti-clotting effect that these enzymes have in plasma, despite their activation of procoagulant enzymes.

We also tested for cleavage of the protein in plasma in order to evaluate whether the adhesins served to target HRgpA to a substrate such as fibrinogen, resulting in faster cleavage (Figure 4). It was shown that cleavage profiles in plasma were similar to those with purified fibrinogen in that all gingipain-R forms cleaved the A α -chain rapidly. However, there were some differences in the cleavage of the B β -chain, with only HRgpA cleaving this chain. This difference was not due to activation of the coagulation cascade (15, 30, 31), since the same cleavage pattern was observed in the presence of the leech extract containing hirudin and other very effective inhibitors of proteases from the coagulation cascade (32, 33).

The results of this study strongly imply that the differences previously noted between different forms of gingipain-R in terms of their cleavage of isolated protein substrates are primarily due to differences at the active site of the enzymes, with the adhesin domains playing a minor role. However, cleavage in complex (patho)physiological fluids such as plasma may be affected by the presence of the competing proteins, since it has been noted that HRgpA is more efficient in a number of biological contexts than RgpB. This enhanced activity has often been attributed to the extra adhesin subunits found on HRgpA compared to RgpB, and indeed, we have shown here that fibrinogen in plasma is cleaved in a different way from purified fibrinogen. However, this difference is limited to the rate of β -chain degradation and accumulation of some cleavage products. Thus, it appears that the adhesin subunits of HRgpA play relatively little overall roles in determining the cleavage rate of peptide or protein substrates in a complex physiological environment.

P. gingivalis is one of the major pathogens associated with adult periodontitis. Since periodontitis is one of the main causes of tooth loss today, and more recently has been linked to cardiovascular diseases, factors contributing to the virulence of the bacterium are attractive targets for the design of drugs or vaccines against the disease (2, 3). Gingipains-R are essential for the survival of *P. gingivalis* and responsible for various intrinsic and extrinsic factors associated with its virulence (14–16, 18). Determination of the P $_2$ ' and P $_3$ ' specificity of the gingipain-R enzymes thus helps to define the properties of their active site and improve our understanding of the specificity of these enzymes, which can be used further to develop selective synthetic inhibitors to combat periodontal disease.

REFERENCES

- Genco, C. A., Potempa, J., Mikolajczyk-Pawlinska, J., and Travis, J. (1999) Role of gingipain R in the pathogenesis of *Porphyromonas gingivalis*-mediated periodontal disease, *Clin. Infect. Dis.* 28, 456–465.
- Beck, J., Garcia, R., Heiss, G., Vokonas, P. S., and Offenbacher, S. (1996) Periodontal disease and cardiovascular disease, *J. Periodontol.* 67, 1123–1137.
- Genco, R. J. (1998) Periodontal disease and risk for myocardial infarction and cardiovascular disease, *Cardiovasc. Rev. Rep.* 19, 34–40.
- Offenbacher, S., Katz, V., Fertik, G., Collins, J., Boyd, D., Maynor, G., McKaig, and Beck, J. (1996) Periodontal infection as a possible risk factor for pre-term low birth weight, *J. Periodontol.* 67, 1103–1113.
- Page, R. C. (1998) The pathobiology of periodontal diseases may affect systemic diseases: inversion of a paradigm, *Ann. Periodontol.* 3, 108–120.
- Cutler, C. W., Kalmar, J. R., and Genco, C. A. (1995) Pathogenic strategies of the oral anaerobe *Porphyromonas gingivalis*, *Trends Microbiol.* 3, 45–51.
- Kuramitsu, H. K. (1998) Proteases of *Porphyromonas gingivalis*: what do not they do?, *Oral. Microbiol. Immunol.* 13, 263–270.
- Holt, S. C., Kesavalu, L., Walker, S., and Genco, C. A. (1999) Virulence factors of *Porphyromonas gingivalis*, *Periodontology* 20, 168–238.
- Genco, C. A., Odusanya, B. M., Potempa, J., Mikolajczyk-Pawlinska, J., and Travis, J. (1998) A peptide domain on gingipain R which confers immunity against *Porphyromonas gingivalis* infection in mice, *Infect. Immun.* 66, 4108–4114.
- Potempa, J., and Travis, J. (1996) *Porphyromonas gingivalis* proteinases in periodontitis, a review, *Acta Biochim. Pol.* 43, 455–466.
- Potempa, J., Pavloff, N., and Travis, J. (1995) *Porphyromonas gingivalis*: a proteinase/gene accounting audit, *Trends Microbiol.* 3, 430–434.
- Curtis, M. A., Kuramitsu, H. K., Lantz, M., Macrina, L. F., Nakayama, K., Potempa, J., Reynolds, E. C., and Aduse-Opoku, J. (1999) Molecular genetics and nomenclature of protease: of *Porphyromonas gingivalis*, *J. Periodontol. Res.* 34, 464–472.
- Mikolajczyk-Pawlinska, J., Kordula, T., Pavloff, N., Pemberton, P. A., Kiefer, M. C., Travis, J., and Potempa, J. (1998) Genetic variation of *Porphyromonas gingivalis* genes encoding gingipains, cysteine proteinases with arginine or lysine specificity, *Biol. Chem.* 277, 205–211.
- Imamura, T., Potempa, J., and Travis, J. (2000) Comparison of pathogenic properties between two types of arginine-specific cysteine proteinases (gingipains-R) from *Porphyromonas gingivalis*, *Microb. Pathog.* 29, 155–163.
- Imamura, T., Potempa, J., Tanase, S., and Travis, J. (1997) Activation of blood coagulation factor X by arginine-specific cysteine proteinases (gingipains-Rs) from *Porphyromonas gingivalis*, *J. Biol. Chem.* 272, 16062–16067.
- DiScipio, R. G., Daffern, P. J., Kawahara, M., Pike, R., Potempa, J., Travis, J., and Hugli, T. E. (1996) Cleavage of human complement components C5 by cysteine proteinases from *Porphyromonas (Bacteroides) gingivalis*. Prior oxidation of C5 augments proteinase digestion of C5, *Immunology* 87, 660–667.
- Lantz, M. S., Allen, R. D., Vail, T. A., Switalski, L. M., and Hook, M. (1991) Specific cell components of *Bacteroides gingivalis* mediate binding and degradation of human fibrinogen, *J. Bacteriol.* 173, 495–504.
- Imamura, T., Pike, R. N., Potempa, J., and Travis, J. (1994) Pathogenesis of Periodontitis: a major arginine-specific cysteine proteinase from *Porphyromonas gingivalis* induces vascular permeability enhancement through activation of the Kallikrein/Kinin pathway, *J. Clin. Invest.* 94, 361–367.
- Calkins, C. C., Platt, K., Potempa, J., and Travis, J. (1998) Inactivation of tumour necrosis factor- α by proteinases (gingipains) from the periodontal pathogen *Porphyromonas gingivalis*, *J. Biol. Chem.* 273, 6611–6614.
- Eichinger, A., Beisel, H. G., Jacob, U., Huber, R., Medrano, F. J., Banbula, A., Potempa, J., Travis, J., and Bode, W. (1999) Crystal structure of gingipain R: an Arg-specific bacterial cysteine proteinase with a caspase-like fold, *EMBO J.* 18, 5453–5462.
- Le Bonniec, B. F., Myles, T., Johnson, T., Knight, C. G., Tapparelli, C., Stone, S. R. (1996) Characterization of the P $_2$ ' and P $_3$ ' specificities of thrombin using fluorescence-quenched substrates and mapping of the subsites by mutagenesis, *Biochemistry* 35, 7114–7122.

22. Chen, Z., Potempa, J., Polanowski, A., Wikstrom, M., and Travis, J. (1992) Purification and characterization of a 50-kDa cysteine proteinase (gingipain) from *Porphyromonas gingivalis*. *J. Biol. Chem.* 267, 18896-18901.
23. Pike, R., McGraw, W., Potempa, J., and Travis, J. (1994) Lysine- and Arginine-specific proteinases from *Porphyromonas gingivalis*: isolation, characterisation and evidence for the existence of complexes with hemagglutinins. *J. Biol. Chem.* 269, 406-411.
24. Pike, R. N., Potempa, J., McGraw, W., Coetzer, T. H. T., and Travis, J. (1996) Characterization of the binding activities of proteinase-adhesins from *Porphyromonas gingivalis*. *J. Biol. Chem.* 271, 2876-2882.
25. Potempa, J., Mikolajczyk-Pawlinska, J., Brassell, D., Nelson, D., Thøgersen, I. B., Enghild, J. J., and Travis, J. (1998) Comparative properties of two cysteine proteinases (Gingipains R), the products of two related but individual genes of *Porphyromonas gingivalis*. *J. Biol. Chem.* 273, 21648-21657.
26. Potempa, J., Pike, R. N., and Travis, J. (1997) Titration and mapping of the active site of cysteine proteinases from *Porphyromonas gingivalis* (gingipains) using peptidyl chloromethanes. *Biol. Chem.* 378, 223-230.
27. Sali, A., and Blundell, T. L. (1993) Comparative protein modelling by satisfaction of spatial restraints. *J. Mol. Biol.* 234, 779-815.
28. Berman, H. M., Westbrook, J., Feng, Z., Gilliland, G., Bhat, T. N., Weissig, H., Shindyalov, I. N., and Bourne, P. E. (2000) The Protein Data Bank. *Nucleic Acids Res.* 28, 235-242.
29. Shagger, H., and von Jagow, G. (1987) Tricine-sodium dodecyl sulfate-polyacrylamide gel electrophoresis for the separation of proteins in the range from 1 to 100 kDa. *Anal. Biochem.* 166, 368-379.
30. Imamura, T., Banbula, A., Pereira, P., Travis, J., and Potempa, J. (2001) Activation of human prothrombin by arginine-specific cysteine proteinases (Gingipains R) from *Porphyromonas gingivalis*. *J. Biol. Chem.* 276, 18984-18991.
31. Imamura, T., Tanase, S., Hamamoto, T., Potempa, J., and Travis, J. (2001) Activation of blood coagulation factor IX by gingipains R, arginine-specific cysteine proteinases from *Porphyromonas gingivalis*. *Biochem. J.* 353, 325-331.
32. Salzet, M. (2002) Leech thrombin inhibitors. *Curr. Pharm. Des.* 8, 493-503.
33. Baskova, I. P., and Zavalova, L. L. (2001) Proteinase inhibitors from the medicinal leech *Hirudo medicinalis*. *Biochemistry (Moscow)* 66, 703-714.

BI0349726

REFERENCES:

Aduse-Opoku, J., Muir, J., Slaney, J.M., Rangarajan, M. and Curtis, M.A. (1995) Characterization, genetic analysis, and expression of a protease antigen (PrpRI) of *Porphyromonas gingivalis* W50. *Infection and Immunity* **63**: 4744-54.

Aleo, J.J. (1980) Stimulation of macromolecular synthesis by endotoxin-treated 3T6 fibroblasts. *Experientia* **36**: 546-7.

Armitage, G.C. (1999) Development of a Classification System for Periodontal Disease and Conditions. *Annals of Periodontology* **4**: 1-6.

Barkocy-Gallagher, G.A., Han, N., Patti, J.M., Whitlock, J., Progulske-Fox, A. and Lantz, M.S. (1996) Analysis of the prtP gene encoding porphypain, a cysteine proteinase of *Porphyromonas gingivalis*. *Journal of Bacteriology* **178**: 2734-41.

Barrett, A.J. and Rawlings, N.D. (2001) Evolutionary lines of cysteine peptidases. *Biological Chemistry* **382**:727-33.

Barua, P.K., Dyer, D.W. and Neiders, M.E. (1990) Effect of iron limitation on *Bacteroides gingivalis*. *Oral Microbiology and Immunology* **5**:263-8.

Baskova, I.P. and Zavalova, L.L. (2001) Proteinase inhibitors from the medicinal leech *Hirudo medicinalis*. *Biochemistry (Moscow)* **66**: 703-14.

Beck, J., Garcia, R., Heiss, G., Vokonas, P.S. and Offenbacher, S. (1996) Periodontal disease and cardiovascular disease. *Journal of Periodontology* **67**: 1123-37.

Berger, A. and Schechter, I. (1970) Mapping the active site of papain with the aid of peptide substrates and inhibitors. *Philosophical Transactions Royal Society London (Biological Sciences)* **257**: 249-64.

Berman, H.M., Westbrook, J., Feng, Z., Gilliland, G., Bhat, T.N., Weissig, H., Shindyalov, I.N. and Bourne, P.E. (2000) The Protein Data Bank. *Nucleic Acids Research* **28**: 235-42.

Bhogal, P.S., Slakeski, N. and Reynolds, E.C. (1997) A cell-associated protein complex of *Porphyromonas gingivalis* W50 composed of Arg- and Lys-specific cysteine proteinases and adhesins. *Microbiology* **143**:2485-95.

Birkedal-Hansen, H. (1993). Role of cytokines and inflammatory mediators in tissue destruction. *Journal of Periodontal Research* **28**: 500-10.

Bordusa, F., Ullmann, D. and Jakubke, H.D. (1997) Subsite specificity studies on the unusual cysteine protease clostripain: charged residues in the P3 position indicate a narrow subsite region. *Journal of Biological Chemistry* **378**: 1193-8.

Bradford, M.M. (1976) A rapid and sensitive method for the quantitation of microgram quantities of protein utilizing the principle of protein-dye binding. *Analytical Biochemistry* **72**: 248-54.

Bramanti, T.E. and Holt, S.C. (1991) Roles of porphyrins and host iron transport proteins in regulation of growth of *Porphyromonas gingivalis* W50. *Journal of Bacteriology* **173**:7330-9.

Calkins, C.C., Sameni, M., Koblinski, J., Sloane, B.F. and Calkins, M.K. (1998) Differential localization of cysteine protease inhibitors and a target cysteine protease, cathepsin B, by immuno-confocal microscopy. *Journal of Histochemistry and Cytochemistry* **46**: 745-51.

Chen, P.B., Neiders, M.E., Millar, S.J., Reynolds, H.S. and Zambon, J.J. (1987) Effect of immunization on experimental *Bacteroides gingivalis* infection in a murine model. *Infection and Immunity* **55**:2534-7.

Chen, Z., Potempa, J., Polanowski, A., Wikstrom, M. and Travis, J. (1992) Purification and characterization of a 50-kDa cysteine proteinase (gingipain) from *Porphyromonas gingivalis*. *Journal of Biological Chemistry* **267**:18896-901.

Cimasoni, G. (1983) Crevicular fluid updated. *Monographs in Oral Science* **12**:III-VII, 1-152.

Coughlin, S.R. (2000) Thrombin signalling and protease-activated receptors. *Nature* **407**: 258-64.

Curtis, M.A., Kuramitsu, H.K., Lantz, M., Macrina, F.L., Nakayama, K., Potempa, J., Reynolds, E.C. and Aduse-Opoku, J. (1999) Molecular genetics and nomenclature of proteases of *Porphyromonas gingivalis*. *Journal of Periodontal Research* **34**: 464-72.

Curtis, M.A., Aduse Opoku, J., Rangarajan, M., Gallagher, A., Sterne, J.A., Reid, C.R., Evans, H.E. and Samuelsson, B. (2002) Attenuation of the virulence of *Porphyromonas gingivalis* by using a specific synthetic Kgp protease inhibitor. *Infection and Immunity* **70**: 6968-75.

Cutler, C.W., Kalmar, J.R. and Genco, C.A. (1995) Pathogenic strategies of the oral anaerobe, *Porphyromonas gingivalis*. *Trends in Microbiology* **3**: 45-51.

Darveau, R.P., Cunningham, M.D., Bailey, T., Seachord, C., Ratcliffe, K., Bainbridge, B., Dietsch, M., Page, R.C. and Aruffo, A. (1995) Ability of bacteria associated with chronic inflammatory disease to stimulate E-selectin expression and promote neutrophil adhesion. *Infection and Immunity* **63**: 1311-7.

Darveau, R.P. (1998) Lipid A diversity and the innate host response to bacterial infection. *Current Opinion in Microbiology* **1**: 36-42.

Darveau, R.P., Belton, C.M., Reife, R.A. and Lamont, R.J. (1998) Local chemokine paralysis, a novel pathogenic mechanism for *Porphyromonas gingivalis*. *Infection and Immunity* **66**: 1660-5.

Dery, O., Corvera, C.U., Steinhoff, M. and Bunnett, N.W. (1998) Proteinase-activated receptors: novel mechanisms of signaling by serine proteases. *American Journal of Physiology* **274**: C1429-52.

Deshpande, R.G., Khan, M. and Genco, C.A. (1999) Invasion strategies of the oral pathogen *Porphyromonas gingivalis*: implications for cardiovascular disease. *Invasion and Metastasis*. **18**: 57-69.

Dickinson, D.P., Kubineic, M.K., Yoshimura, F., and Genco, R.J. (1988) Molecular cloning and sequencing of the gene encoding the fimbrial subunit of *Bacteroides gingivalis*. *Journal of Bacteriology* 170: 1658-65.

Discipio, R.G., Daffern, P.J., Kawahara, M., Pike, R., Travis, J., Hugli, T.E. and Potempa, J. (1996) Cleavage of human complement component C5 by cysteine proteinases from *Porphyromonas (Bacteroides) gingivalis*. Prior oxidation of C5 augments proteinase digestion of C5. *Immunology* 87: 660-7.

Dom, B.R., Dunn, W.A.Jr., and Progulsk-Fox, A. (1999) Invasion of Human Coronary Artery Cells by Periodontal Pathogens. *Infection and Immunity* 67: 5792-98.

Dom, B.R., Dunn, W.A. Jr., and Progulsk-Fox, A. (2001) *Porphyromonas gingivalis* Traffics to Autophagosomes in Human Coronary Artery Endothelial Cells. *Infection and Immunity* 69: 5698-708.

Eichinger, A., Beisel, H.G., Jacob, U., Huber, R., Medrano, F.J., Banbula, A., Potempa, J., Travis, J. and Bode, W. (1999) Crystal structure of gingipain R: an Arg-specific bacterial cysteine proteinase with a caspase-like fold. *The EMBO Journal* 18: 5453- 62.

Fletcher, J., Reddi, K., Poole, S., Nair, S., Henderson, B., Tabona, P. and Wilson, M. (1997) Interactions between perodontopathic bacteria and cytokines. *Journal of Periodontology Research* 32: 200-5.

Fujimura, S., Shibata, Y., Hirai, K. and Nakamura, T. (1995) Some binding properties of the envelope of *Porphyromonas gingivalis* to hemoglobin. *FEMS Immunology and Medical Microbiology* 10:109-14.

Fujimura, S., Hirai, K., Shibata, Y., Nakayama, K. and Nakamura, T. (1998) Comparative properties of envelope-associated arginine-gingipains and lysine-gingipain of *Porphyromonas gingivalis*. *FEMS Microbiology Letters* 163:173-9.

Genco, C.A. (1995) Regulation of hemin and iron transport in *Porphyromonas gingivalis*. *Advances in Dental Research* 9:41-7.

Genco, C.A., Odusanya, B.M., Potempa, J., Mikolajczyk-Pawlinska, J. and Travis, J. (1998) A peptide domain on gingipain R which confers immunity against *Porphyromonas gingivalis* infection in mice. *Infection and Immunity* **66**: 4108-14.

Genco, C.A., Potempa, J., Mikolajczyk-Pawlinska, J. and Travis, J. (1999) Role of gingipains R in the pathogenesis of *Porphyromonas gingivalis*-mediated periodontal disease. *Clinical and Infectious Diseases* **28**: 456-65.

Genco, R.J. (1998) Periodontal disease and risk for myocardial infarction and cardiovascular disease. *Cardiovascular Reviews and Reports* **19**: 34-40.

Greenstein G. (1984) The role of bleeding upon probing in the diagnosis of periodontal disease. A literature review. *Periodontology* **55**: 684-8.

Grenier, D., Roy, S., Chandad, F., Plamondon, P., Yoshioka, M., Nakayama, K. and Mayrand, D. (2003) Effect of inactivation of the Arg- and/or Lys-gingipain gene on selected virulence and physiological properties of *Porphyromonas gingivalis*. *Infection and Immunity* **71**:4742-8.

Haapasalo, M., Shah, H., Gharbia, S., Seddon, S. and Lounatmaa, K. (1989) Surface properties and ultrastructure of *Porphyromonas gingivalis* W50 and pleiotropic mutants. *Scandinavian Journal of Dental Research* **97**:355-60.

Haffajee A.D. and Socransky, S.S. (1994) Microbial etiological agents of destructive periodontal diseases. *Periodontology 2000* **5**: 78-111.

Hamada, S., Fujiwara, T., Morishima, S., Takahashi, I., Nakagawa, I., Kimura, S. and Ogawa, T. (1994) Molecular and immunological characterization of the fimbriae of *Porphyromonas gingivalis*. *Microbiology Immunology* **38**: 921-30.

Harrington, D.J. (1996) Bacterial collagenases and collagen-degrading enzymes and their potential role in human disease. *Infection and Immunity* **64**: 1885-91.

Holt, S.C. and Bramanti, T.E. (1991) Factors in virulence expression and their role in periodontal disease pathogenesis. *Critical Reviews in Oral Biology and Medicine* 2: 177-281.

Holt, S.C., Kesavalu, L., Walker, S. and Genco, C.A. (1999) Virulence factors of *Porphyromonas gingivalis*. *Periodontology* 2000 20: 168-238.

Hosotaki, K., Imamura, T., Potempa, J., Kitamura, N. and Travis, J. (1999) Activation of protein C by arginine-specific cysteine proteinases (gingipains-R) from *Porphyromonas gingivalis*. *Biological Chemistry* 380: 75-80.

Huang, G.T.J., Haake, S.K., Kim, J.W. and Park, N.H. (1998) Differential expression of interleukin-8 and intercellular adhesion molecule-1 by human gingival epithelial cells in response to *Actinobacillus actinomycetemcomitans* or *Porphyromonas gingivalis* infection. *Oral Microbiology and Immunology* 13: 301-9.

Imamura, T., Pike, R., Potempa, J. and Travis, J. (1994) Pathogenesis of periodontitis: a major arginine-specific cysteine proteinase from *Porphyromonas gingivalis* induces vascular permeability enhancement through activation of the kallikrein/kinin pathway. *Journal of Clinical Investigations* 94: 361-7.

Imamura, T., Potempa, J., Tanase, S. and Travis, J. (1997) Activation of blood coagulation factor X by arginine-specific cysteine proteinases (gingipain-Rs) from *Porphyromonas gingivalis*. *Journal of Biological Chemistry* 272:16062-67.

Imamura, T., Potempa, J. and Travis, J. (2000) Comparison of pathogenic properties between two types of arginine-specific cysteine proteinases (gingipains-R) from *Porphyromonas gingivalis*. *Microbial Pathogenesis* 29: 155-63.

Imamura, T., Banbula, A., Periera, P., Travis, J., and Potempa, J. (2001a) Activation of human prothrombin by arginine-specific cysteine proteinases (gingipains R) from *Porphyromonas gingivalis*. *Journal of Biological Chemistry* 276: 18984-91.

Imamura, T., Tanase, S., Hamamoto, T., Potempa, J. and Travis, J. (2001) Activation of blood coagulation factor IX by gingipains R, arginine-specific cysteine proteinases from *Porphyromonas gingivalis*. *Biochemical Journal* 353: 325-31.

Ishihara, H., Connolly, A.J., Zeng, D., Kahn, M.L., Zheng, Y.W., Timmons, C., Tram, T. and Coughlin, S.R. (1997) Protease-activated receptor 3 is a second thrombin receptor in humans. *Nature* 386:502-6.

Jagels, M.A., Travis, J., Potempa, J., Pike, R. and Hugli, T.E. (1996) Proteolytic inactivation of the leukocyte C5a receptor by proteinases derived from *Porphyromonas gingivalis*. *Infection and Immunity* 64:1984-91.

Kahn, M.L., Zheng, Y.W., Huang, W., Bigornia, V., Zeng, D., Moff, S., Farese, R. V., Jr., Tam, C. and Coughlin, S.R. (1998) A dual thrombin receptor system for platelet activation. *Nature* 394: 690-4.

Kaplan, A.P., Joseph, K., Shibayama, Y., Reddigari, S., Ghebrehiwet, B. and Silverberg, M. (1997) The intrinsic coagulation/kinin-forming cascade: Assembly in plasma and cell surfaces in inflammation. *Advances in Immunology* 66: 225-72.

Kilian, M. Systemic disease: manifestations of oral bacteria, *In Dental Microbiology*. Ed. J.R. McGhee, S.M. Michalek, and G.H. Cassell. Harpers & Row, Philadelphia, Pa. 1982. p832-38.

Kirszbaum, L., Sotiropoulos, C., Jackson, C., Cleal, S., Slakeski, N. and Reynolds, E.C. (1995) Complete nucleotide sequence of a gene *prtR* of *Porphyromonas gingivalis* W50 encoding a 132 kDa protein that contains an arginine-specific thiol endopeptidase domain and a haemagglutinin domain. *Biochemical Biophysical Research Communications* 207: 424-31.

Kontani, M., Ono, H., Shibata, H., Okamura, Y., Tanaka, T., Fujiwara, T., Kimura, S. and Hamada, S. (1996) Cysteine protease of *Porphyromonas gingivalis* 381 enhances binding of fimbriae to cultured human fibroblasts and matrix proteins. *Infection and Immunity*. 64: 756-62.

Kuramitsu, H.K., Yoneda, M. and Madden, T. (1995). Proteases and collagenases of *Porphyromonas gingivalis*. *Advances in Dental Research* **9**:37-40.

Kuramitsu, H.K. (1998) Proteases of *Porphyromonas gingivalis*: what don't they do? *Oral Microbiology Immunology* **13**: 263-70.

Lamont, R.J. and Jenkinson, H.F. (1998) Life below the gum line: pathogenic mechanisms of *Porphyromonas gingivalis*. *Microbiology and Molecular Biology Review* **62**: 1244-63.

Lamont, R.J. and Jenkinson, H.F. (2000) Subgingival colonization by *Porphyromonas gingivalis*. *Oral Microbiology and Immunology* **15**: 341-9.

Lamont, R.J. and Yilmaz, O. (2002) In or out: the invasiveness of oral bacteria. *Periodontology 2000* **30**: 61-9.

Lantz, M.S., Allen, R.D., Vail, T.A., Switalski, L.M. and Hook, M. (1991) Identification of *Porphyromonas gingivalis* components that mediate its interaction with fibronectin. *Journal of Bacteriology* **173**: 495-504.

Le Bonniec, B.F., Myles, T., Johnson, T., Knight, C.G., Tapparelli, C., Stone, S.R. (1996) Characterization of the P2' and P3' specificities of thrombin using fluorescence-quenched substrates and mapping of the subsites by mutagenesis. *Biochemistry* **35**: 7114-22.

Lewis, J.P. and Macrina, F.L. (1998) IS195, an insertion sequence-like element associated with protease genes in *Porphyromonas gingivalis*. *Infection and Immunity* **66**: 3035-42.

Littlewood, A.J., Russell, J., Harvey, G.R., Hughes, D.E., Russell, R.G. and Gowen, M. (1991). The modulation of the expression of IL-6 and its receptor in human osteoblasts *in vitro*. *Endocrinology* **129**:1513-20.

Loesche, W.J. (1993) Bacterial mediators in periodontal disease. Anaerobic bacteria and anaerobic infections. *Clinical and Infectious Diseases* **16**: S203-10.

Loesche, W.J. and Grossman, N.S. (2001) Periodontal disease as a specific, albeit chronic, infection: diagnosis and treatment. *Clinical and Microbiological Reviews* **14**:727-52.

Lourbakos, A., Chinni, C., Thompson, P., Potempa, J., Travis J., Mackie, E.J. and Pike, R.N. (1998) Cleavage and activation of proteinase-activated receptor-2 on human neutrophils by gingipain-R from *Porphyromonas gingivalis*. *FEBS Letters* **435**: 45-48.

Lourbakos, A., Potempa, J., Travis, J., D'Andrea, M.R., Andrade-Gordon, P., Santulli, R., Mackie, E.J. and Pike, R.N. (2001a) Arginine-specific protease from *Porphyromonas gingivalis* activates protease-activated receptors on human oral epithelial cells and induces interleukin-6 secretion. *Infection and Immunity*. **69**: 5121-30.

Lourbakos, A., Yuan, Y., Jenkins, A.L., Travis, J., Andrade-Gordon, P., Santulli, R., Potempa, J. and Pike, R.N. (2001b) Activation of protease-activated receptors by gingipains from *Porphyromonas gingivalis* leads to platelet aggregation: a new trait in microbial pathogenicity. *Blood* **97**:3790-97.

Maeda, H. and Yamamoto, T. (1996) Pathogenic mechanisms induced by microbial proteases in microbial infections. *Biological Chemistry* **377**: 217-26.

Mayrand, D. and Holt, S.C. (1988) Biology of asaccharolytic black-pigmented *Bacteroides* species. *Microbiology Reviews* **52**:134-52.

Mikolajczyk-Pawlinska, J., Kordula, T., Pavloff, N., Pemberton, P.A., Kiefer, M.C., Travis, J. and Potempa, J. (1998) Genetic variation of *Porphyromonas gingivalis* genes encoding gingipains, cysteine proteinases with arginine or lysine specificity. *Biological Chemistry* **237**: 205-11.

Millar, S.J., Goldstein, E.G., Levine, M.J. and Hausmann, E. (1936) Modulation of bone metabolism by two chemically distinct lipopolysaccharide fractions from *Bacteroides gingivalis*. *Infection and Immunity* **51**: 302-6.

Moore, W.E., Holdeman, L.V., Smibert R.M., Hash, D.E., Burnmeister, J.A. and Ranney, R.R. (1982) Bacteriology of severe periodontitis in young adult humans. *Infection and Immunity* **38**:1137-48.

Mundy, G.R. (1991) Inflammatory mediators and the destruction of bone. *Journal of Periodontological Research* **26**: 213-17.

Naito, Y., Tohda, H., Okuda, K. and Takazoe, I. (1993) Adherence and hydrophobicity of invasive and non-invasive strains of *Porphyromonas gingivalis*. *Oral Microbiology and Immunology* **8**: 195-202.

Nakayama, K. (1997) Domain-specific rearrangement between the two Arg-gingipain-encoding genes in *Porphyromonas gingivalis*: possible involvement of nonreciprocal recombination. *Microbiology and Immunology* **41**: 185-195.

O'Brien-Simpson, N.M., Paolini, R.A. and Reynolds, E.C. (2000) RgpA-Kgp peptide-based immunogens provide protection against *Porphyromonas gingivalis* challenge in a murine lesion model. *Infection and Immunity* **68**:4055-63.

O'Brien-Simpson, N.M., Paolini, R.A., Hoffmann, B., Slakeski, N., Dashper, S.G. and Reynolds, E.C. (2001) Role of RgpA, RgpB, and Kgp proteinases in virulence of *Porphyromonas gingivalis* W50 in a murine lesion model. *Infection and Immunity* **69**:7527-34.

Ofek, I., and J.D. Doyle. Bacterial Adhesion to Cells and Tissues. 1994. Chapman and Hall, New York.

Offenbacher, S. (1996) Periodontal diseases: pathogenesis. *Annals in Periodontology* **1**:821-78.

Offenbacher, S., Katz, V., Fertik, G., Collins, J., Boyd, D., Maynor, G., McKaig, and Beck, J. (1996) Periodontal infection as a possible risk factor for preterm low birth weight. *Journal of Periodontology* **67**: 1103-1113.

Ogawa, T.Y., Kusumoto, S., Hamada, J.R., McGhee, and Kiyono, H. (1990). *Bacteroides gingivalis*-specific serum IgG and IgA subclass antibodies in periodontal diseases. *Clinical and Experimental Immunology* **82**: 318-325.

Ogawa, T. (1994) The potential protective immune responses to synthetic peptides containing conserved epitopes of *Porphyromonas gingivalis* fimbrial protein. *Journal of Medical Microbiology* **41**: 349-58.

Okamoto, K., Misumi, Y., Kadowaki, T., Yoneda, M., Yamamoto, K. and Ikehara, Y. (1995) Structural characterization of argingipain, a novel arginine-specific cysteine proteinase as a major periodontal pathogenic factor from *Porphyromonas gingivalis*. *Archives of Biochemistry and Biophysics* **316**: 917-925.

Okamoto, K., Kadowaki, T., Nakayama, K., and Yamamoto, K. (1996). Cloning and sequencing of the gene encoding a lysine-specific cysteine proteinase (lys-gingipain) in *Porphyromonas gingivalis*: structural relationship with the arginine-specific cysteine proteinase (arg-gingipain). *Journal of Biochemistry* **120**: 398-406.

Page, R.C. (1998) The pathobiology of periodontal diseases may affect systemic diseases: inversion of a paradigm. *Annals of Periodontology* **3**: 108-120.

Pavloff, N., Potempa, J., Pike, R.N., Prochazka, V., Kiefer, M.C., Travis, J. and Barr, P.J. (1995) Molecular cloning and structural characterization of the Arg-gingipain proteinase of *Porphyromonas gingivalis*. Biosynthesis as a proteinase-adhesin polyprotein. *Journal of Biological Chemistry* **270**: 1007-10.

Pavloff, N., Pemberton, P.A., Potempa, J., Chen, W.C.A., Pike, R.N., Prochazka, V., Kiefer, M.C., Travis, J. and Barr, P.J. (1997) Molecular Cloning and Characterization of *Porphyromonas gingivalis* Lysine-specific Gingipain. A new member of an emerging family of pathogenic bacterial cysteine proteinases. *Journal of Biological Chemistry* **272**: 1595-1600.

Pike, R., McGraw, W., Potempa, J. and Travis, J. (1994). Lysine- and arginine-specific proteinases from *Porphyromonas gingivalis*. Isolation,

characterization, and evidence for the existence of complexes with hemagglutinins. *Journal of Biological Chemistry* **269**: 406-411.

Pike, R.N., Potempa, J., McGraw, W., Coetzer, T.H.T. and Travis, J. (1996) Characterization of the binding activities of proteinase-adhesin complexes from *Porphyromonas gingivalis*. *Journal of Bacteriology* **178**: 2876-2882.

Potempa, J., Pavloff, N. and Travis, J. (1995a) *Porphyromonas gingivalis*: a proteinase/gene accounting audit. *Trends in Microbiology* **3**: 430-434.

Potempa, J., Pike, R. and Travis, J. (1995) The multiple forms of trypsin-like activity present in various strains of *Porphyromonas gingivalis* are due to the presence of either Arg-gingipain or Lys-gingipain. *Infection and Immunity* **63**: 1176-82.

Potempa, J. and Travis, J. (1996). *Porphyromonas gingivalis* proteinases in periodontitis, a review. *Acta Biochimica. (Pol)*. **43**: 455-466.

Potempa, J., Pike, R.N. and Travis, J. (1997) Titration and mapping of the active site of cysteine proteinases from *Porphyromonas gingivalis* (Gingipains) using peptidyl chloromethanes. *Biological Chemistry* **378**: 223-230.

Potempa, J., Mikolajczyk-Pawlinska, J., Brassell, D., Nelson, D., Thogersen, I.B., Enghild, J.J. and Travis, J. (1998). Comparative Properties of Two Cysteine Proteinases (Gingipains R), the Products of Two Related but Individual Genes of *Porphyromonas gingivalis*. *Journal of Biological Chemistry* **273**: 21648-21657.

Rangarajan, M., Smith, S.J., and Curtis, M.A. (1997) Biochemical characterization of the arginine-specific proteases of *Porphyromonas gingivalis* W50 suggests a common precursor. *Biochemical Journal*. **323**: 701-9.

Rajapakse, P.S., O'Brien-Simpson, N.M., Slakeski, N., Hoffmann, B. and Reynolds, E.C. (2002) Immunization with the RgpA-Kgp proteinase-adhesin complexes of *Porphyromonas gingivalis* protects against periodontal bone loss in the rat periodontitis model. *Infection and Immunity* **70**:2480-6.

Reife, R.A., Shapiro, R.A., Bamber, B.A., Berry, K.K., Mick, G.E. and Darveau R.P. (1995) *Porphyromonas gingivalis* lipopolysaccharide is poorly recognized by molecular components of innate host defense in a mouse model of early inflammation. *Infection and Immunity*. **63**: 4686-94.

Sali, A., and Blundell, T.L. (1993) Comparative protein modelling by satisfaction of spatial restraints. *Journal of Molecular Biology* **234**: 779-815.

Salvesen, G. and Nagase, H. Inhibition of proteolytic enzymes. In Proteolytic enzymes : A practical approach. Ed., Beynon, R.J., Bond, J.S. Oxford: IRL Press, 1989. pg83-102.

Salzet, M. (2002) Leech thrombin inhibitors. *Current Pharmacological developments*. **8**: 493-503.

Sawyer, S.J., Macdonald, J.B. and Gibbons, R.J. (1962) Biochemical characteristics of *Bacteroides melaninogenicus*. A study of thirty-one strains. *Archives of Oral Biology*.**7**:685-91.

Schenkein, H.A., Fletcher, H.M., Bodnar, M. and Macrina, F.L. (1995) Increased opsonization of a prtH-defective mutant of *Porphyromonas gingivalis* W83 is caused by reduced degradation of complement-derived opsonins. *Journal of Immunology* **154**: 5331-7.

Schenkein, H.A. (1998) Inheritance as a determinant of susceptibility for periodontitis. *Journal of Dental Education* **62**: 840-51.

Schifferle, R.E., Reddy, M.S., Zambon, J.J., Genco, R.J. and Levine, M.J. (1989) Characterization of a polysaccharide antigen from *Bacteriodes gingivalis*. *Journal of Immunology* **143**: 3035-3042.

Shägger, H. and von Jagow, G. (1987) Tricine-sodium dodecyl sulfate-polyacrylamide gel electrophoresis for the separation of proteins in the range from 1 to 100 kDa. *Analytical Biochemistry* **166**: 368-379.

Shah, H.N. and Gharbia, S.E. (1989) Lysis of erythrocytes by the secreted cysteine proteinase of *Porphyromonas gingivalis* W83. *FEMS Microbiology Letters* **52**:213-7.

Shapira, L., Gordon, B., Warbington, M. and Van Dyke, T.E. (1994) Priming effect of *Porphyromonas gingivalis* lipopolysaccharide on superoxide production by neutrophils from healthy and rapidly progressive periodontitis subjects. *Journal of Periodontology* **65**: 129-33.

Slakeski, N., Bhogal, P.S., O'Brien-Simpson, N.M. and Reynolds, E.C. (1998) Characterization of a second cell-associated Arg-specific cysteine proteinase of *Porphyromonas gingivalis* and identification of an adhesin-binding motif involved in association of the prtR and prtK proteases and adhesins into large complexes. *Microbiology* **144**: 1583-92.

Slakeski, N., Cleal, S.M., Bhogal, P.S. and Reynolds, E.C. (1999) Characterization of a *Porphyromonas gingivalis* gene prtK that encodes a lysine-specific cysteine proteinase and three sequence-related adhesins. *Oral Microbiology and Immunology* **14**: 92-7.

Socransky, S.S., Haffajee, A.D., Smith, C. and Dibart, S. (1991) Relation of counts of microbial species to clinical status at the sampled site. *Journal of Clinical Periodontology* **18**:766-75.

Socransky, S.S. and Haffajee, A.D. (1992) The bacterial etiology of destructive periodontal disease: current concepts. *Journal of Periodontology* **63**:322-31.

Socransky, S.S., Haffajee, A.D., Cugini, M.A., Smith, C. and Kent, R.L. Jr. (1998) Microbial complexes in subgingival plaque. *Journal of Clinical Periodontology* **25**:134-44.

Sorsa, T., Ingman, T., Suomalainen, K., Haapasalo, M., Konttinen, Y.T., Lindy, O., Saari, H. and Uitto, V.J. (1992) Identification of proteases from

periodontopathogenic bacteria as activators of latent human neutrophil and fibroblast-type interstitial collagenases. *Infection and Immunity* **60**: 4491-5.

Supuran, C.T., Scozzafava, A., and Clare, B.W. (2002) Bacterial Protease Inhibitors, *Medicinal Research Reviews* **22**: 329-372.

Travis, J., Pike, R., Imamura, T. and Potempa, J. (1994) The role of proteolytic enzymes in the development of pulmonary emphysema and periodontal disease. *American Journal of Respiratory and Critical Care Medicine* **150**: S143-6.

Travis, J., Pike, R., Imamura, T. and Potempa, J. (1997) Porphyromonas gingivalis proteinases as virulence factors in the development of periodontitis. *Journal of Periodontal Research* **32**: 120-5.

Travis, J., Potempa, J. and Maeda, H. (1995) Are bacterial proteinases pathogenic factors? *Trends in Microbiology*. **3**: 405-7.

Travis, J. and Potempa, J. (2000) Bacterial proteinases as targets for the development of second-generation antibiotics. *Biochimica Biophysica Acta* **1477**: 35-50.

Watanabe, A.A. Takeshita, S., Kitano, and Hanazawa, S. (1996) CD14-mediated signal pathway of *Porphyromonas gingivalis* lipopolysaccharide in human gingival fibroblasts. *Infection and Immunity* **64**: 4488-4494.

Weibe, C.B. and Putnins, E.E. (2000). The Periodontal Disease Classification System of the American Academy of Periodontology- An Update. *Journal of the Canadian Dental Association* **66**: 594-597.

Wingrove, J.A., DiScipio, R.G., Chen, Z., Potempa, J., Travis, J. and Hugli, T.E. (1992) Activation of complement components C3 and C5 by a cysteine proteinase (gingipain-1) from *Porphyromonas (Bacteroides) gingivalis*. *Journal of Biological Chemistry* **267**: 18902-7.

Xie, H., Cai, S. and Lamont, R.J. (1997) Environmental regulation of fimbrial gene expression in *Porphyromonas gingivalis*. *Infection and Immunity*. **65**: 2265-71.

Xu, W.F., Andersen, H., Whitmore, T.E., Presnell, S.R., Yee, D.P., Ching, A., Gilbert, T., Davie, E.W. and Foster, D.C. (1998) Cloning and characterization of human protease-activated receptor 4. *Proceedings of the National Academy of Sciences* **95**: 6642-46.

Yonezawa, H., Ishihara, K. and Okuda, K. (2001) Arg-gingipain a DNA vaccine induces protective immunity against infection by *Porphyromonas gingivalis* in a murine model. *Infection and Immunity* **69**:2858-64.